

General Disclaimer

One or more of the Following Statements may affect this Document

- This document has been reproduced from the best copy furnished by the organizational source. It is being released in the interest of making available as much information as possible.
- This document may contain data, which exceeds the sheet parameters. It was furnished in this condition by the organizational source and is the best copy available.
- This document may contain tone-on-tone or color graphs, charts and/or pictures, which have been reproduced in black and white.
- This document is paginated as submitted by the original source.
- Portions of this document are not fully legible due to the historical nature of some of the material. However, it is the best reproduction available from the original submission.

OU TM-47 (NASA)

NASA CR- 145178

A MICROCOMPUTER-BASED LOW-COST
OMEGA SENSOR PROCESSOR

(NASA-CR-145178) A MICROCOMPUTER-BASED
LOW-COST OMEGA SENSOR PROCESSOR M.S. Thesis
(Ohio Univ.) 146 p HC AC7/MF A01 CSCI 17G

N77-22063

Unclassified
G3/04 25116

by

Richard J. Salter, Jr.
Avionics Engineering Center
Department of Electrical Engineering
Ohio University
Athens, Ohio 45701

February 1977

Supported by

National Aeronautics and Space Administration

Grant NGR 36-009-017



FOREWORD

This paper was submitted to and approved by the Department of Electrical Engineering and the Graduate College of Ohio University on March 4, 1977 as a master's thesis.

ABSTRACT

A microcomputer-based, low-cost Omega sensor processor (OSP) has been designed, implemented with minimum hardware, and tested. The feasibility of implementing a minimum hardware/maximum software system of less complexity and lower cost than is currently available has been verified. The design approach and hardware/software details are presented for this low-cost navigation aid.

The long-range project goal of developing a general aviation Omega navigation system (ONS) for a cost under \$1000 is now feasible. The microcomputer-based OSP presented here represents nearly all the system hardware needed for an airborne ONS. An area navigation routine is the additional component needed to complete the ONS for general aviation. This navigation routine can readily be added to the present system since it is additional software and not hardware.

This paper describes the OSP design and engineering approach used in achieving this design. In reflecting a structured program design approach, the project goal of designing a low-cost OSP is presented initially. Succeeding chapters document the efforts made in support of this goal. The OSP operations are functionally described in the text, as is the system hardware and software. Circuit details of the hardware modules and program listings for the FORTRAN and microcomputer software are reserved for the appendices.

TABLE OF CONTENTS

	PAGE
ABSTRACT	ii
List of Figures	v
I. INTRODUCTION	1
II. OMEGA SENSOR PROCESSOR	3
A. Design Approach	4
B. System Hardware	6
1. Receiver	6
2. Computer Interface	10
3. Microcomputer	13
C. System Software	16
1. Interrupt Servicing	16
2. Automatic Synchronization	16
3. PLL Phase Tracking	24
III. OSP OUTPUTS AND USES	36
A. Output Data	36
B. OSP Uses	46
IV. SUMMARY AND CONCLUSIONS	47
V. RECOMMENDATIONS FOR FUTURE WORK	48
VI. ACKNOWLEDGEMENTS	49
VII. REFERENCES	50
VIII. APPENDICES	53
A. The Worldwide Omega Navigation System	53
B. Omega Data Base	60
C. Omega Sensor Processor Circuitry	64
D. JOLT Microcomputer System	64
1. Hardware	64
2. Software	71
E. FORTRAN Simulation Analysis	71
1. Noise Modeling	75
2. Automatic Synchronization Simulation	76
3. Phase Locked Loop Simulation	85

	PAGE
F. OSP Microcomputer Routines	116
1. Main Routine	116
2. Interrupt Service Routine	116
3. Automatic Synchronization Subroutine	123
4. SMAPLL2 Tracking Subroutine	123
5. Data Output Subroutine	123

LIST OF FIGURES

	PAGE
Figure 1. Summary Block Diagram - Microcomputer-Based Omega Sensor Processor.	7
Figure 2. Preamplifier Characteristics.	8
Figure 3. Front-End, Computer Interface, and Microcomputer Modules Block Diagram.	9
Figure 4. Front-End Module Response Curve.	11
Figure 5. Microcomputer System Organization.	14
Figure 6. Memory-Mapped Data Output Port.	15
Figure 7. Interrupt Service Routine Flow Chart.	17
Figure 8. Automatic Synchronization Routine Flow Chart.	19
Figure 9. Computer Plot of Raw Omega Data.	23
Figure 10. First-Order Software Memory-Aided Phase Locked Loop (SMAPLL1) Block Diagram.	25
Figure 11. Second-Order Software Memory-Aided Phase Locked Loop (SMAPLL2) Block Diagram.	27
Figure 12. SMAPLL2 Transient (Lock-Up Mode) Response to 180° Step(Top) and 300-Knot Ramp (Bottom) Inputs at 0 dB SNR.	30
Figure 13. Steady-State Response of SMAPLL2 to Zero Velocity Inputs.	31
Figure 14. Steady-State Response of SMAPLL2 to 300-Knot Ramp Inputs.	32
Figure 15. Normalized Histogram of -10 dB Input Signal-Plus-Noise.	33
Figure 16. Normalized Histogram of SMAPLL2, Output Estimates of Phase for -10 dB Input SNR.	34

	PAGE
Figure 17. Data Output Routine Flow Chart.	37
Figure 18. User-Inserted Code Words for Output Routine.	38
Figure 19. Single Station Phase of North Dakota Minus Clock.	40
Figure 20. Single Station Phase of Trinidad Minus Clock and Argentina Minus Clock.	40
Figure 21a. 24 Hours Diurnal Data: Hawaii-North Dakota LOP.	41
Figure 21b. 24 Hours Diurnal Data: North Dakota - Trinidad LOP.	41
Figure 22. 24 Hours Diurnal Data: North Dakota - Argentina LOP.	42
Figure 23. Omega LOP Output Traces -- Software Loop Output on Bottom.	44
Figure 24. An Example of Signal Quality Data.	45
Figure 25. Multiplexed LOP Outputs (90 Seconds MUX Time).	45
Figure A-1. Omega Station Locations.	54
Figure A-2. Omega Signal Transmission Format.	54
Figure A-3. Omega Transmitting Antenna Structures.	55
Figure A-4. Propagation Modes for VLF Signals.	56
Figure A-5. Omega Lines-of-Position (LOP's) Formed by North Dakota (D) and Temporary Station Trinidad (B).	59
Figure A-6. VLF Signal Levels as Received in 30 Hz Bandwidth in New York.	56
Figure B-1. Omega Data Collection Setup.	62
Figure B-2. Omega Data Base Summary.	63
Figure C-1. Dual Purpose Preamplifier Module.	65

	PAGE
Figure C-2a. Receiver Front-End Module, Two-Stage VLF Bandpass Amplifier.	66
Figure C-2b. Receiver Front-End Module, Limiter - Comparator Circuit.	67
Figure C-3. Microcomputer Interface Module Circuit Diagram.	68
Figure D-1. JOLT CPU Board Schematic Diagram.	69
Figure D-2. JOLT 4K RAM Memory Board Schematic Diagram.	70
Figure D-3. Instruction Set for MOS Technology 6502 CPU.	72
Figure D-4. JOLT System TTY Monitor Commands Summary.	73
Figure D-5. JOLT System Memory Map.	74
Figure E-1. Normalized Histogram of Simulated Noise Phase Vs. Phase in cec for +20 dB SNR.	77
Figure E-2. Autocorrelation for Simulated Noise Phase for +20 dB SNR.	78
Figure E-3. Normalized Histogram of Real Omega Noise Phase Vs. Phase in cec for +20 dB SNR.	79
Figure E-4. Autocorrelation of Real Omega Noise Phase for +20 dB SNR.	80
Figure E-5. Automatic Synchronization Flow Chart.	81
Figure E-6. 10 Second Frame of Data Plotted 10 Points Per Line. Top = Real Data, Bottom = Mirrored Data.	82
Figure E-7. Sample-to-Sample Phase Differences Plotted Ten Points Per Line.	84
Figure E-8. SMAPLL1 Steady-State Response to O-Velocity Input for First-Order Filter Equal to 2 Counts (1), 4 counts (2), 8 counts (3), 16 counts (4) and 32 counts (5).	88
Figure E-9. SMAPLL2 Steady-State Response to Zero-Velocity Input for Second-Order Gain Equal to Zero (1), .125 (2), .250 (3), .375 (4), .500 (5).	89

	PAGE
Figure E-10. SMA.PLL2 Steady-State Response to 300-Knot Ramp Input for Second-Order Gain Equal to .125 (1), .250 (2), .375 (3), .500 (4), .625 (5).	90
Figure E-11. SMAPLL2 Transient (Lock-Up Mode) Response to 180° Step (Top) and 300-Knot Ramp (Bottom) Input of -10 dB SNR.	92
Figure E-12. SMAPLL2 Transient (Lock-Up Mode) Response to 180° Step (Top) and 300-Knot Ramp Inputs (Bottom) of +10 dB SNR.	93
Figure E-13. FORTRAN Program RSRAND Used to Analyze Real and Simulated Omega Noise.	94
Figure E-14. FORTRAN Program RSOSP Used to Simulate Automatic Synchronization Routine.	99
Figure E-15. FORTRAN Program RSSIM Used to Simulate SMAPLL2 and Evaluate Performance.	108
Figure F-1. Main (Initialization) Routine Flow Chart.	117
Figure F-2. Microcomputer Program INIT Listing.	118
Figure F-3. Interrupt Service Routine Flow Chart.	120
Figure F-4. Microcomputer Program OSERV Listing.	121
Figure F-5. Automatic Synchronization Subroutine Flow Chart.	124
Figure F-6. Microcomputer Program SYNC Listing.	126
Figure F-7. SMAPLL2 Subroutine Flow Chart.	130
Figure F-8. Microcomputer Program SMAPLL2 Listing.	131
Figure F-9. Data OUTPUT Subroutine Flow Chart.	135
Figure F-10. Microcomputer Program OUTPUT Listing.	136

I. INTRODUCTION

This project was sponsored by the NASA/Langley Research Center under a grant effort known as the NASA Tri-University Program in Air Transportation Systems. The program was begun in 1971 and includes MIT, Ohio University, and Princeton University in a cooperative effort to improve the safety, reliability, and efficiency of our National Airspace System. Each University offers a unique area of specialized interest and expertise, thereby complementing each others' efforts; Ohio University's area of specialization being avionics.

Early in the program's development it was determined that the Tri-University Program might make a contribution to general aviation by developing a low-cost area navigation system for small aircraft. Studies pointed to the Omega navigation system as a low-cost system which could provide all-altitude signal coverage, and the major emphasis in the program became the development of a low-cost Omega navigation system for the general aviation pilot.

While MIT studied the systems integration aspects and Princeton University the flight dynamics aspects, Ohio University turned its efforts towards designing a more sensitive and lower cost Omega receiver than was commercially available. An early result was an Omega sensor processor incorporating all TTL circuitry, and this unit was flight-tested aboard the Avionics Engineering Center's DC-3 flying laboratory enroute to Langley Field, Virginia in October, 1974. After this successful flight demonstration, Ohio University embarked on a project to build five Omega prototype receivers for the other Universities and NASA. These prototypes were designed using low power CMOS circuitry and were delivered to the recipients in September, 1976.

The Omega sensor processor outputs, Omega phase and phase differences, are the inputs needed by a navigation processor to derive pilot-useable information such as cross-track error and down-track distance. Due to the recent availability of low-cost microcomputers, efforts were channeled toward using a commercially-available microcomputer as the navigation processor for the airborne Omega navigation system (ONS). When incorporating a microcomputer into the ONS, however, it became obvious that, in addition to performing the area navigation functions, the sensor processor functions could also be performed in microcomputer software.

Therefore, a project was begun to explore the feasibility of a minimum hardware/maximum software OSP. This paper reports results of this project: a minimum hardware system has been designed, and the OSP functions of automatic synchronization, phase tracking, and line-of-position (LOP) generation have been implemented in microcomputer software. The microcomputer-based OSP thus consists of a 10.2 KHz TRF receiver module, an interface module which samples the receiver outputs, and a microcomputer module to process the Omega phase data.

The design approach was to first develop the system hardware (receiver and interface modules) and use these modules to supply Omega data to a digital magnetic tape recorder. A data base of real Omega ground and flight data was collected for use in a FORTRAN language simulation analysis of OSP functions. Algorithms to perform the OSP functions were developed and optimized via this simulation. The routines were then assembled into microcomputer code and loaded into the OSP microcomputer module. With the receiver and interface supplying

Omega data to the microcomputer module, the output data consistently equaled or exceeded the quality of the all-hardware OSP outputs, thus verifying the feasibility of the software-based system.

The hardware and software for the microcomputer-based low-cost OSP are functionally described herein, and the type of outputs available and the results obtained are presented. The hardware circuit details and software routines program listings are documented in the appendices.

II. OMEGA SENSOR PROCESSOR

The worldwide Omega navigation system is a network of eight VLF transmitting stations. The stations transmit in a time-multiplexed fashion on the frequencies of 10.2 KHz, 13.6 KHz, and 11.333 KHz. A brief system description is given in Appendix A, while a more thorough treatment is afforded by U.S. Coast Guard publication "Omega Navigation System User Handbook".^[1] In-depth treatment of Omega system details has been given by Pierce^[2] and Morris.^[3]

Information on the design of airborne receiving and navigating systems using the Omega signals is less accessible. Although commercial manufacturers are understandably secretive with their receiver hardware/software designs, reports on those systems whose development has been funded by government agencies should be available to the public (e.g., "Omega Navigation Set: An/ARN-99 Final Engineering Report"^[4]). An all-hardware Omega sensor processor designed by Ohio University for NASA is described in "Ohio University Omega Prototype Receiver".^[5]

An Omega navigation system for airborne use can consist of three functional units: an Omega sensor processor (OSP), navigation processor, and a cockpit display. The OSP receives the Omega signals and provides amplification and signal-to-noise ratio improvement. The OSP must provide Omega data usable by the navigation processor. This navigation processor must convert the Omega information into pilot-usable information to be displayed on the cockpit display. A simple display sufficient for general aviation could take the form of analog or digital readout of cross-track error and down-track distance.

A. Design Approach. The project effort to develop a low-cost Omega navigation system for general aviation has been greatly aided by the recent commercial availability of inexpensive microcomputers. The reasons for choosing to use a microcomputer to perform navigation processing are well known: high reliability, small size, low cost, low power consumption, and off-the-shelf availability in addition to software design flexibility. Using a microcomputer for sensor processing as well as navigation processing has the advantages noted above, but it can present some complex systems problems to the designer (particularly time sharing of the computer for several functions and prioritizing of work). Therefore, this project was undertaken to explore the feasibility of implementing an Omega sensor processor with a minimum hardware/maximum software combination.

The design approach taken was to use the previously developed Ohio University low-cost front-end receiver module [6] in conjunction with an interface module to collect a data base of real Omega ground and flight data. This data base was then used as the input for a FORTRAN language simulation analysis

of the OSP functions. After the OSP functions had been simulated and optimized in FORTRAN, they were rewritten in microcomputer language and tested in the final system configuration. The power of this approach lies in the fact that the software routines were developed not only with computer-generated data as input, but they were optimized to perform with the actual Omega data as collected with the OSP hardware.

The OSP is functionally illustrated in Figure 1, and the hardware modules and software algorithms are described in the following two sections. For the purpose of data collection, the microcomputer module of Figure 1 was replaced with a digital magnetic tape recorder. This setup was used in the laboratory for the collection of ground-based data, while the collection of flight data was accomplished with this configuration onboard Ohio University's DC-3 aircraft N4002. Complete documentation of the Omega phase data base is given in Appendix B.

Figure 1 shows that the basic system operation is as follows: the receiver front-end module receives the Omega signal from the antenna-preamplifier and provides filtering, amplification, and hard-limiting before sending Omega zero-crossings to the interface module. The microcomputer interface module measures and samples the Omega phase information at some predetermined rate and generates a microcomputer interrupt signal. The microcomputer (or data recorder) receives the digitized phase sample, and this information is used by the OSP software routines.

The OSP software routines for automatic synchronization, phase tracking, and LOP generation perform the bulk of the Omega phase processing work.

B. System Hardware. The Omega sensor processor design is intended to be a minimum hardware configuration with emphasis on low cost. The use of a general purpose microcomputer to perform as many OSP functions as possible reflects this design objective. The OSP is functionally illustrated in the block diagram of Figure 1, and a description for each of the hardware modules follows. Circuit details for each module are given in Appendix C.

1. Receiver. The antenna used for airborne operation is the aircraft's ADF sense antenna. If the aircraft is not equipped with an ADF sense wire, another high-impedance E-field antenna may be used (such as a bent dipole nav-com antenna). For ground-based operation it is desirable to mount the antenna as high above buildings, etc., as possible and in an area free of 60 Hz interference (10.2 KHz being the 170th harmonic of 60 Hz).

The signal developed across the antenna is amplified by a preamplifier which is colocated with the antenna. This colocation is necessary to overcome signal attenuation due to capacitance of the receiver module lead-in cable. The preamplifier is primarily an impedance-matching device and has two outputs. The Omega output provides a gain of 20 decibels at 10.2 KHz in a -3 dB bandwidth of several kilohertz. The phase shift is adjusted to zero degrees at 10.2 KHz. The ADF output provides a flat response of -6 dB across the band from 10 KHz to 1 MHz, and the phase shift is zero degrees across the ADF band. The preamplifier response characteristics are shown in Figure 2. The preamplifier has been described by Wright.^[7]

Accepting the signal from the preamplifier is a 10.2 KHz TRF receiver front-end module (see Figure 3). The front-end module provides additional gain,

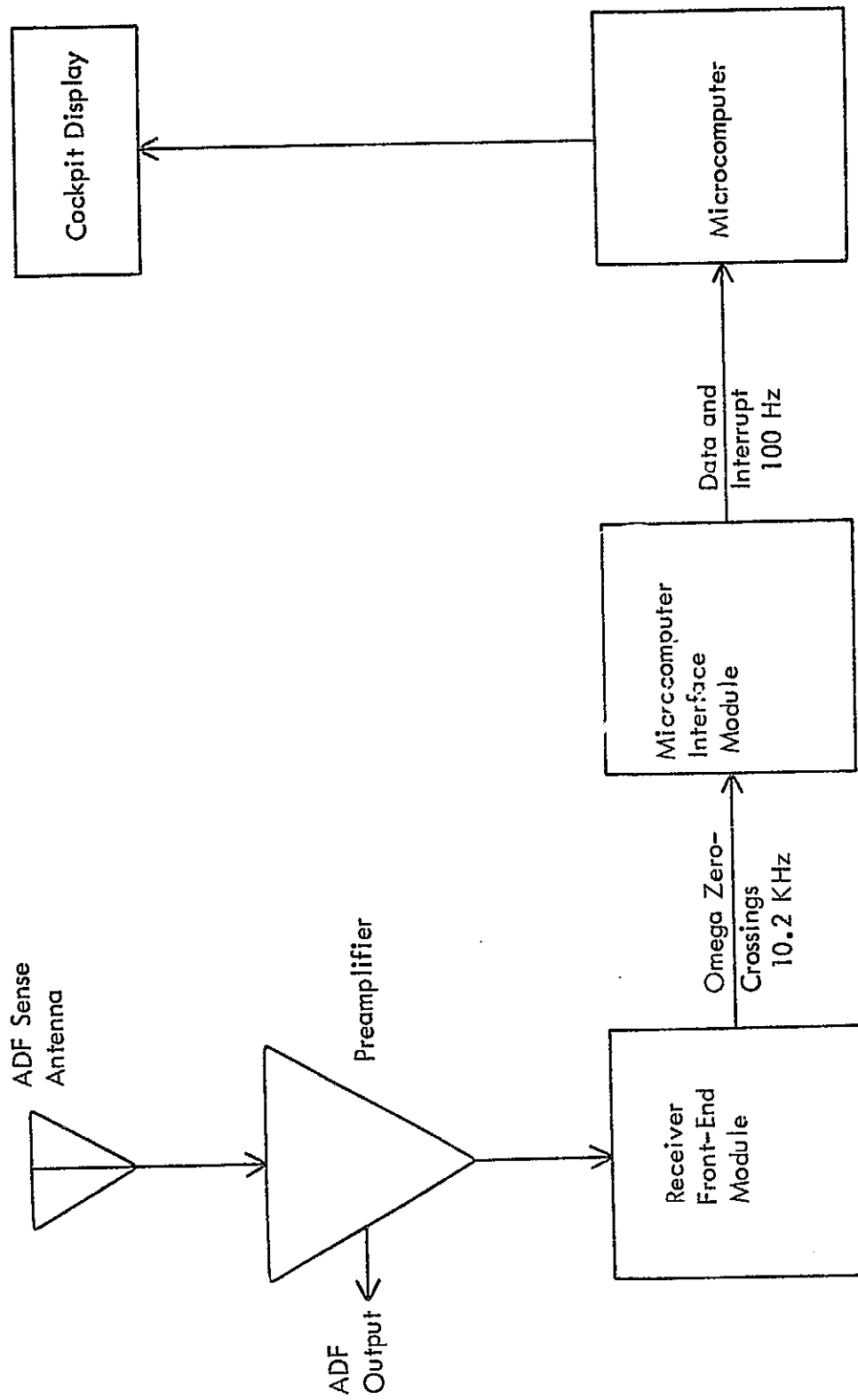


Figure 1. Summary Block Diagram - Microcomputer-Based Omega Sensor Processor.

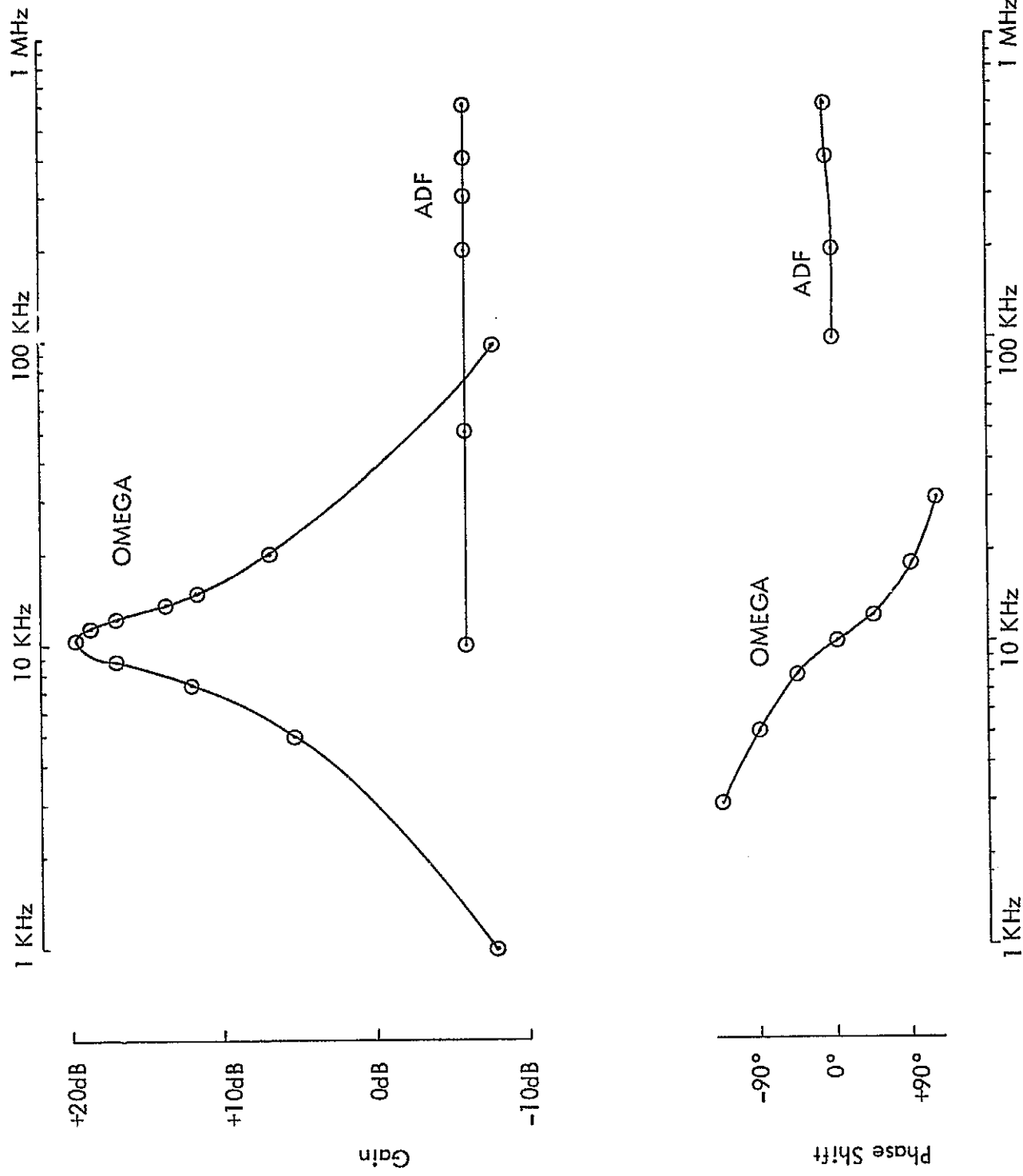


Figure 2. Preamp characteristics.

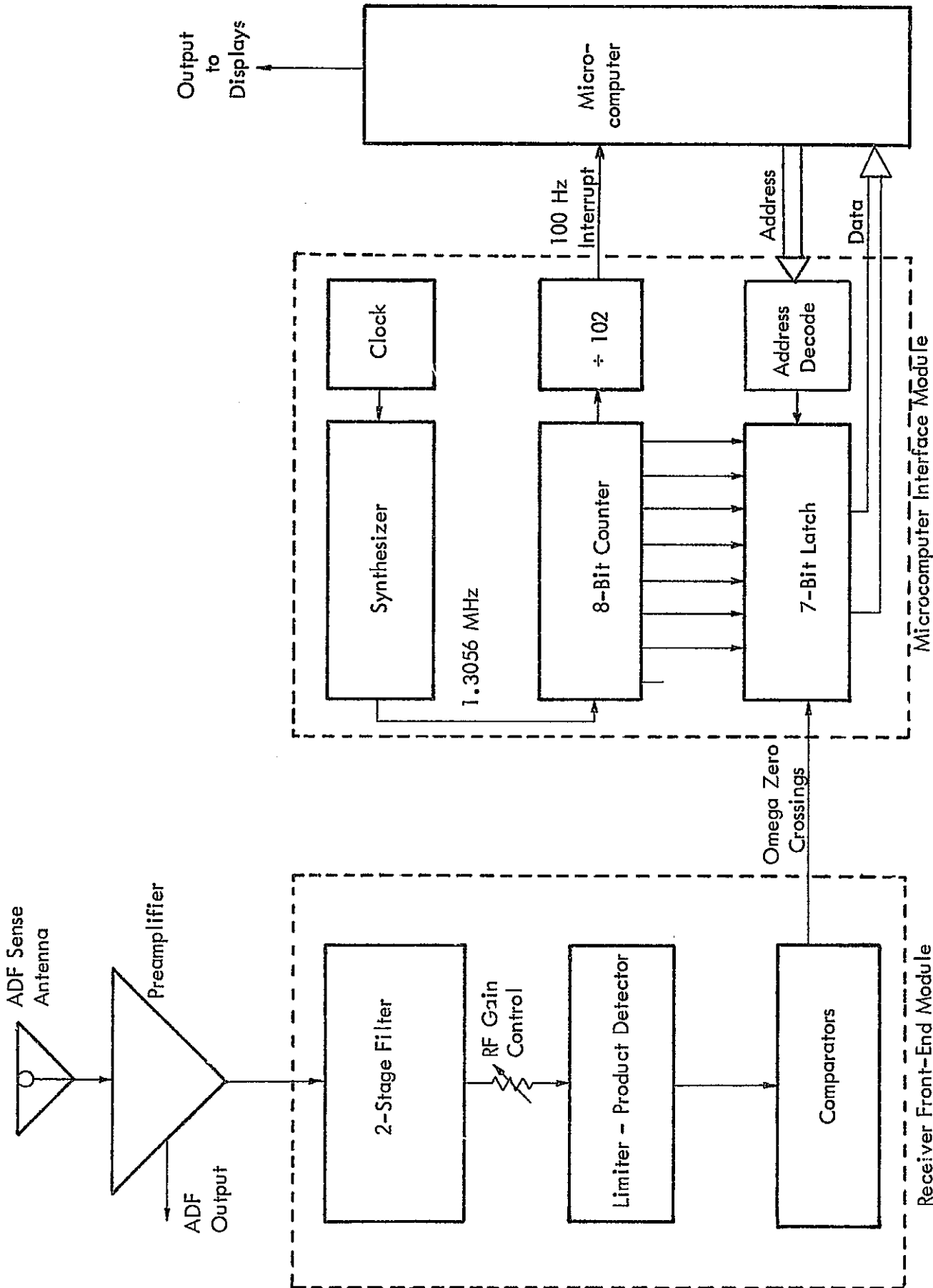
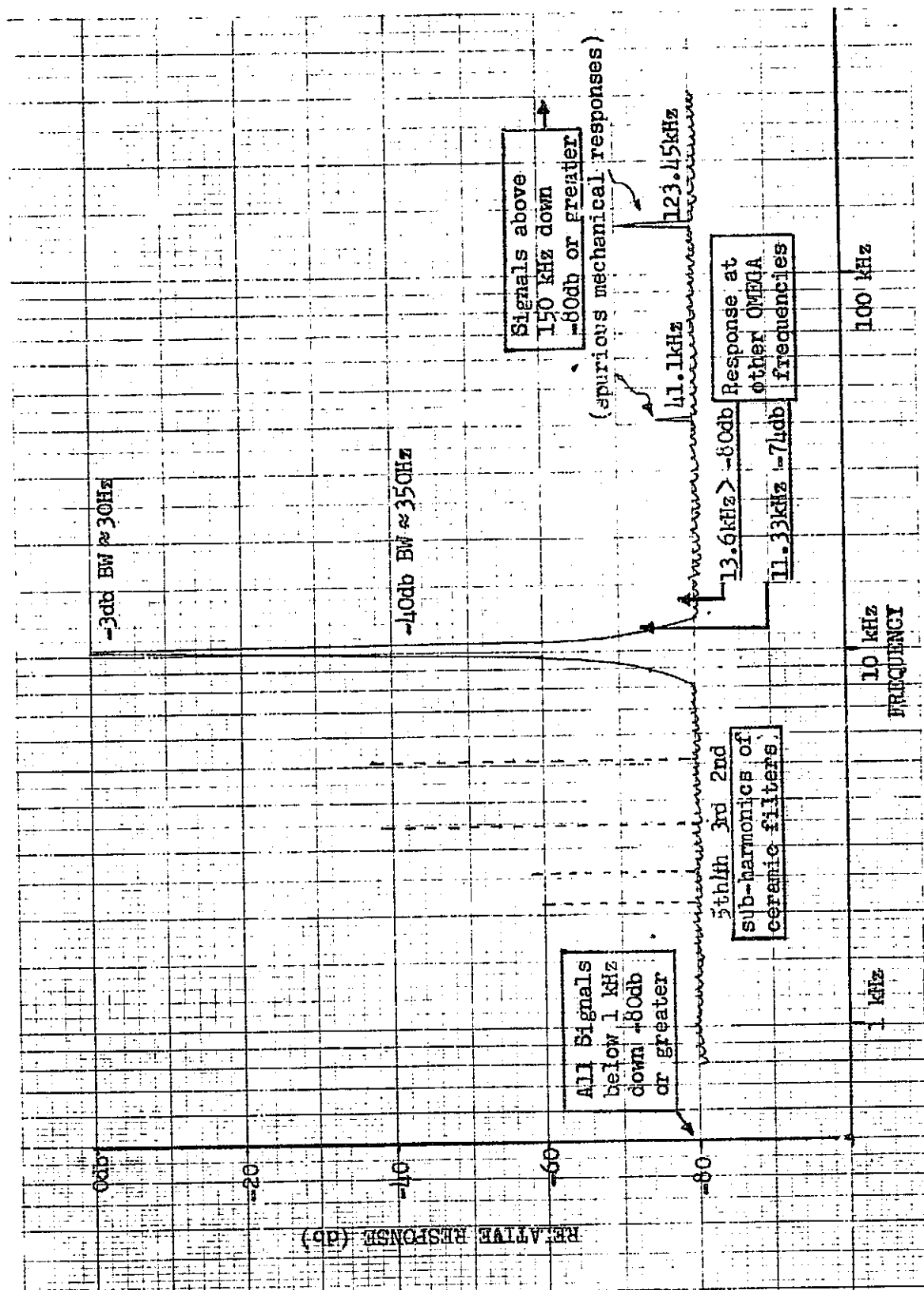


Figure 3. Front-End, Computer Interface, and Microcomputer Modules Block Diagram.

narrowband filtering, and hard-limiting (i.e. provides pulse outputs coincident with the 10.2 KHz Omega zero-crossings). The unit consists of three integrated circuit chips and two ceramic filters providing a bandwidth of 30 Hz at 10.2 KHz. The module is equipped with an RF gain control which permits gain adjustment from 160 to 200 dB. The front-end frequency response curve is shown in Figure 4. As can be seen from this curve, the response is down nearly 80 dB at the other Omega frequencies of 11.333 KHz and 13.6 KHz. The sensitivity and recommended operating range is 1 microvolt to 10,000 microvolts. The front-end module has [6] been described by Burhans.

2. Computer Interface. After the bandpass filtering and hard-limiting provided by the front-end, pulses coincident with the Omega zero-crossings are sent to the microcomputer interface module. This module is also illustrated in Figure 3. The functions of phase detection and data sampling are performed by this interface hardware, and it also generates the interrupt signals necessary for reading the phase data into the microcomputer. Besides the Omega zero-crossings, a clock signal of 1.3056 MHz is used by the microcomputer interface module. This clock signal is synthesized from a 5 MHz temperature compensated crystal oscillator. The choice of 5 MHz as the basic oscillator frequency permits operation by an external, more stable clock of this standard frequency should this be desired.

Phase detection is performed in an open loop fashion: the $2^7 \times 10.2$ KHz clock signal is input to a 7-bit reference counter, and the seven counter outputs are used as data inputs to a 7-bit latch. The Omega zero-crossings clock the latch, thus providing a relative phase measurement of Omega compared to the local clock approximately 10,200 times per second.



ORIGINAL PAGE IS
OF POOR QUALITY

Figure 4. Front-End Module Response Curve.

There are at least two considerations which suggest sampling the Omega phase measurements at a rate slower than the 10.2 KHz carrier rate:

- (1) Since an extremely precise measurement is not required, it is unnecessary to use the phase measurement of every cycle of the carrier to gain a filtered estimate of the true phase.
- (2) Using the data at the maximum available raw-data rate implies a prohibitively high interrupt rate for most micro-computers.

The choice of a particular sampling rate is also based on these considerations. In this implementation a sampling rate of 100 Hz has been chosen for the following reasons:

- (1) Sampling of the 15 Hz post-detection bandwidth phase at 100 Hz is a rate high enough to avoid severe aliasing of the sampled data spectrum, and it provides a sufficient statistical base of data points for each Omega time-slot.
- (2) 100 Hz is an acceptable microcomputer interrupt rate, and it is easily generated from the existing timing circuitry.

The microcomputer interface module derives the 100 Hz sampling frequency, samples the phase data at this rate, and sends an interrupt signal to the microcomputer. Having received the interrupt signal, the microcomputer services the interrupt request by loading the new phase data from the interface module. The inexpensive technique known as memory-mapping is used to accomplish this loading of data. The microcomputer address bus is decoded, thereby enabling

the data onto the data bus and into the microcomputer (as indicated in Figure 3).

The interface module and memory-mapping have been previously addressed by this author in references 8,9, and 10.

3. Microcomputer. The microcomputer module consists of a commercially available microcomputer system made up of a central processing unit (CPU), random access memory (RAM), peripheral interface adapter (PIA), teletypewriter interface circuitry, and teletypewriter monitor software in permanent read-only storage (ROM) as illustrated in Figure 5. The CPU utilizes a sixteen-line address bus, enabling addressing up to 65 kilobytes of memory. An eight-bit bidirectional data bus allows for data transfer among the CPU, memory, and input/output (I/O) devices.

The computer's clock is a 1 MHz adjustable RC oscillator or crystal oscillator, resulting in a machine cycle time of one microsecond. Most instructions require 2 or 3 machine cycles to execute. CPU registers include one accumulator, two index (scratch-pad) registers, a processor status register, a stack pointer, and a program counter. All of these are eight-bit registers except the program counter which is sixteen bits. Appendix C gives the microcomputer specifics, and its operation is explained in detail in the manufacturer's manuals.^[11,12]

Figure 6 shows the simple, inexpensive method for output of the microcomputer data, which is the same technique used for data input mentioned previously. An output latch is memory-mapped to a particular address by decoding the microcomputer address bus lines. The address decoder output signal is gated with the microcomputer's "write" signal. This gate's output enables a latch which stores the logic levels appearing on the data bus at that

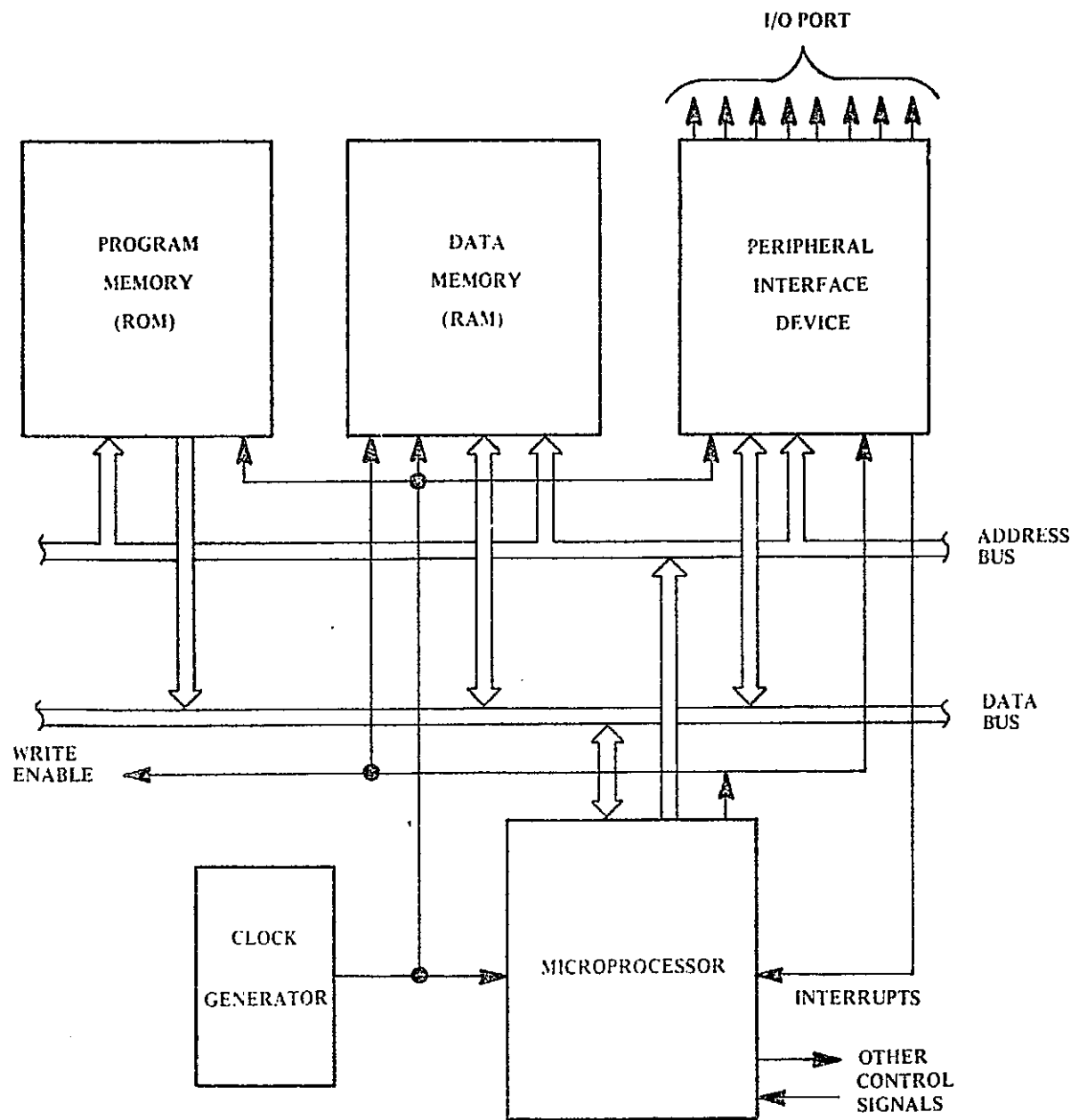


Figure 5. Microcomputer System Organization.

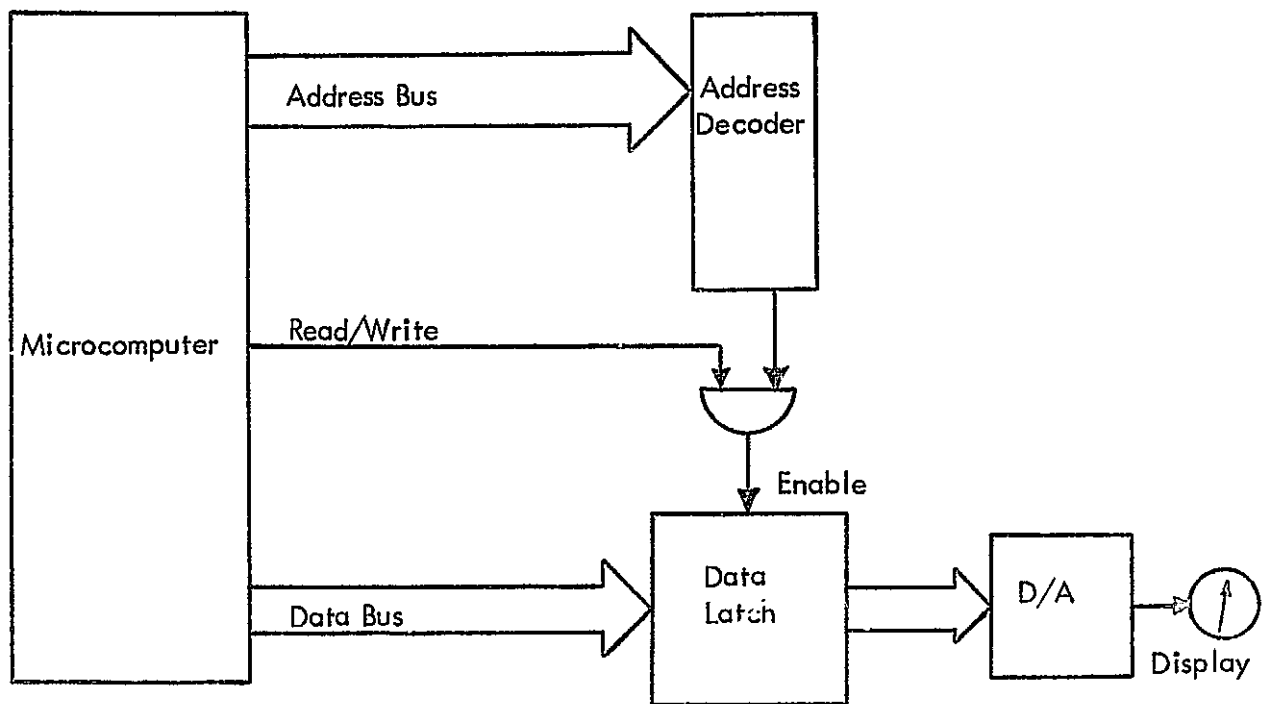


Figure 6. Memory-Mapped Data Output Port.

time. This data is then fed to a digital-to-analog (D/A) converter for display on a chart recorder or meter.

C. System Software.

1. Interrupt Servicing. When the microcomputer interface module sends an interrupt signal to the microcomputer, the interrupt service routine loads the new data into the computer. Then the software process as flowcharted in Figure 7 begins. The basic interrupt service routine serves as a system time-keeper and data "traffic cop": it loads in new data as it becomes available and hands it off to the proper data-processing subroutine. If the OSP is not in sync with the Omega transmission format, synchronization must be achieved first. Otherwise, the data is sent to the tracking loop subroutine if it is time-slot data, whereas the data is simply ignored if it is from an Omega transmission gap. A data output subroutine is executed if it is the correct time for it.

The automatic synchronization, tracking loop, and data output subroutines called by this interrupt service routine are functionally described in the subsequent text material, while the FORTRAN and microcomputer language programs are listed and described in Appendices E and F. The interrupt service routine requires 150 bytes of memory and performs its time and data management in a few tens of microseconds following each interrupt request signal.

2. Automatic Synchronization. The Omega system consists of eight stations transmitting on three VLF channels in a fixed, time-multiplexed format. As described in Appendix A, a unique pattern is formed by the scheduled length (in time) of each station's transmission which repeats every ten seconds. Thus, to use the phase measurements supplied by the microcomputer interface module,

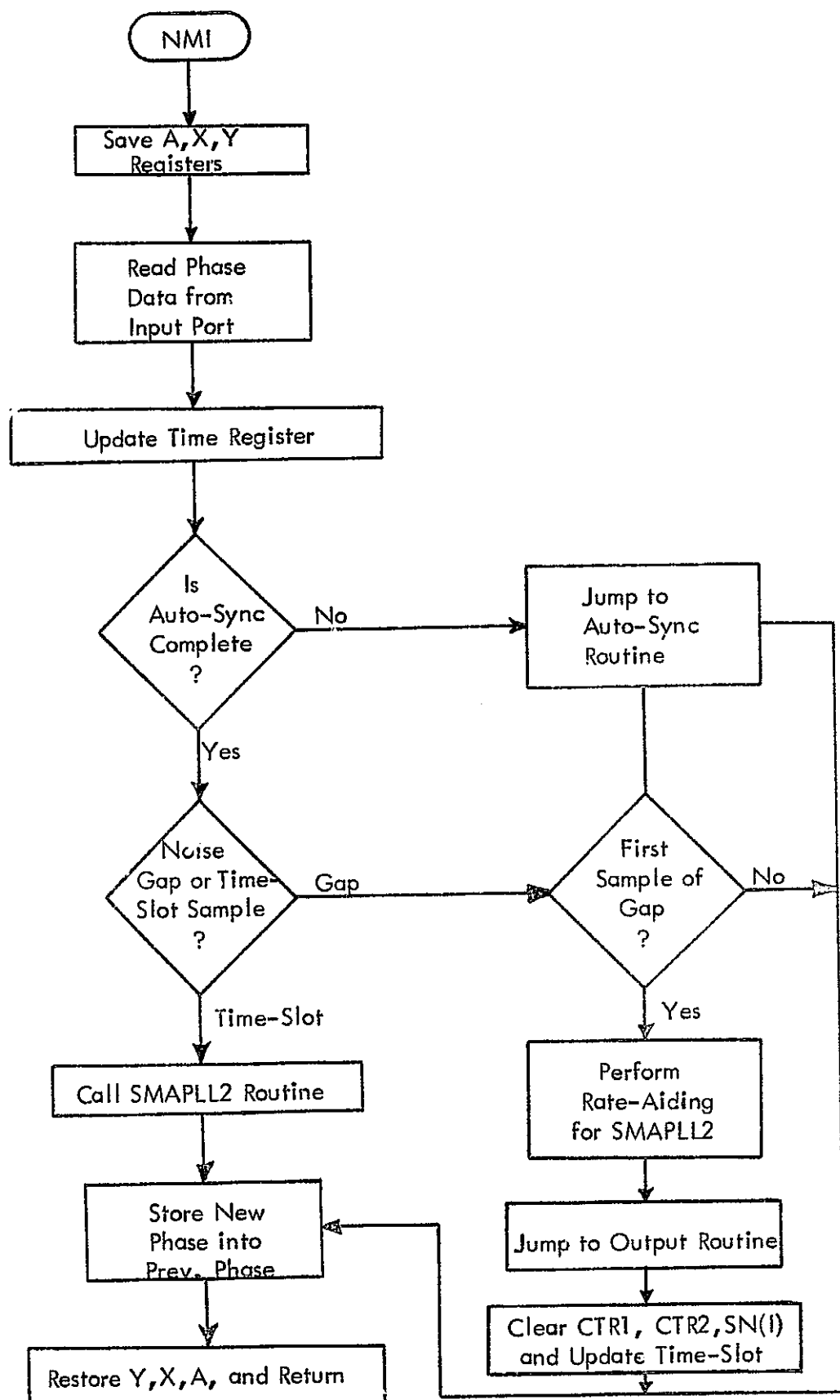


Figure 7. Interrupt Service Routine Flow Chart.

some means must be provided for synchronizing the OSP timing with the Omega transmission pattern. Only after the OSP is "in sync" can the phase of each station's signal be followed by tracking filters to give position-fixing information.

It should be pointed out that precision sync (better than plus or minus 100 msec) is unnecessary. A .2 second gap between each transmission burst allows for propagation delays from transmitter to receiver and for signal build-up on the transmitting antenna and through the narrowband receiver module without signal overlap into another station's time-slot. Therefore, sync within plus or minus 100 msec insures that only one station will be received during each of the eight time-slots.

A description of the automatic synchronization procedure simulated in FORTRAN and implemented in the OSP microcomputer follows, and a logic flow diagram appears in Figure 8. Although the routine is described here in terms of a single-frequency OSP, the technique is applicable to multiple-frequency systems as well. Performing the routine on multiple channels simultaneously would give the OSP a redundancy check. By averaging the results obtained for all channels a best estimate of the true sync point could be obtained.

To establish sync a pattern of station transmission lengths is derived from the received data, and the entire frame of data is shifted until the received pattern coincides with the unique transmission pattern stored in the computer. The received pattern of transmission lengths can be established by determining the amount of coherence between consecutive 10 msec phase samples. A high level of coherence indicates the presence of a strong signal, while the lack of phase coherence (i.e. phase jitter) is indicative of a weak signal or noise. The absolute value of phase

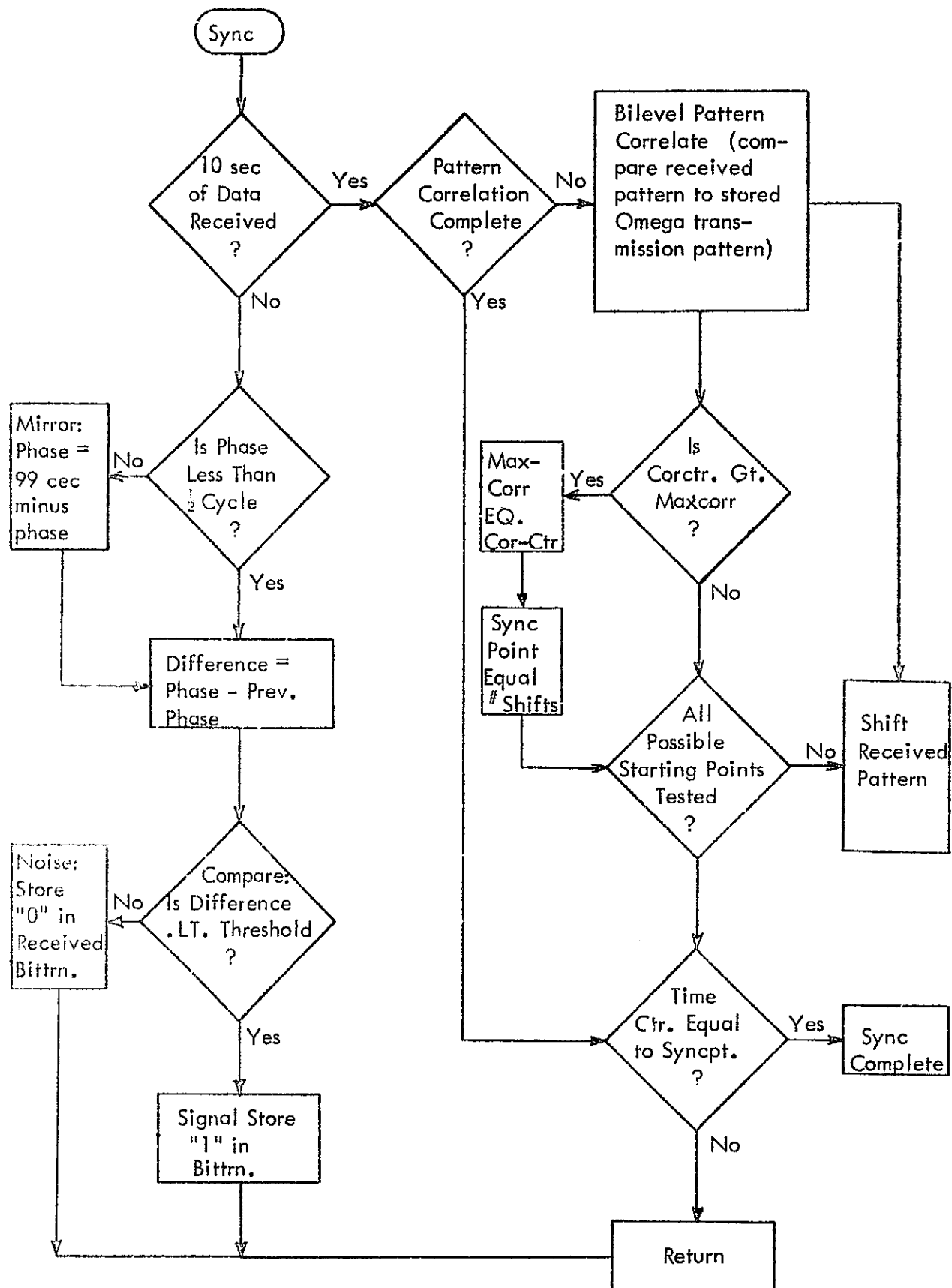


Figure 8. Automatic Synchronization Routine Flow Chart.

measurements is meaningless during the sync process; only the phase coherence from sample to sample is useful in determining the received transmission pattern (i.e. in determining whether each sample is signal or noise).

An Omega phase measurement is supplied by the microcomputer interface module every 10 msec (100 Hz sampling rate). Starting at a random point in time (power on time) and taking data for ten seconds (one complete Omega frame) yields 1000 phase samples. This is all the information needed to accomplish sync. The Omega signal is contaminated with noise, causing a series of measurements to result in a dispersion of phase points rather than a constant value. The units of centicycles (cec) are commonly used in Omega Iargon. One cec is 1/100 of an Omega carrier cycle; at 10.2 KHz a cycle is about 16 nautical miles long, making one cec equal to about .16 miles. If the phase of the received signal with respect to the OSP clock is near the 0 or 99 cec measurement extremes (near the edge of a cycle), the measured value may "bobble" between these extremes. To remove this bobble each data point above 49 cec is "mirrored" about the 50% full-scale value (mirrored about 49 cec). Points at $x = 99$ cec are thus reflected to $99-x = 0$ cec. Since only the phase coherence is of interest and not the absolute value of phase, the mirroring process merely puts the data into a better form from which coherence can be determined.

A simple routine yielding a measure of the point-to-point coherence is to take the difference of each two successive phase points. That is, subtracting each measurement from the previous yields 1000 difference values for the 10 second data frame. Each difference is inversely proportional to the coherence between the two phase samples.

By comparing each difference value to a predetermined "threshold constant", a decision can be made as to whether signal or noise exists in each 10 msec sample slot. However, it is desirable to first smooth or average the difference values over several sample slots before comparison to the threshold constant is made. If the smoothed difference is less than the threshold, a "1" is stored for the sample slot; whereas, if the smoothed difference is greater than the threshold, a "0" is stored for the slot (low difference \longrightarrow high coherence \longrightarrow signal present). After all 1000 comparisons have been performed, a pattern of 1000 1's and 0's represents the signal and noise sample slots, respectively. The "high-low" or "on-off" pattern created by the 1000 binites resembles the Omega transmission format shown in Appendix A, the amount of resemblance being proportional to each station's signal-to-noise ratio (SNR).

Note that the 1000 bits can be stored in 125 eight-bit bytes of memory (an amount of storage not prohibitive for simple microcomputer systems). Also bear in mind that the entire microcomputer will be dedicated to the auto-sync routine during the sync process, since no Omega navigation information is available until sync is completed.

The 1000 sample bits are next compared to the stored Omega pattern in a bilevel correlation process. Use is made of the time-slot and transmission gap information; whenever the received slot binit is equal to the stored slot binit, a correlation counter is incremented by one. After all 1000 slots have been compared, the stored pattern is shifted by one slot and the correlation of points sequence is repeated. This shift and correlate iteration is continued until all 1000 possible shifted patterns have been tested. The number of shifts necessary

to obtain the highest bilevel correlation value is used to obtain the starting point for the "A" time-slot (assuming the microcomputer's interrupt service routine has been keeping time (counting 1000 Hz interrupts) in a modulo 10-second fashion since the auto-sync process began).

Having found the sync-point in the simulation data, Figure 9 shows the original 1000 byte record of phase data plotted ten points per line. The higher the SNR of the station being received in each time-slot, the less dispersion there is in the phase points plotted.

The OSP operator's a priori knowledge of which stations are on the air and which ones will be well received in his particular geographic area can be incorporated into the creation of the unique transmission pattern stored in the computer. This facilitates the bilevel correlation process, resulting in a more accurate sync point.

Although it was not used in this version of the OSP, for an additional confidence measure the entire sync process can be performed several times and a best estimate of the sync point computed. If multiple frequency channels are available, the process can be performed on each channel and the sync points averaged (or a sync point can be considered acceptable only if it results on two of three channels, etc.). Another possibility is to save the second highest correlation value as well as the highest, and consider the sync point acceptable only if the highest value is better than the second highest by some predetermined amount.

In summary, the technique presented requires very simple microcomputer instructions (compare, subtract, shift), uses very little scratch-pad RAM storage

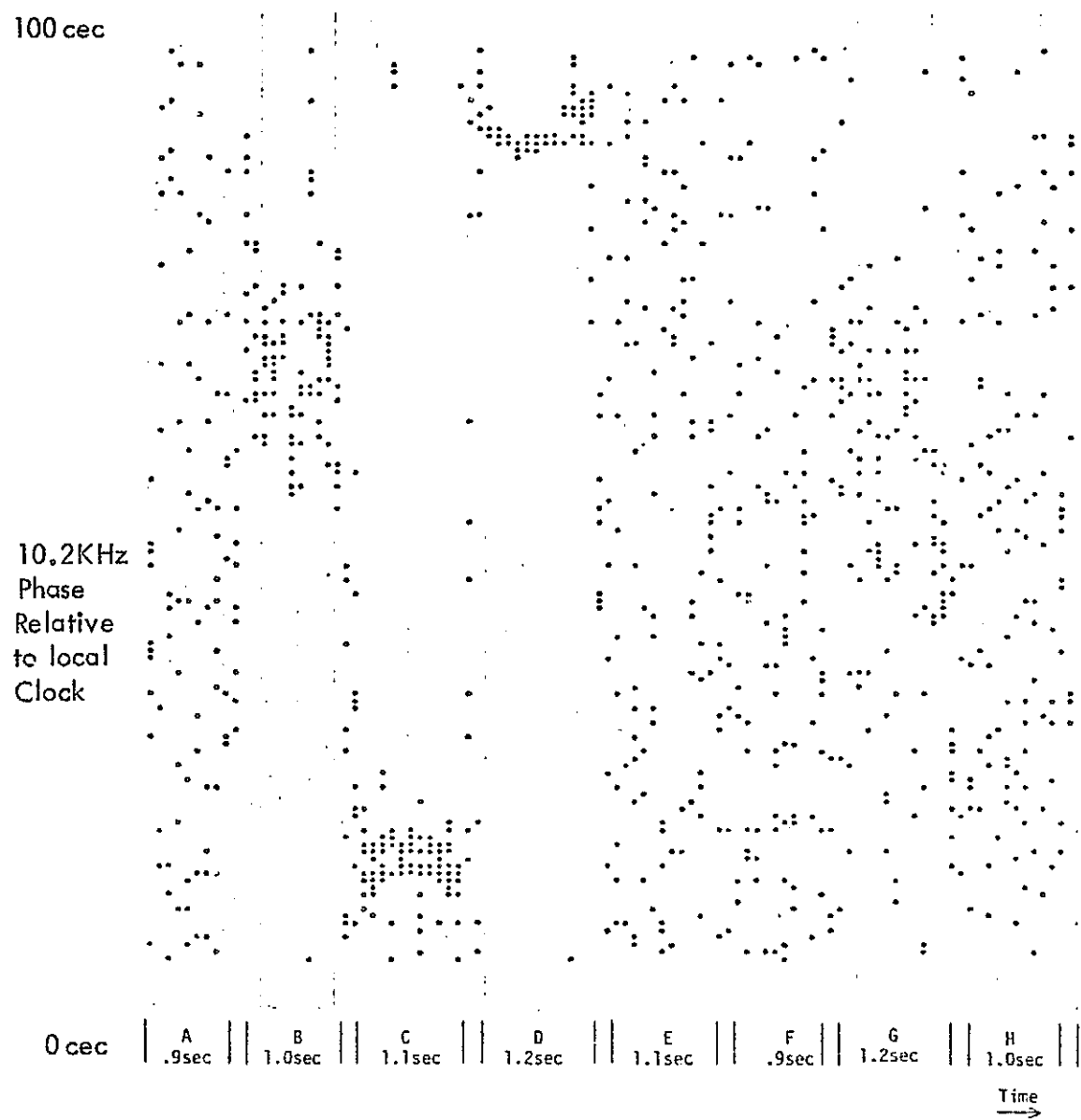


Figure 9. Computer Plot of Raw Omega Data. This is the 30 Hz bandwidth phase plotted 10 points per line.

(125 bytes), and usually accomplishes sync in about 100 seconds (depending on the redundancy constraints imposed). The technique has demonstrated acceptable accuracy (within \pm 100 msec of true sync) and the microcomputer program is about 300 bytes long.

3. PLL Phase Tracking. After the OSP is in sync with the Omega transmissions, the phase of each station's signal can be tracked using correlation techniques, and SNR improvement can be made. The correlation detection structure known as the memory-aided phase locked loop (MAPLL) has been found to be a successful tracking filter for the Omega signals.^[13] Since previous experience with hardware versions of the MAPLL had revealed its usefulness for Omega tracking, it was desirable to duplicate this configuration in software.

The first-order version of the software memory-aided phase locked loop (SMAPLL1) is functionally illustrated in Figure 10. The loop operation can be generally explained as follows: the loop's bilevel quantizing phase detector compares the incoming phase measurement with a filtered loop control word (LCW) at the 100 Hz sampling rate. The output of the phase detector is an increment command if the incoming phase is ahead of the LCW; it is a decrement command if the incoming phase lags behind the LCW. The increment/decrement commands are filtered in a bidirectional loop counter. Loop filtering is achieved by requiring the loop counter to receive several correlated signals (counts in the same direction) before it affects the LCW. When the loop counter has received sufficient correlated up/down commands, it outputs an increment/decrement command to the LCW register. This new LCW is in turn compared to the new incoming phase measurements in the phase detector.

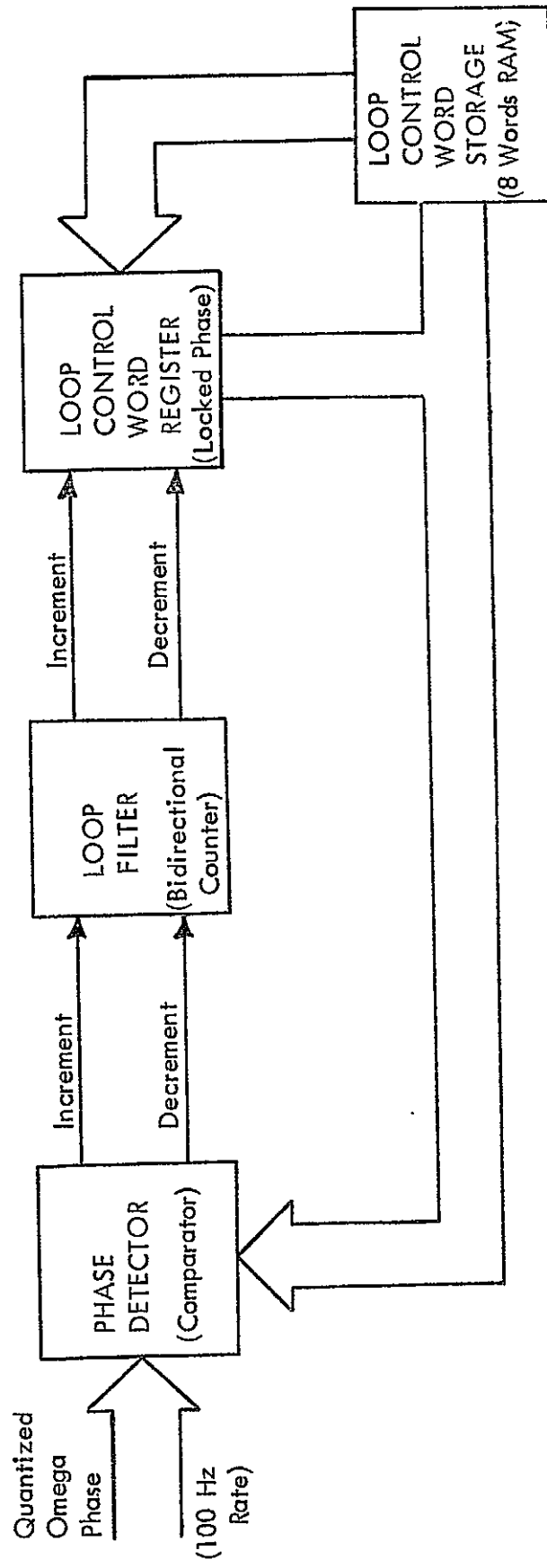


Figure 10. First-Order Software Memory-Aided Phase Locked Loop (SMAPLL1) Block Diagram.

The memory-aiding feature allows a single phase locked loop (PLL) routine to be utilized to track all eight Omega stations' phase. At the end of a current time-slot the LCW is stored in a memory location, and the LCW for the next time-slot is retrieved from memory and used to track the new time-slot's phase.

Atmospheric noise in the VLF-Omega frequency range is known to be caused primarily by lightning. [14] The noise is made up of both gaussian and impulsive noise. The bilevel quantizing phase detector is thought to discriminate against the impulsive noise better than a linear detector [13] (in addition to being simpler to implement). Omega signal levels are such that the PLL must be able to track signals at a -20 dB SNR in the 30 Hz predetection bandwidth. The loop filter (bidirectional counter) provides a narrow post-detection bandwidth of a fraction of a Hertz to enable tracking of these low-level signals. However, the increment/decrement type of phase detector and narrowband loop filter severely limit the tracking speed of the loop. Increased loop filtering gives SNR improvement but decreases the maximum tracking speed of the loop, and vice-versa.

The PLL must be capable of tracking the motion of a general aviation aircraft (nominally 200 knots velocity). The frequency offset of the receiver's local oscillator (TCXO) appears as a velocity offset in phase, thereby adding a few more tens of knots to be tracked by the PLL. This speed requirement coupled with the narrowband filtering restraint dictates the need for a higher order tracking loop (i.e. one that can track a constant velocity offset without sacrificing the needed integration). Therefore, the second-order memory-aided PLL (SMAPLL2) structure illustrated in Figure 11 has been implemented.

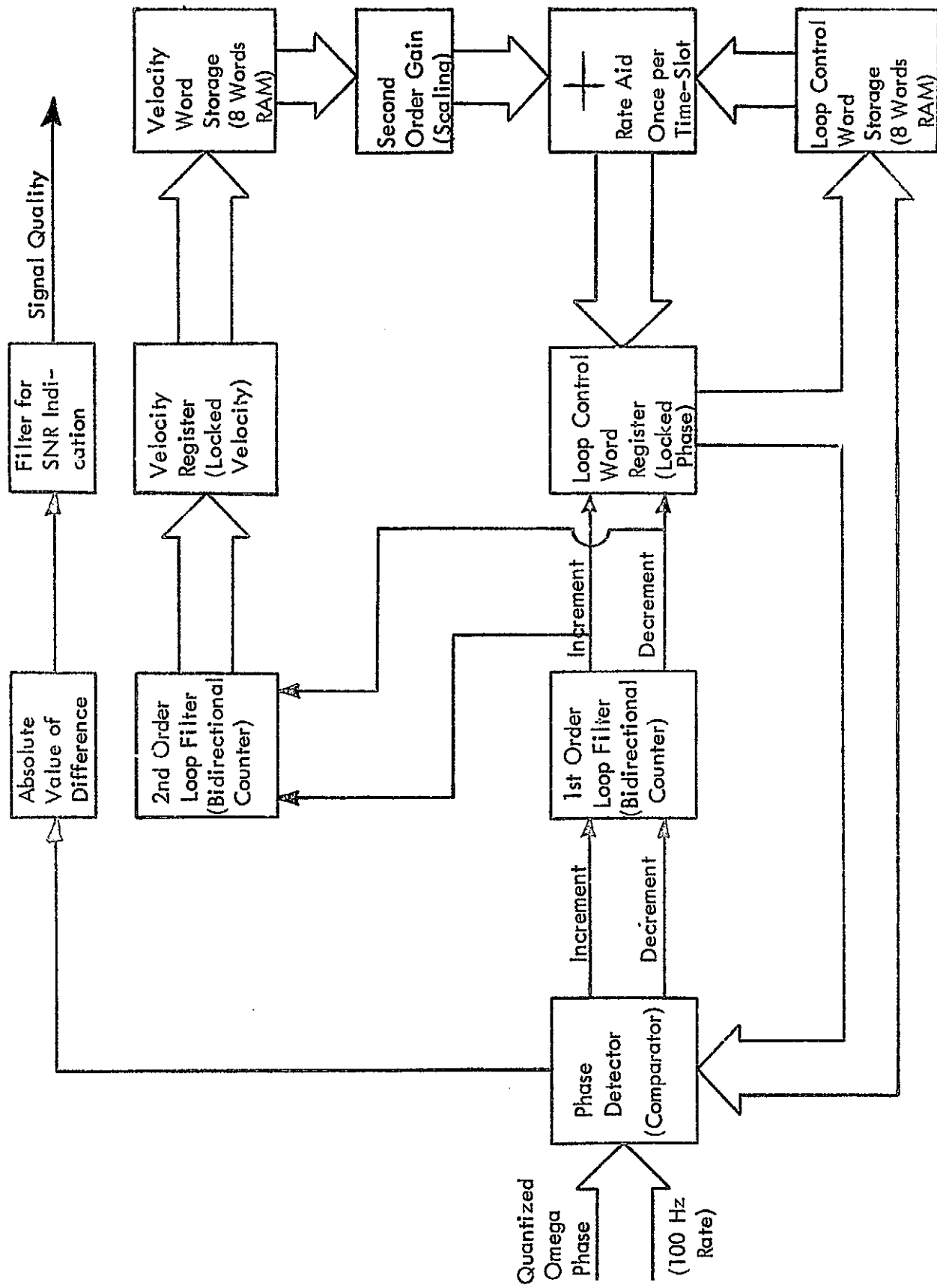


Figure 11. Second-Order Software Memory-Aided Phase Locked Loop (S\APLL2) Block Diagram.

The operation of this PLL is similar to that of the first order loop, but a second-order loop counter and a velocity register have been added. [15] When the first-order loop counter increments or decrements the LCW, it also increments or decrements the second-order loop counter. At the end of the time-slot the contents of the second-order loop counter are added to the velocity register. The velocity register contents are then scaled by a second-order gain factor and used to rate-aid the LCW before its use in the next time-slot measurement 10 seconds later. It should be noted that the SMAPLL2 exhibits first-order loop characteristics during each time-slot, with second-order characteristics (rate-aiding) only between time-slots.

Additionally, a SNR measurement is derived from the phase detector output. As shown in Figure 11, the phase detector compares the incoming phase measurement with the LCW. This is accomplished by differencing the two numbers. This difference is a measure of how "tightly" the loop is locked, which is in turn a function of the received SNR. The absolute (unsigned) values of these differences are accumulated over all measurements in a time-slot. For a high SNR case the accumulation will be small (loop tightly locked), while for a low SNR case the sum will be large.

The SMAPLL2 parameters of first order bandwidth and second order gain have been optimized via FORTRAN simulation as documented in Appendix E. Worst-case conditions of 200 knot aircraft velocity and 100 knot TCXO clock drift in a radial direction to/from Omega stations, as well as a SNR range of -20 dB to +20 dB in the 30 Hz predetection bandwidth have been taken into account in the optimization procedure. A first order filter of 16 counts (about

.05 Hz bandwidth) combined with a second order gain of .25 have been chosen to yield the best combination of transient and steady-state responses.

Figure 12 shows SMAPLL2 transient (lock-up) response to 180 degree step and 300 knot ramp inputs. The input SNR for this Figure is 0 dB, and it can be seen that the loop requires about two and one half minutes to lock to this low-level signal. The loop requires longer times to lock to lower SNR signals and shorter times for high SNR inputs (e.g. about 15 minutes for -15 dB and 2 minutes for +10 dB SNR).

Figure 13 shows the steady-state response of the SMAPLL2 to the desired range of SNR's of step inputs. Figure 14 gives the same data for the 300 knot ramp inputs. The vertical axis is the standard deviation of the SMAPLL2 output estimates of phase in units of cec. Both of these Figures show that the loop's steady-state error will be less than plus or minus 3 cec 62.5% of the time whether airborne at 300 knots or on the ground motionless.

A further demonstration of the improvement in signal variance provided by the SMAPLL2 is provided by plots of the histograms for signal plus noise input phase and the loop output estimates of phase. Figure 15 gives the input histogram for a -10 dB SNR case and Figure 16 gives the loop's output histogram. The improvement made in signal variance by the SMAPLL2 is obvious from this Figure, and is directly proportional to the SNR improvement through the loop.

All SMAPLL2 parameters have been optimized for tracking in the noisy -20 dB SNR case and with the 300-knot velocity constraint imposed. Performance is considerably enhanced by higher SNR's and slower velocities. The SMAPLL2 routine requires about 150 bytes of microcomputer memory and takes about 200

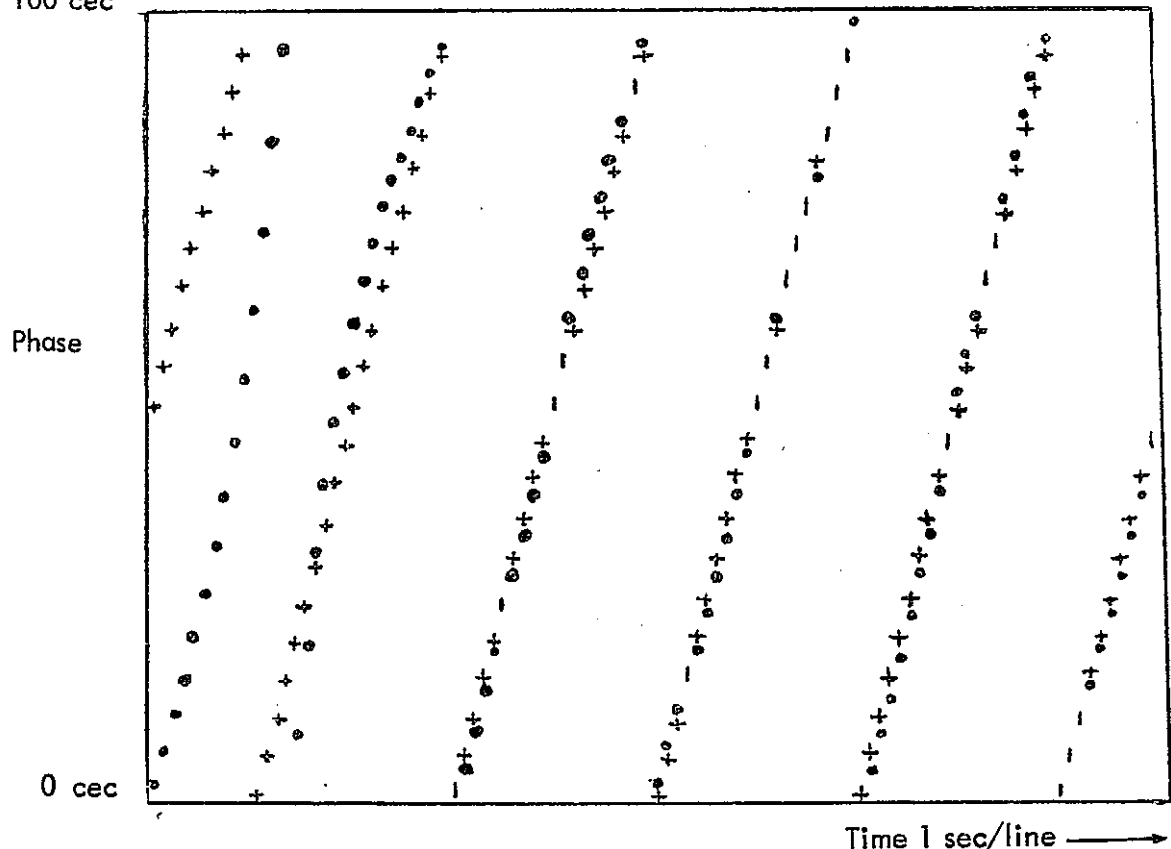
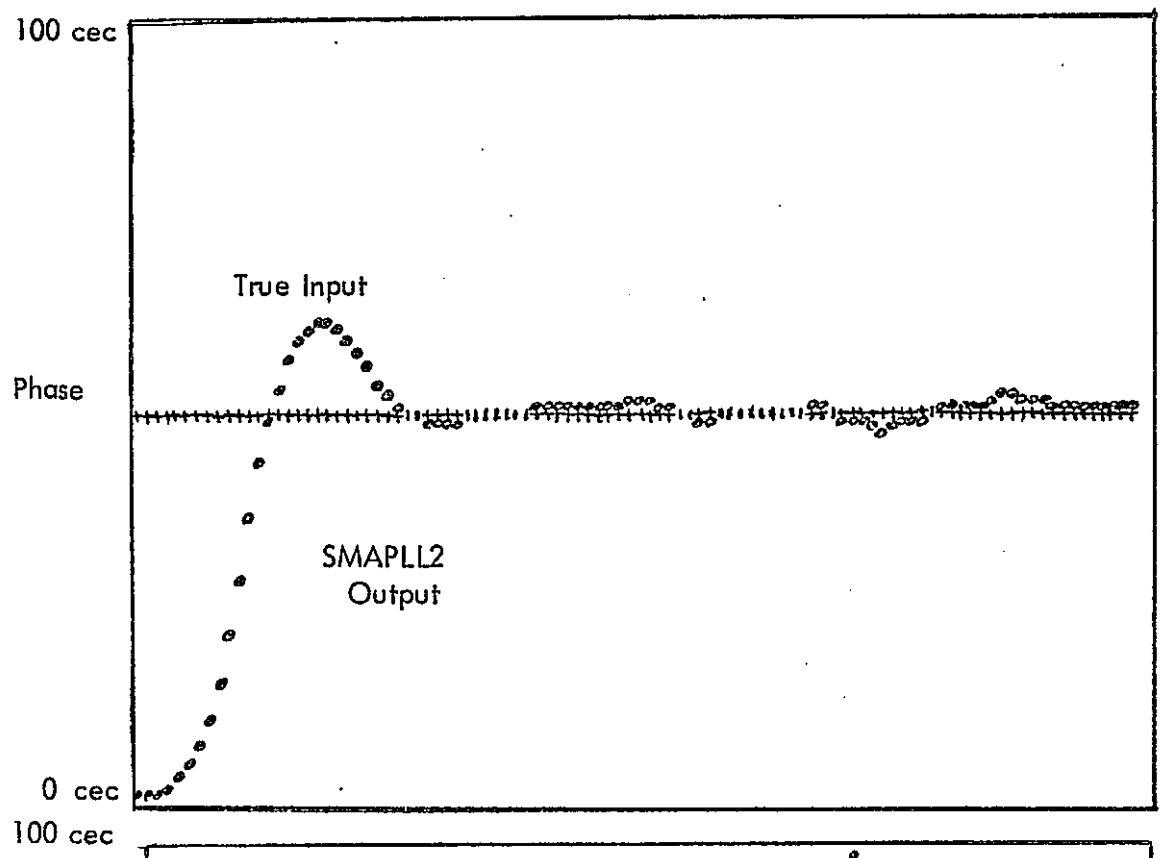


Figure 12. SMAPLL2 Transient (Lock-Up Mode) Response to 180° Step (Top) and 300-Knot Ramp Inputs (Bottom) of 0 dB SNR.

ORIGINAL PAGE IS
OF POOR QUALITY

-31-

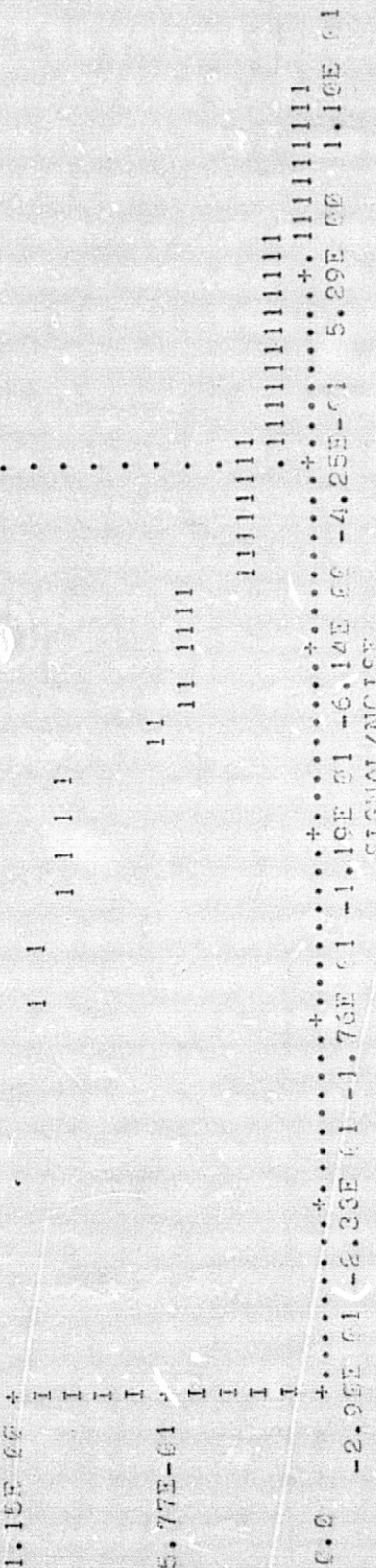


Figure 13. Steady-State Response of SMAPLL2 to Zero Velocity Inputs: Standard deviation of loop outputs in cec vs. range of inputs SNR's in dB.

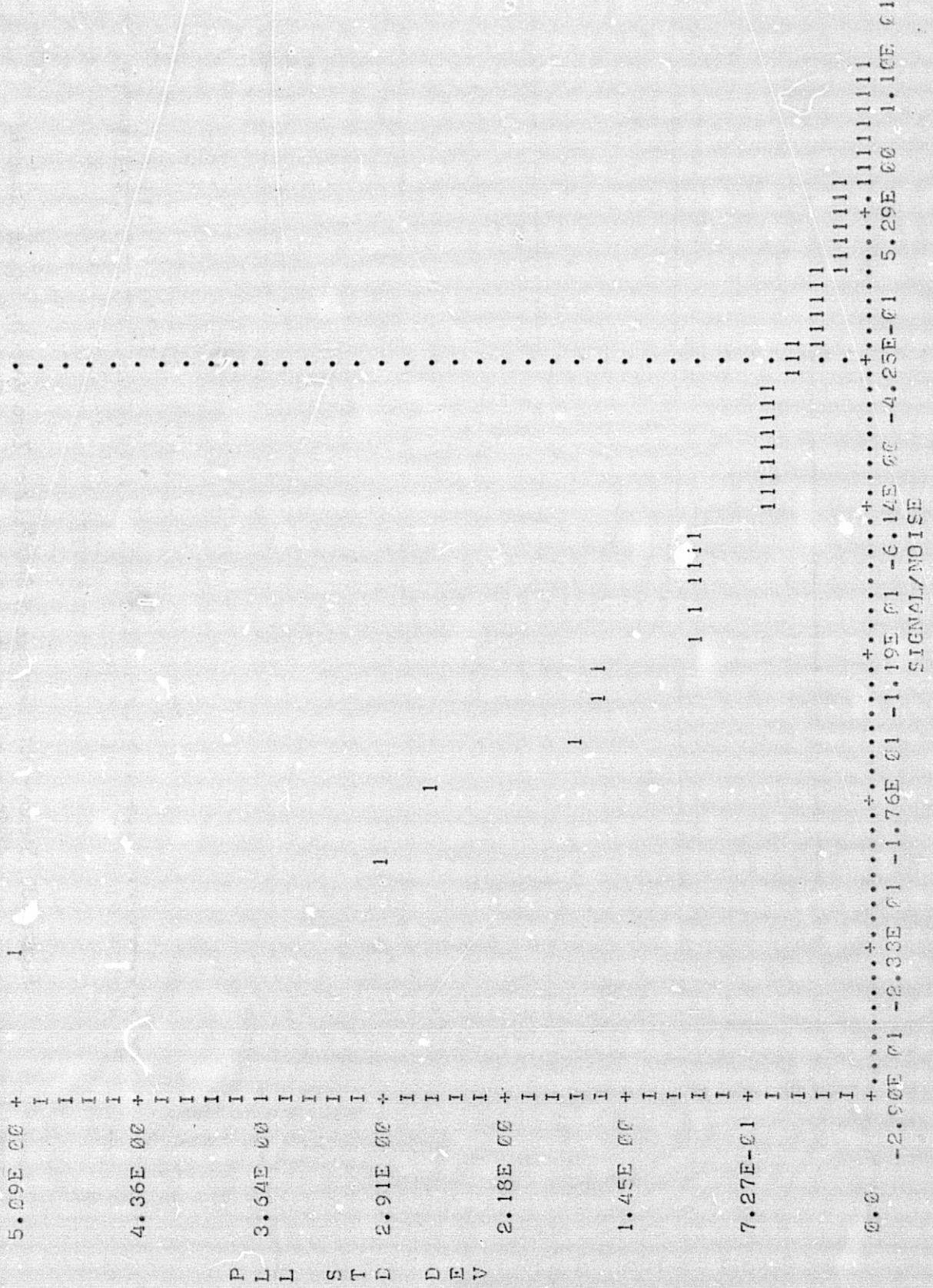


Figure 14. Steady-State Response of SIMPLL2 to 300-Knot Ramp Inputs: Standard deviation of loop outputs in cec vs. range of input SNR's.

MEAN = 0.26020
 VARIANCE = 53E-02
 SNR = -9.91182

$\varrho \cdot \varrho$ -5.60E-01 -3.57E-01 -2.14E-01 -7.14E-02 7.14E-02 2.14E-01 3.57E-01 5.60E-01
 NOISE PHASE

3.96E-02 +
 3.39E-02 +
 H I 2.83E-02 +
 S T O G R 2.26E-02 +
 A M

ORIGINAL PAGE IS
OF POOR QUALITY

Figure 15. Normalized Histogram of -10 dB Input Signal-Plus-Noise.

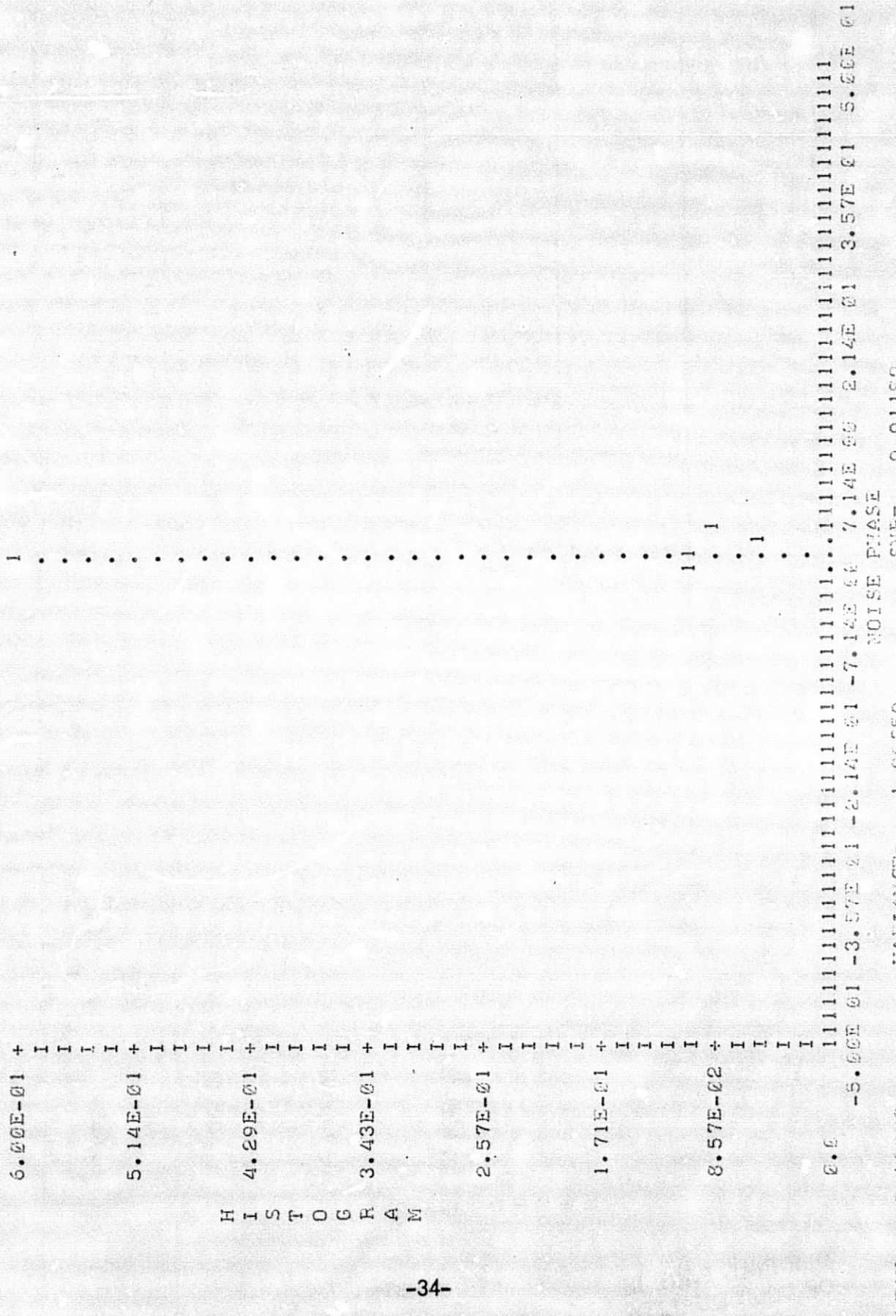


Figure 16. Normalized Histogram of SMAPLL2 Output Estimates of Phase for -10 dB Input SNR.

microseconds to execute. Appendix E gives the details of the simulation and additional plots describing the loop's performance. Appendix F gives the microcomputer program listing for the SMAPLL2.

In addition to the interrupt service routine, auto-sync subroutine, and SMAPLL2 subroutine already described (and the data output subroutine to be described in the next chapter), the OSP employs a "main", or idling, routine. At system turn-on time this routine initializes all necessary memory locations to their proper contents; it then simply idles (wasting time) until it is interrupted by the microcomputer interface module with new Omega data. This main routine would take the form of an airborne navigation program in a full-blown ONS. In its current form it requires 100 bytes of memory to initialize OSP parameters and takes about 100 microseconds to execute.

By accumulating the CPU time and program memory requirements for all the OSP algorithms presented, it is possible to estimate the CPU time and program storage currently unused (that which is available for future navigation processing algorithms). After system initialization and automatic synchronization during the first 100 seconds after turn-on, the SMAPLL2 requires about 200 microseconds after each Omega interrupt every 10 milliseconds. This leaves about 98% of the available CPU time currently unused (i.e. available for navigation processing). All OSP algorithms, including the Data Output Routine described in the next chapter, require a total of about 1000 bytes (1K) of program memory. Therefore, about 3K of the available storage is currently unused and is available for the navigation algorithms.

III. OSP OUTPUTS AND USES

A. Output Data. The Omega sensor processor receives the Omega signal off-the-air, performs automatic synchronization to the Omega transmission format, and tracks the phase of each receivable station. The data which the OSP makes available is the relative phase of each transmitting station and an indication of the relative signal strength of each station's signal with respect to the atmospheric noise level. This is the data needed by a navigation processor to derive the receiver's position.

The microcomputer-based OSP makes maximum use of the inherent design flexibility afforded by the software by utilizing a data output subroutine. The output routine is flowcharted in Figure 17, and the actual program is listed in Appendix F. The routine is built around three user-inserted code words, as illustrated in Figure 18. (Appendix D explains the insertion of data into the microcomputer). One bit of the "option" code word selects a single output or two outputs to be time multiplexed to the output latch (this latch is described in the hardware section). Another bit selects output of the phase or signal quality of the channels chosen by the second and third code words. The last six bits of the option code word dictate the multiplex time in tens of seconds to be spent on the output of each channel's data (if the multiplex option was selected by bit one). The second and third code words select the stations for which data is to be displayed. Each code word is treated as two four-bit station identifiers, and each station identifier is a number between zero and eight (corresponding to zero and the Omega stations A through H).

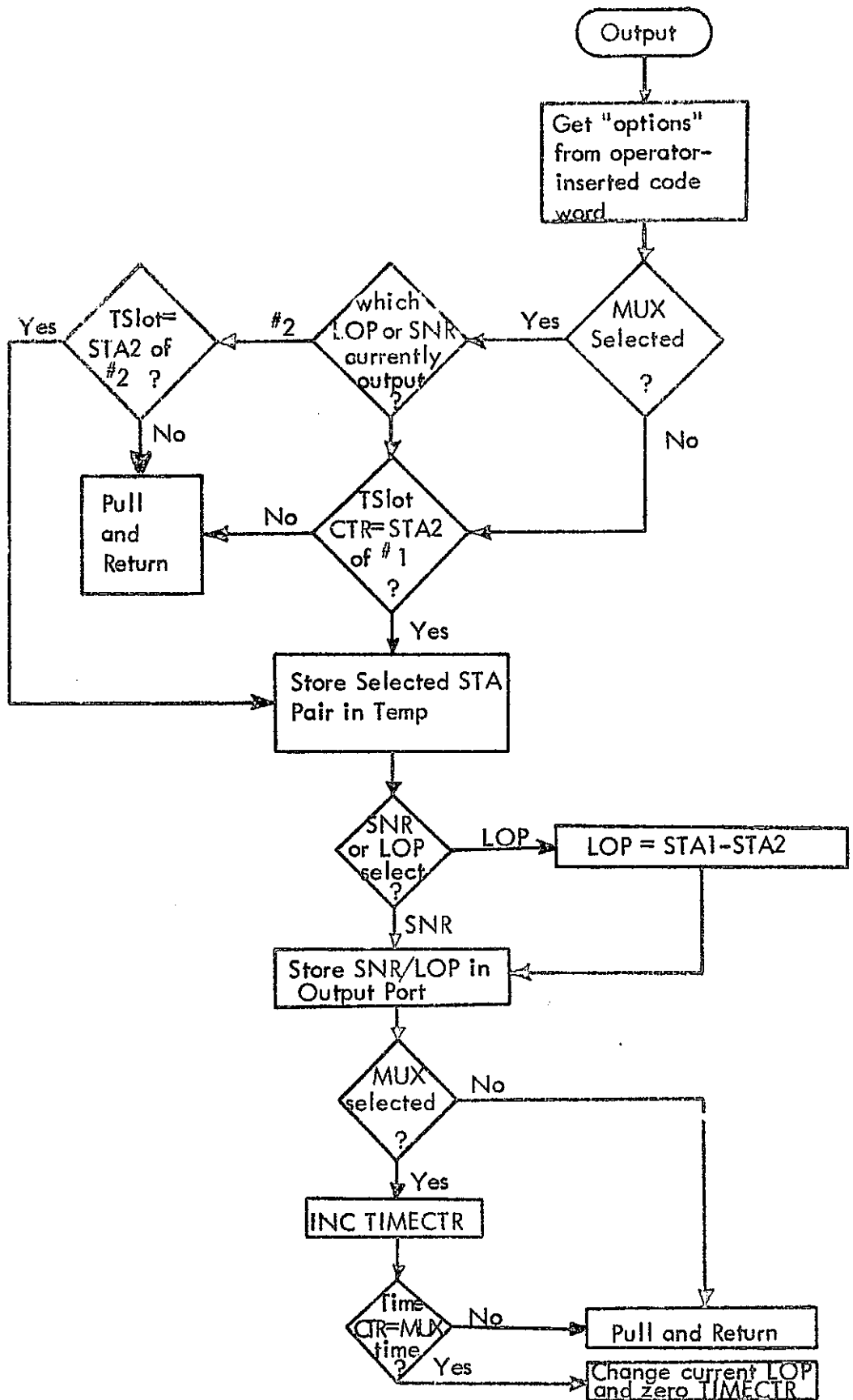
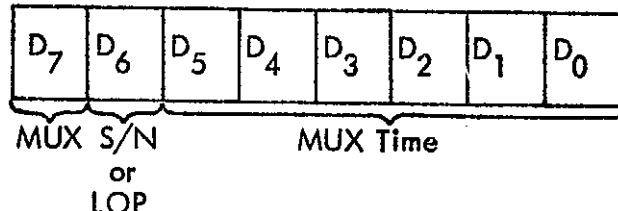


Figure 17. Data Output Routine Flow Chart.

Option
Code Word

Address
0000



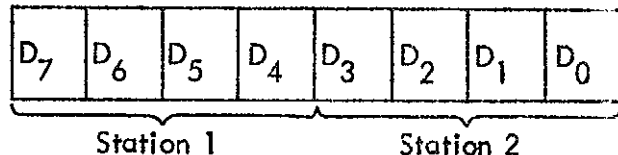
MUX (Bit D₇) is set = 1 for multiplexing two outputs. (D₇ = 0 will result in LOP(1) or S/N(1) output only.)

S/N or LOP (Bit D₆) is set = 1 for LOP output (D₆ = 0 will result in S/N output).

MUX Time (Bits D₅ - D₀) is set to a binary number corresponding to the number of 10 second intervals to be spent outputting each LOP or S/N before switching to other LOP or S/N.

LOP and S/N
Code Words

Addresses
0001 and 0002



Station 1 (Bits D₇ - D₄) is a binary number between 0 and 8. The number 0 selects clock drift only; while 1-8 select Omega stations A-H.

LOP is generated by taking phase of station 1 - station 2.

If S/N is selected by making D₆ bit of option code word = 0, then the S/N of station 2 is output.

Figure 18. User-Inserted Code Words for Output Routine.

If the phase option has been selected, the numbers in the first channel code word represent the phase of station #1 minus the phase of station #2 to be output. If the number inserted for station #1 is zero, and the number of station #2 is 1-8, the phase of the station selected in station #2 with respect to the OSP TCXO will be output. This measurement of "single station phase" is exactly that which has been tracked by the SMAPLL2 tracking filter described in the software section. An example of the single station phase output appears in Figures 19 and 20. Figure 19 shows the phase of a strong SNR station (as received in Ohio) versus the OSP clock. The Omega signals are phase-locked to a stable atomic standard at the transmitter, so that the constant velocity offset in phase is caused by an offset in frequency of the OSP clock. Figure 20 shows the single station phase of a station whose received SNR is lower than in the previous graph. This signal also exhibits the ramping phase measurements, but the track is less constant or noiser than the strong station's plot.

If the phase option has been selected and neither of the numbers in the first channel word are zero, the phase difference of station #1 minus station #2 will be output. The phase difference of two Omega signals gives a line-of-position (LOP) as explained in Appendix A. Figures 21 and 22 show the LOP's plotted for various station pairs as received in Ohio. The phase ramping noted in the single station phase plots is eliminated in the LOP's by virtue of the fact that subtracting two phases measured against the same clock reference effectively cancels the clock from the measurement. Figure 21a shows the strong station pair C-D, and also illustrates the predictable diurnal phase shifting effects caused by sunrise

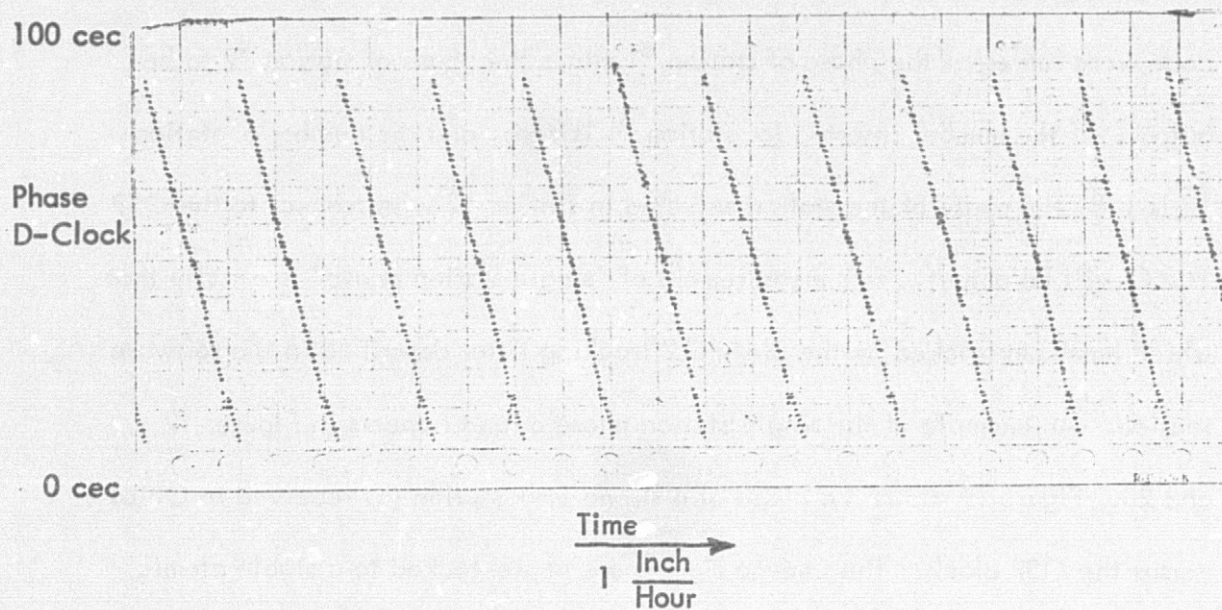


Figure 19. Single Station Phase of North Dakota Minus Clock.

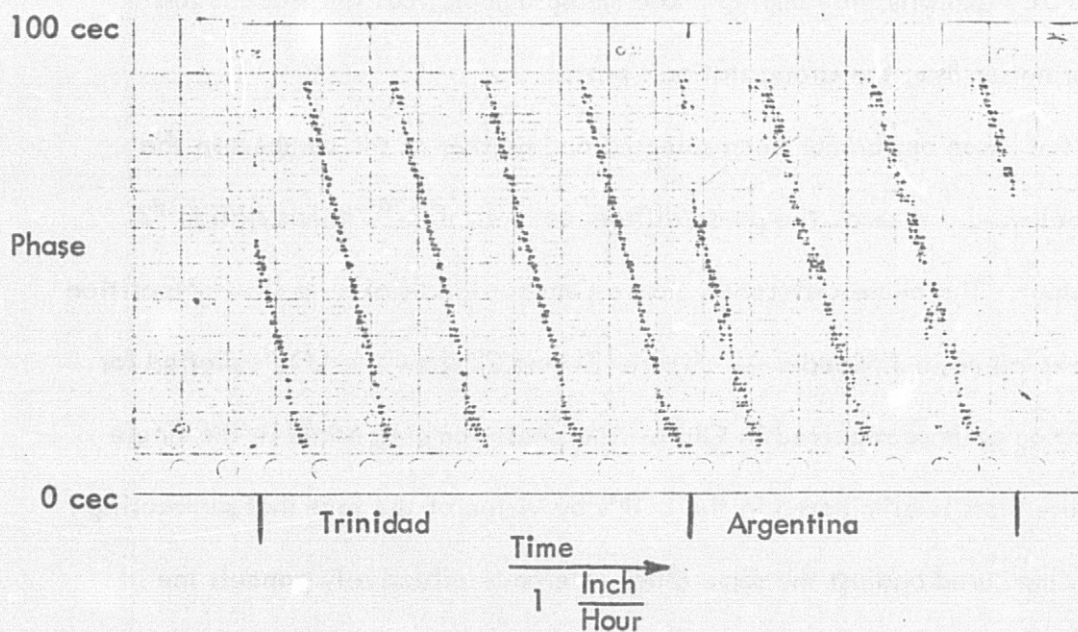


Figure 20. Single Station Phase of Trinidad Minus Clock and Argentina Minus Clock.

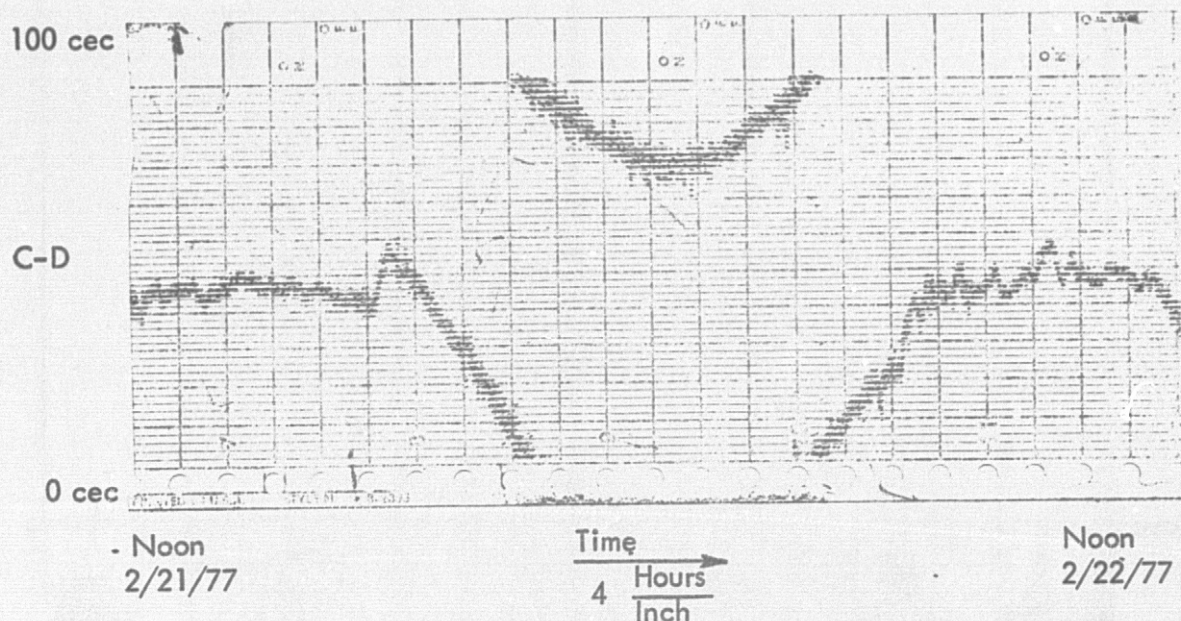


Figure 21a. 24 Hours Diurnal Data: Hawaii - North Dakota LOP.

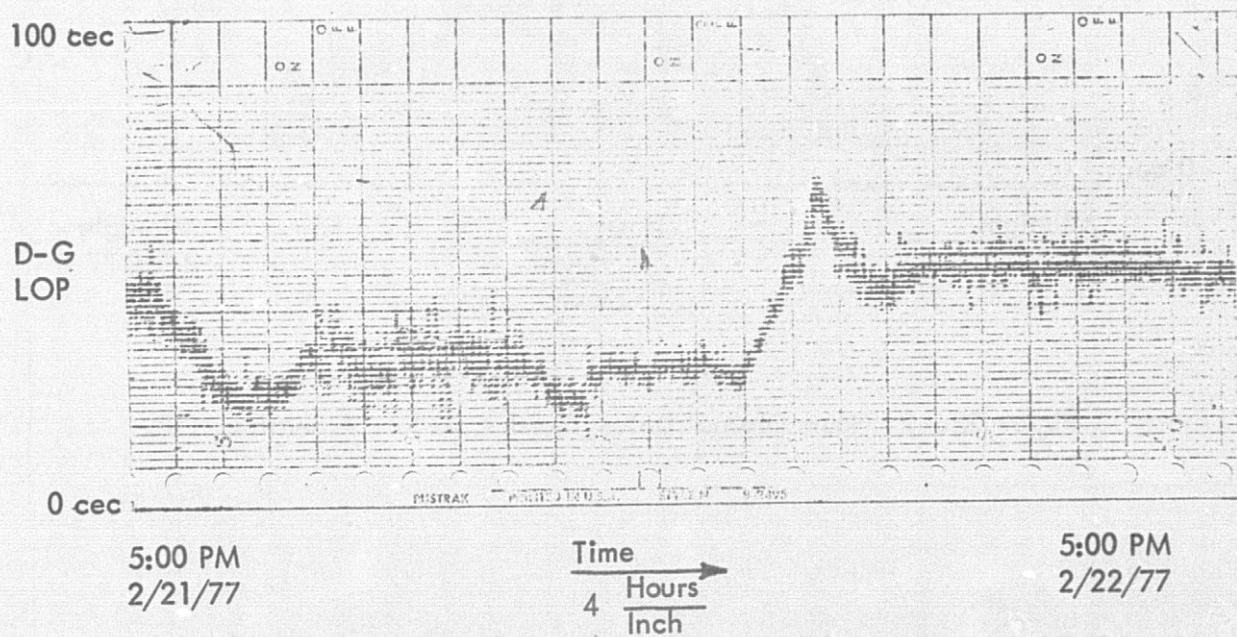


Figure 21b. 24 Hours Diurnal Data: North Dakota - Trinidad LOP.

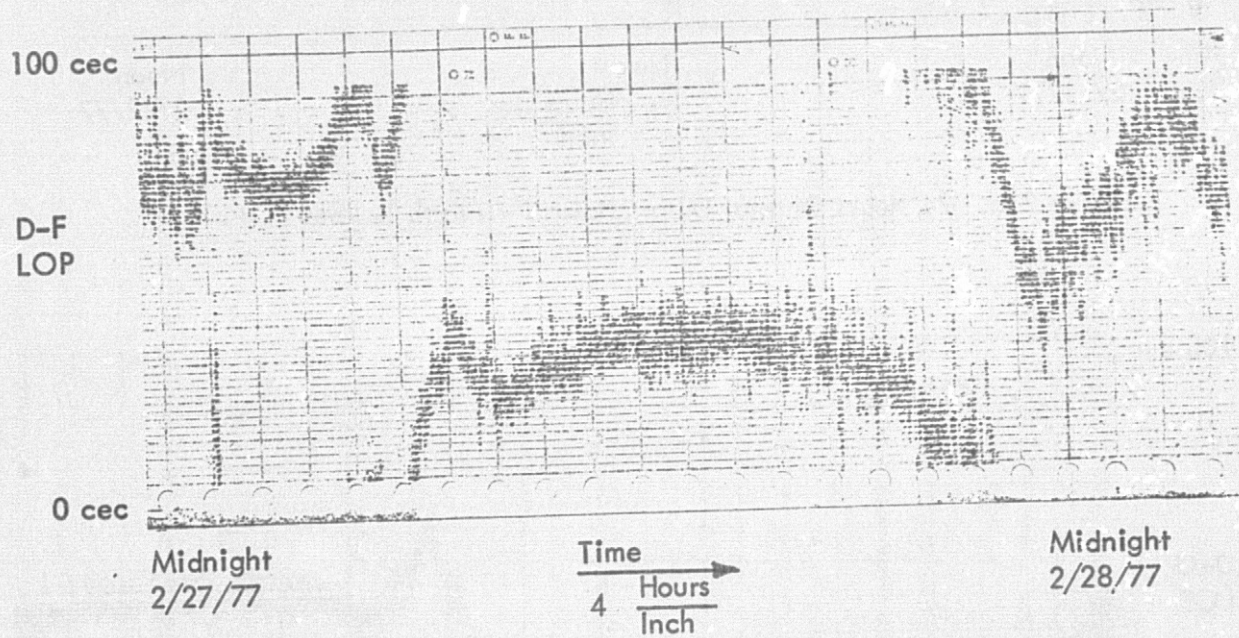


Figure 22. 24 Hours Diurnal Data: North Dakota - Argentina LOP.

and sunset. Figure 21b shows the D-GLOP which is a noisier pair, but one which is still highly usable for navigation. Figure 22 shows the D-F LOP which is very noisy, and is most useful for navigation during the atmospherically "quieter" night-time hours (when the propagation path is in darkness).

For means of comparing the software-based OSP with an all hardware OSP, Figure 23 is given which shows LOP outputs for both designs. This chart illustrates that both OSP designs track the Omega signal when in a ground-based environment. However, the second-order tracking loop employed in the software-based OSP enables the tracking of high speed aircraft with more SNR improvement than is possible with the first-order hardware version. This is verified by the computer simulation described in Appendix E.

If signal quality is selected in the option word instead of phase, the output will be the signal quality of station #2 of the first channel word. Figure 24 shows plots of the signal quality for several stations. Note that this gives only a relative SNR indication in its present form; although this measurement could be calibrated to give true SNR.

The multiplex option represents a means for time-sharing a single chart recorder or other output device. If this option is selected in the option code word, the output routine will multiplex phase or signal quality (whichever is selected) of the first and second channel code words to the output latch. The multiplex time, or time spent outputting the data for each channel word, is determined from the last six bits in the option word. This six-bit binary number represents the number of ten second intervals to be spent on each channel's data before switching to output the data indicated for the other channel word. Figure 25 gives an example

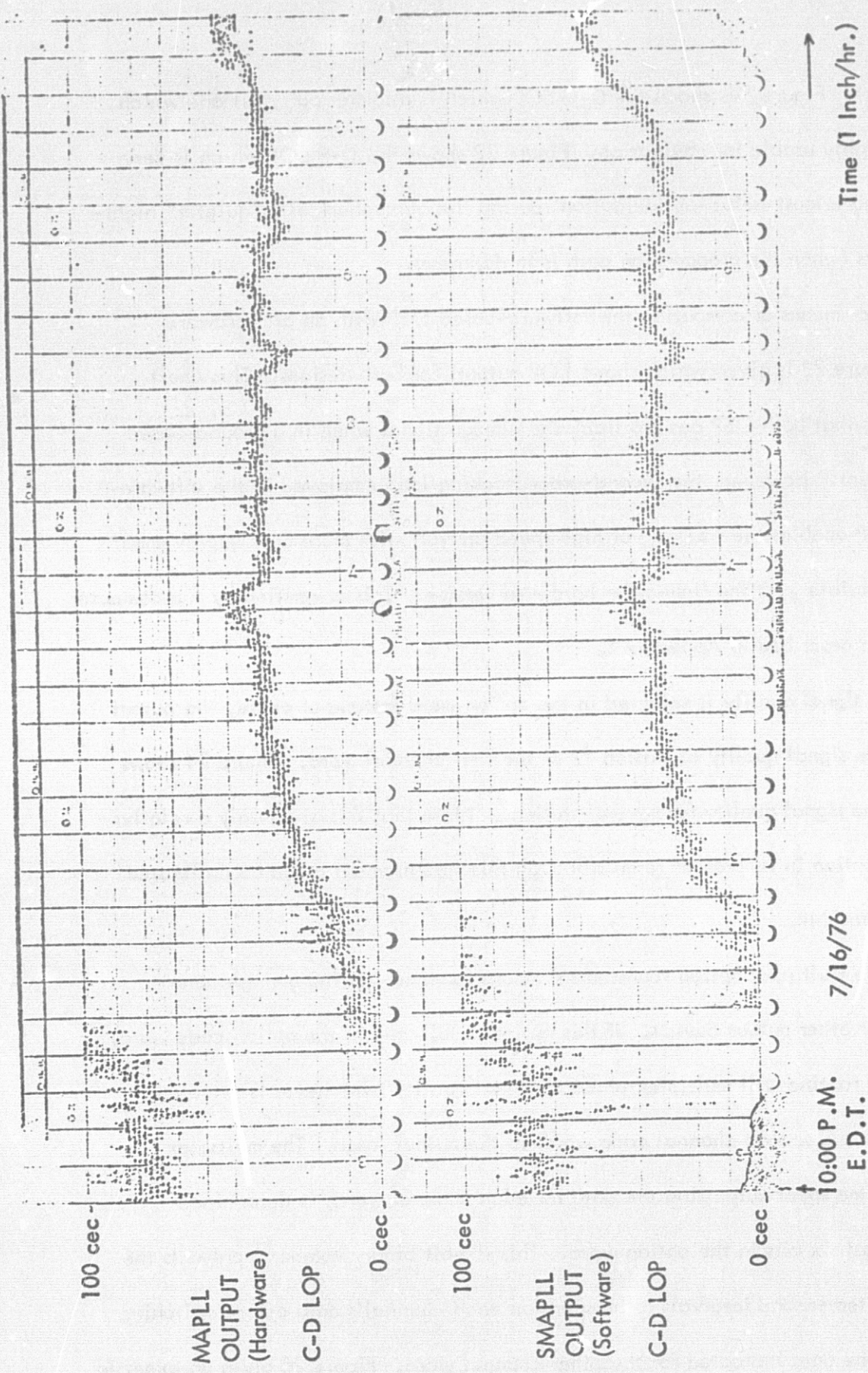


Figure 23. Omega LOP Output Traces -- Software Loop Output on Bottom.

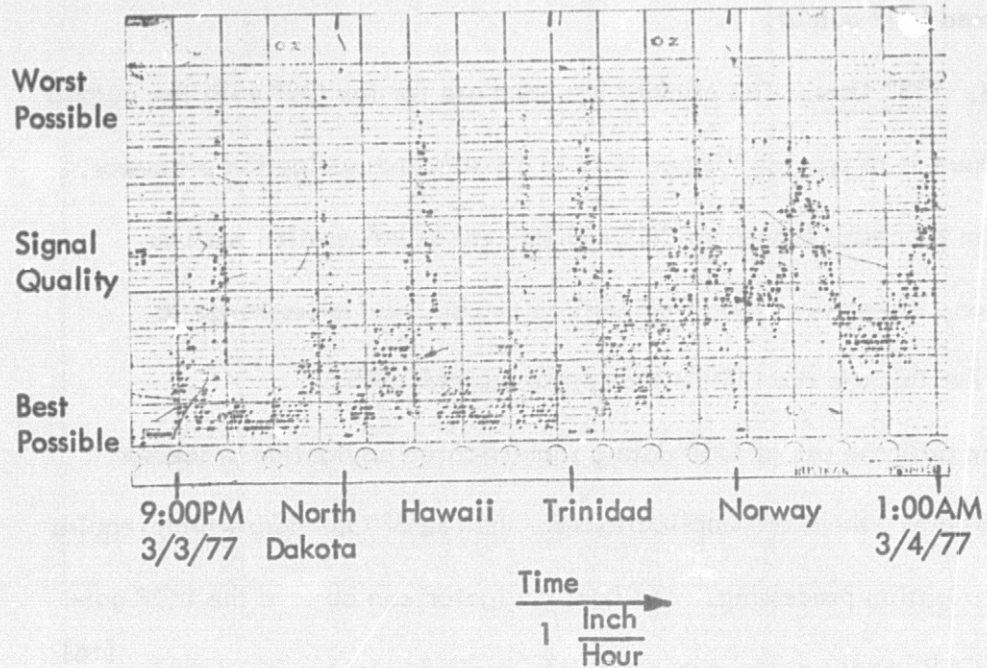


Figure 24. An Example of Signal Quality Data.

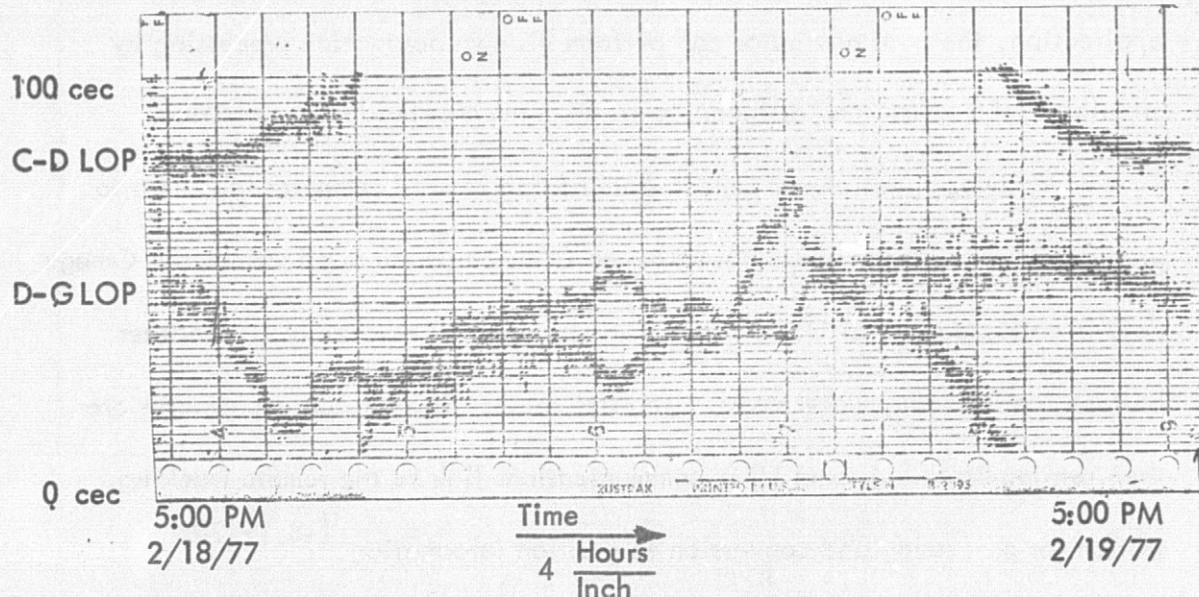


Figure 25. Multiplexed LOP Outputs (90 Seconds MUX Time).

of a multiplexed LOP output.

B. OSP Uses. The primary intended use for the OSP with the outputs as presented here is to provide Omega data to an airborne navigation processor. This navigation processor is then to derive pilot-usable information such as current position, course deviation from desired course, and miles-to-go to destination. For this use the OSP is thought to perform well.

For the airborne use of OSP data a sophisticated navigation processor is needed; however, there are applications for the use of OSP data which require little or no navigation processing. The boat navigator can observe the LOP outputs from the OSP, apply a skywave correction available in published tables [16], and find his current position on published Omega charts. [17] In this slow-speed application, the boat navigator can perform his own navigation processing by calculating the course and distance-to-go from his charted Omega position.

Many applications of Omega data utilize remote computer facilities to process the raw Omega phase data from an OSP. In these applications the Omega data is collected via an OSP on board an object to be tracked (e.g. weather balloon, radiosonde, water buoy, life raft, etc.). The Omega coordinates are then retransmitted via some other communications link to the remote tracking station for processing and conversion to position information. [18, 19, 20]

The U.S. Coast Guard is the U.S. government agency responsible for maintaining the Omega network in navigationally-precise, working order. [1] This entails providing a network of Omega monitor stations to receive and record the Omega signals at several geographic locations around the world for transmitter fault detection purposes and signal propagation studies. The OSP presented herein

is ideal for monitoring purposes such as this. The data can be stored on a digital or analog output device for later collection, or it can be transmitted to the monitoring headquarters via phone lines in near real time.

Finally, the single station phase measurements such as illustrated in Figure 19 can be used to calibrate laboratory oscillators to near atomic clock precision. Since the Omega signals are locked to atomic standards at the transmitters, the received signal versus local clock measurement shows the offset of the local clock. By adjusting the frequency of the local clock until the phase ramping gives way to a straight line (constant phase measurement) the local oscillator can be calibrated.

IV. SUMMARY AND CONCLUSIONS

A microcomputer-based low-cost Omega sensor processor for general aviation use has been designed, implemented with minimum hardware and innovative software and tested. The sensor processor hardware configuration has been presented and the software has been described.

A FORTRAN simulation analysis of the functions of automatic synchronization and PLL phase tracking has been performed to optimize routines to be performed by the OSP microcomputer. A data base of real Omega data was collected using the system's receiver and interface modules and was used as the simulation input to obtain realistic results.

The microcomputer routines developed have been shown to output data comparable to an all-hardware OSP and, in addition, the software-based OSP offers data options and capabilities not available with the all-hardware model. The OSP provides outputs suitable for use by a navigation processor, and the

system presented includes nearly all the hardware needed for an airborne Omega navigation system.

The feasibility of implementing a minimum hardware software-based OSP of higher performance and lower cost than is currently available has been demonstrated. Further research is encouraged to develop navigation processing microcomputer software to complete the Omega navigation system for general aviation use.

V. RECOMMENDATIONS FOR FUTURE WORK

The OSP presented herein represents nearly all the hardware needed for a complete Omega navigation system. The software OSP routines provide Omega data usable by a navigation processor to derive pilot-usable information. Needed to complete the system for general aviation use is a microcomputerized area navigation routine. One possible navigation technique using Omega data has been functionally described by Zervos.^[21] In addition, a propagation correction routine or some other means for applying skywave corrections is needed. More work also needs to be done to develop a lower-cost, effective pilot display.

A software-based navigation system is afforded inherent flexibility in that the computer memory can be reprogrammed to perform other functions. The OSP design presented can be used for some other navigation system by augmenting or replacing the Omega front-end module with a LORAN, GPS, or other front-end and modifying the software. The potential for a hybrid Omega-LORAN system seems great, considering the possible sharing of system hardware and software by the two systems.

Aside from the noted receiving system developmental work, additional research is needed to determine means for improving the redundancy and reliability offered by the Omega transmitting network. Whether this takes the form of a supplemental navigating system in the receiver-computer or an actual transmitter station augmentation, pilot confidence in an area navigation system must be justified and earned. Thereafter, a means for efficiently integrating Omega into the National Airspace System needs to be pursued.

VI. ACKNOWLEDGEMENTS

The author wishes to thank Mr. Jack Reid of the NASA/Langley Research Center for his support of this project as the Project Monitor of the NASA Tri-University Program. Gratitude is expressed to Dr. Richard McFarland, Director of Avionics at Ohio University for his support and encouragement. Dr. J. E. Essman of the Electrical Engineering faculty is also acknowledged for his constructive advice.

Special appreciation is reserved for Mr. Ralph Burhans, Avionics Research Engineer, and Dr. Robert Lilley, Assistant Director of Avionics, without whose technical expertise and enthusiastic support this thesis would not have been possible. Mr. Kent Chamberlin and Mr. Paul Blasche, Graduate Research Associates, have the author's sincere thanks for their technical consultation.

The author's Tri-University Program student colleagues at Ohio University, Princeton University, and MIT are also acknowledged as being instrumental in this project's completion. Thanks also go to Mrs. Roma Beverage and Mrs. Hope Mills for their work on the manuscript.

VII. REFERENCES

- [1] Department of Transportation, U.S. Coast Guard, Omega Navigation System User Manual, CG-ONSOD, 2100 2nd St. SW, Washington, D.C., preliminary draft in January, 1976.
- [2] Pierce, J.A., et.al., Omega: A World-Wide Navigation System: System Specification and Implementation, AD 630 900, National Technical Information Service, Springfield, Virginia, issued May, 1966.
- [3] Morris, Peter, and Milton Cha, Omega Propagation Corrections: Background and Computational Algorithm, Report No. ONSOD-01-74, Department of Transportation, U.S. Coast Guard, Washington, D.C., December, 1974.
- [4] Radio Navigation Group, Northrop Corporation, Omega Navigation Set AN/ARN-99 (XN-2), Phase II, Final Engineering Report, 2301 W. 120th St., Hawthorne, California, December, 1973.
- [5] Ohio University Avionics Engineering Center, Prototype Omega Receivers for Use in Data Collection and Evaluation, Athens, Ohio, September, 1976.
- [6] Burhans, R.W., Low-Cost, High-Performance, VLF Receiver Front-End, Technical Memorandum (NASA) 18, Avionics Engineering Center, Ohio University, Athens, Ohio, September, 1975.
- [7] Wright, Lee, Improvements for Omega RF Preamplifiers, Technical Memorandum (NASA) 24, Avionics Engineering Center, Ohio University, Athens, Ohio, April, 1976.
- [8] Lilley, R. W., and R. J. Salter, Simulation Analysis of a Microcomputer-Based, Low-Cost Omega Navigation System, Proceedings of the Bi-centennial National Aerospace Symposium of the Institute of Navigation, Warminster, Pennsylvania, April, 1976.
- [9] Lilley, R. W., and R. J. Salter, A Microcomputer-Based Low-Cost Omega Navigation System, Proceedings of the First Annual Meeting of the International Omega Association, Arlington, Virginia, July, 1976.
- [10] Salter, R. J., "Navigation with Mini-O, Part 3, Software", Byte Magazine, Peterborough, New Hampshire, Vol. 2, No. 4, April 1977.
- [11] MOS Technology, Inc., MCS6500 Microcomputer Family Hardware Manual, 950 Rittenhouse Road, Norristown, Pennsylvania, August, 1975.

- [12] MOS Technology, Inc., MCS6500 Microcomputer Family Programming Manual, 950 Rittenhouse Road, Norristown, Pennsylvania, August, 1975.
- [13] Chamberlin, K. A., Digital Correlation Detector for Low-Cost Omega Navigation, Technical Memorandum (NASA) 19, Avionics Engineering Center, Ohio University, Athens, Ohio, February, 1976.
- [14] Raab, Frederick H., and Jerome R. Waechter, The Use of a Counting Phase Detector to Preprocess VLF Radionavigation Signals, to be published in IEEE Transactions on Aerospace and Electronics Systems.
- [15] Chamberlin, K. A., and R. W. Lilley, The Memory-Aided Phase-Locked Loop: A Model and Proposed LSI Chip Implementation, Final Report prepared for Naval Avionics Facility, Indianapolis, Indiana, No. EER 26-1, Avionics Engineering Center, Ohio University, Athens, Ohio, March 1976.
- [16] H.O. Pub. No. 224 (111-C) Series: Omega Propagation Correction Tables, U.S. Naval Oceanographic Office, Washington, D.C., 1971.
- [17] Omega Navigational Charts, 7500 Series, U.S. Naval Oceanographic Office, Washington, D.C.
- [18] Beukers, John M., Windfinding Using Navigational Aids, presented at The Third Symposium on Meteorological Observations and Instrumentation of The American Meteorological Society, February, 1975.
- [19] Baker, Donald L., and Christopher S. Welch, A Prototype Legrangian Current Buoy Using the Carrier Plus Sideband (CSB) Retransmission of Omega Navigation Signals, Proceedings of the First Annual Meeting of the International Omega Association, Arlington, Virginia, July, 1976.
- [20] Rupp, Walter E., GRAN: Experiences and Activities, Proceedings of the First Annual Meeting of The International Omega Association, Arlington, Virginia, July, 1976.
- [21] Zervos, Arthouros, K., A Performance Simulation of a Potential Class of Low-Cost Omega/Air Data Navigation Systems, Masters Thesis, Princeton University, Department of Aerospace and Mechanical Sciences, September, 1975.
- [22] JOLT CPU Hardware Manual and JOLT DEMON Software Manual, Microcomputer Associates, Inc., Santa Clara, California, First Edition, 1975.

- [23] Lilley, Robert W., An Assembler for the MOS Technology 6502 Microprocessor as Implemented in the JOLT (TM) and KIM-1 (TM), Technical Memorandum (NASA) 44, Avionics Engineering Center, Ohio University, Athens, Ohio, November, 1976.
- [24] Schwartz, Mischa, Information Transmission, Modulation and Noise, Second Edition, McGraw Hill Book Company, New York, 1970.

VIII. APPENDICES

A. The Worldwide Omega Navigation System. The worldwide Omega System is a network of very low-frequency (VLF) transmitters located at eight locations around the world, as shown in Figure A-1. Each station transmits for approximately one second out of each ten seconds on the frequencies of 10.2, 13.6, and 11.333 KHz. As shown in Figure A-2, a unique transmission pattern is formed by the scheduled length of each station's transmission.

Omega was originally conceived by Professor J. Pierce of Harvard University following his successful demonstration of the long-range phase stability of VLF signals in the 1940's. Originally developed by the U.S. Navy for use on seagoing ships, Omega has only recently been used in airborne applications. Operational responsibility for the system was transferred to the U.S. Coast Guard in 1971, a move indicative of increasing civilian use of Omega. As of this writing, seven of the eight permanent transmitters are in operation, and the Coast Guard is beginning implementation of approximately forty monitor receiving stations around the world.

Since the wavelength of a 10.2 KHz signal is about 16 nautical miles, an effective antenna for radiating this frequency must be on the order of several miles long. Two types of antenna structures are utilized for Omega transmission. As diagrammed in Figure A-3, these are the tower and valley span antennas. Signals in the VLF region propagate in the waveguide mode using the conducting earth and ionosphere as waveguide bounds. As shown in Figure A-4, a single waveguide mode dominates when several hundred miles from a transmitter, and due to this single, stable mode of propagation the VLF signals can be received in

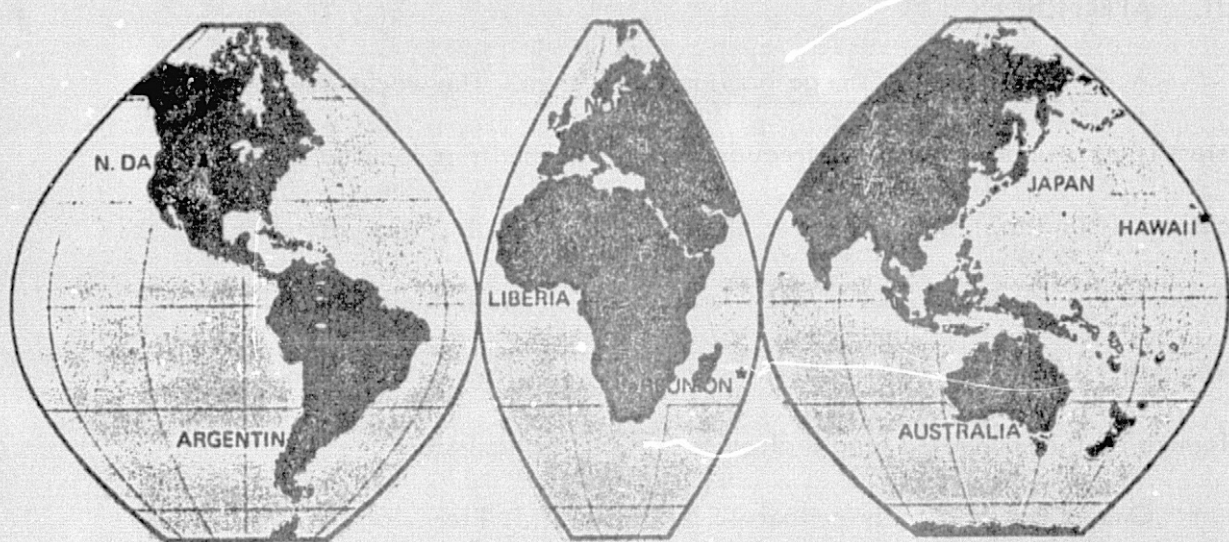


Figure A-1. Omega Station Locations.

	10 SECONDS								
TRANSMISSION INTERVAL	0.9	1.0	1.1	1.2	1.1	0.9	1.2	1.0	0.9
STATION	A	10.2	13.6	11.33	$f_1 \rightarrow$	-	-	-	$10.2 \rightarrow$
	B	$f_2 \rightarrow$	10.2	13.6	11.33	$f_2 \rightarrow$	-	-	-
	C	-	$f_3 \rightarrow$	10.2	13.6	11.33	$f_3 \rightarrow$	-	-
	D	-	-	$f_4 \rightarrow$	10.2	13.6	11.33	$f_4 \rightarrow$	-
	E	-	-	-	$f_5 \rightarrow$	10.2	13.6	11.33	$f_5 \rightarrow$
	F	-	-	-	-	$f_6 \rightarrow$	10.2	13.6	11.33
	G	11.33	-	-	-	-	$f_7 \rightarrow$	10.2	13.6
	H	13.6	11.33	-	-	-	-	$f_8 \rightarrow$	10.2

→ ← 0.2 SEC.

Figure A-2. Omega Signal Transmission Format.

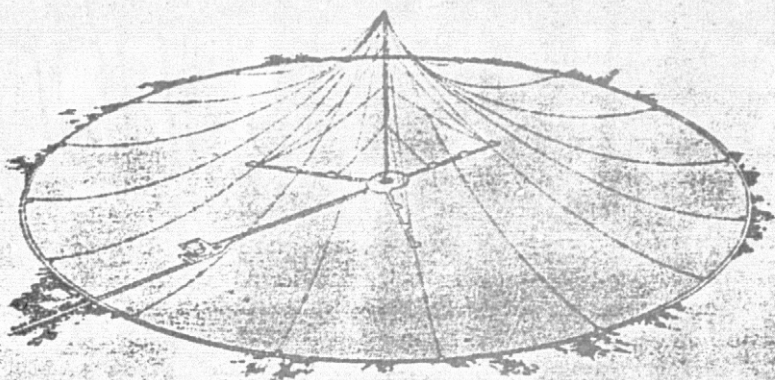


Figure 3
North Dakota Omega Transmitting Station (Typical Tower)

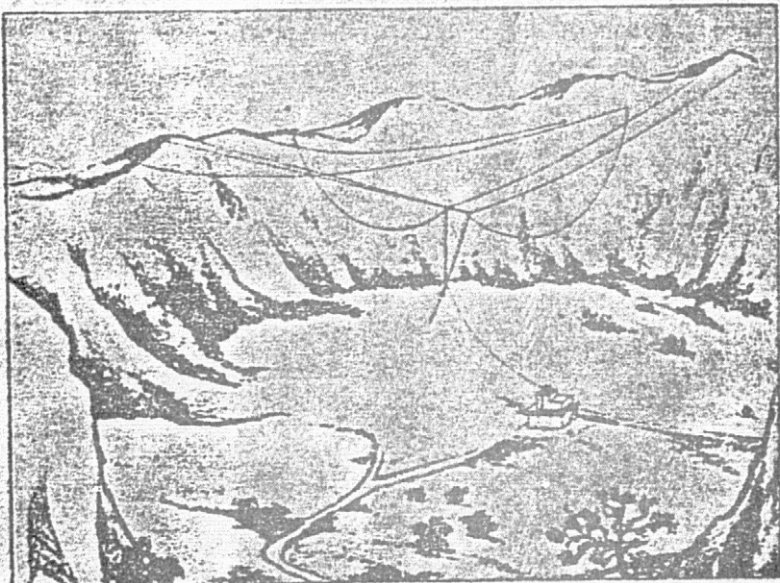


Figure 4
Haiku, Hawaii Omega Transmitting Station (Valley Span)

Figure A-3. Omega Transmitting Antenna Structures.

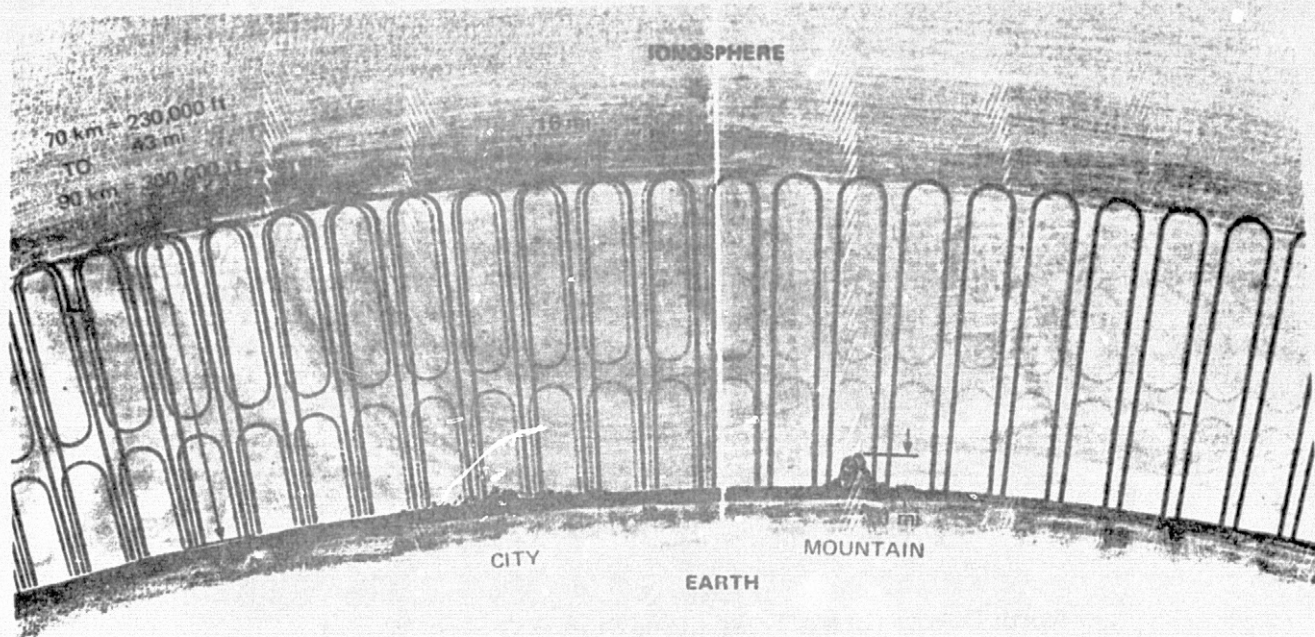


Figure A-4. Propagation Modes for VLF Signals.

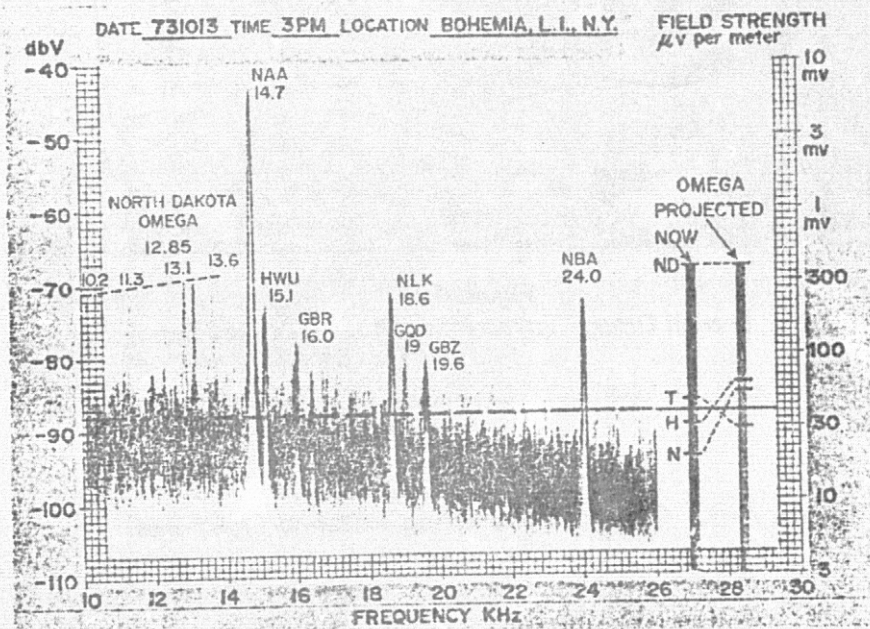


Figure A-6. VLF Signal Levels as Received in 30 Hz Bandwidth in New York.

excess of 6,000 miles and at all altitudes (even between mountains and beneath the surface of water).

The height and smoothness of the ionosphere boundary is changed by varying amounts of radiation received from the sun, and this effective change in waveguide height results in a signal phase velocity change. The phase velocity change occurs when the signal propagation path to the receiver changes from light to darkness and vice-versa, and is, therefore, referred to as "diurnal" shift. This diurnal shift is highly predictable, and the received phase can be adjusted by applying a skywave correction (SWC) factor which is unique for month, day, time-of-day, and receiver location. Another highly predictable factor is the varying conductivity of the earth waveguide boundary. Ground conductivity maps have been prepared and a propagation correction can be applied for particular receiver location. Ionospheric disturbances caused by sunspot activity and solar flares are not as highly predictable and limit the position-fix accuracy attainable with Omega.

Techniques for the reception of the Omega carrier signal differ; however, detection of the signal's phase involves comparing the received signal to a locally generated signal of the same frequency. Differing degrees of sophistication are possible in the phase detection process; more sophisticated meaning more accurate local clock signals. If a clock frequency on the order of a part in 10^{12} (atomic standard accuracy) is available, and it is possible to synchronize the phase of the local clock to the time standards employed at the Omega transmitters, the Omega system can be used in the rho-rho positioning mode by simply measuring the time-of-arrival of two or more Omega signals (propagation time being

proportional to distance traveled). If a local clock of this high accuracy is available, but it is not possible to synchronize its phase with the Omega time standards, it is still possible to navigate in the rho-rho mode. However, it is first necessary to determine the receiver's position within \pm eight nautical miles (since a cycle at 10.2 KHz is 16 nautical miles long and each phase repeats every 16 miles). This is known as lane resolution, and several techniques exist for resolving lanes to within needed limits.

If a local clock of atomic standard accuracy is not available, a less stable (and less expensive) clock may be used provided short-term stability constraints are obeyed. For example, a clock stability of one part in 10^5 per day will drift no more than one centicycle (1/100 of a 360 degree cycle) in ten seconds. Therefore, if this local reference clock is, in effect, used within each ten second Omega frame separately, very little accuracy is sacrificed. Specifically, phase differencing can be performed by first detecting each station's signal with respect to the local clock and then subtracting two phase measurements. This effectively subtracts the clock from the measurement. Each phase difference is a point on a hyperbolic contour. Geometrically, lines of constant phase difference form hyperbolic contours referred to as hyperbolic lines-of-position (LOP's), as shown in Figure A-5.

Navigation by reference to these LOP's is known as the hyperbolic mode, and it is again necessary to determine initial position to within one-half lane (lane resolution). It is necessary to use two LOP's (at least three stations) to determine position, and greatest accuracy is achievable when using LOP's which intersect at close to a 90 degree angle.

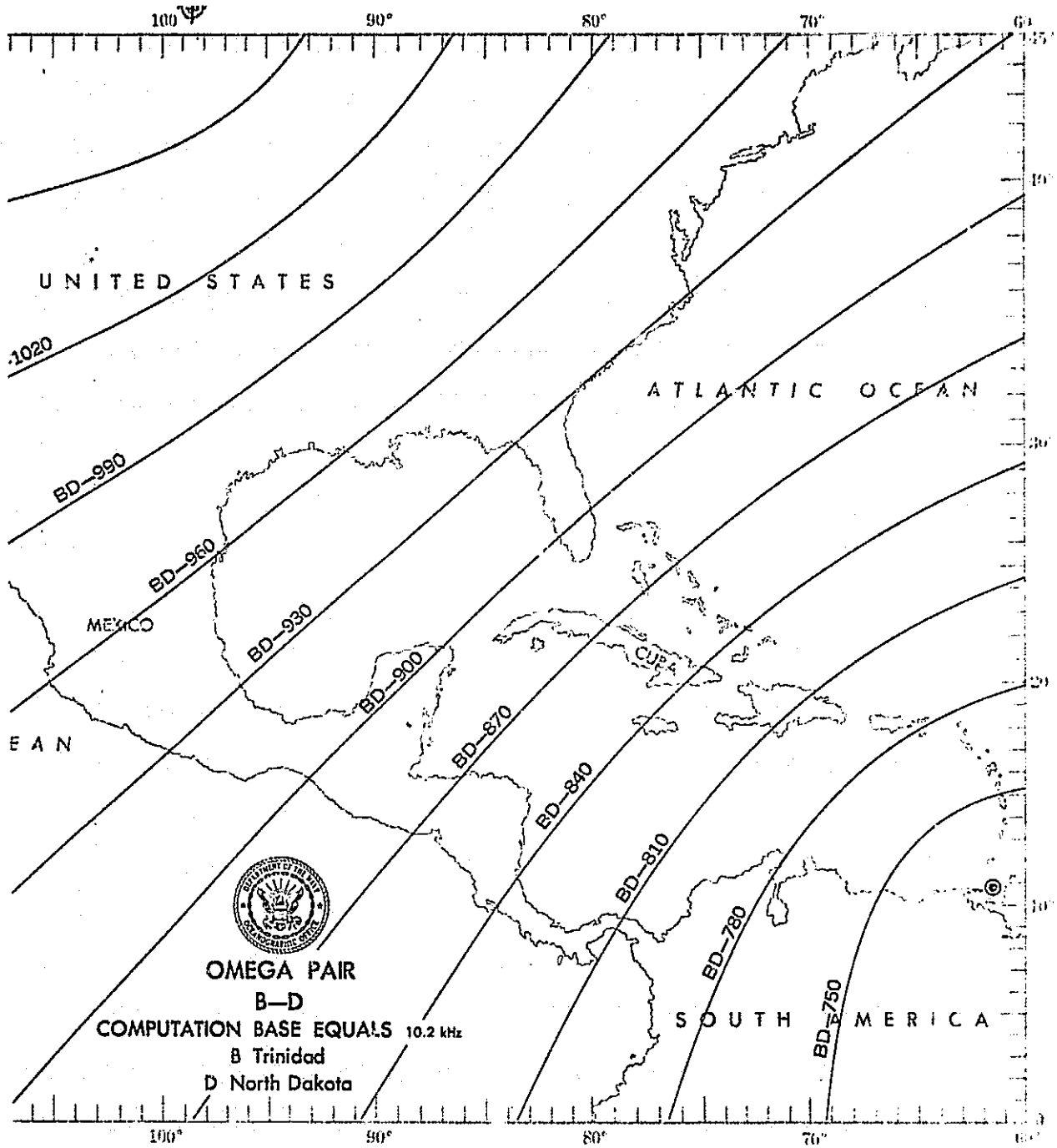


Figure A-5. Omega Lines-of-Position (LOPs) Formed by North Dakota (D) and Temporary Station Trinidad (B).

Paramount in the detection and estimation of Omega phase is the problem of noise. Amplitude noise in the VLF region is caused primarily by lightning and is made up of both gaussian distributed noise (a conglomeration of many distant lightning sources of various strengths and distances) and impulsive noise (closer lightning sources). Transmitted power of all Omega stations is ten kilowatts, and a representative sample of received signal and noise amplitudes appears in Figure A-6. Also of importance is the noise caused by precipitation upon the aircraft and antenna. These additive amplitude noises cause the detected phase to be contaminated with noise (i.e. phase jitter). Due to the several contributing noise sources and allowing for less than perfect propagation corrections, the stated Omega system position fix accuracy is \pm one nautical mile (daytime) to \pm two nautical miles (nighttime). This basic accuracy limitation constrains Omega use to an area (non-precision) navigation aid.

B. Omega Data Base. For purposes of obtaining realistic data for a simulation analysis of Omega sensor processor (OSP) functions, a data base of real Omega ground and flight data was collected. So that the data used as input to the simulation would be the same as that seen by the OSP microcomputer algorithms, the data was collected using the OSP hardware front-end and interface modules which had been fabricated and perfected before the OSP software was developed.

For purposes of evaluating the performance of the simulated automatic synchronization and PLL tracking processes it was necessary to collect Omega data under the following conditions: (1) ground-based receiver with noise conditions found throughout a 24-hour day; (2) ground-based receiver with and without the overwhelming strong station (North Dakota) being received; and (3) airborne receiver in a general aviation aircraft.

The Omega phase data was collected via the equipment set-up as shown in Figure B-1. The microcomputer provides an interrupt signal when new data is latched and ready to be read. For data collection the 100 Hz interrupt signal was used as a magnetic tape recorder "write" signal (one phase sample written every ten milliseconds). In addition, it was possible to collect data only during every other ten second time frame. This was to allow time to write an end-of-record on the tape to separate the ten second data frames. Note that this is wideband 10.2 KHz Omega phase data taken directly from the 30 Hz bandwidth receiver front-end and sampled by the interface module every ten milliseconds.

The ground-based data was collected at Ohio University's Clippinger Laboratories. A 6.1 meters long wire, mounted on the roof of Clippinger Laboratories was used as the receiving antenna. An active preamplifier was colocated at the antenna and feeds the signal through approximately 30.5 meters of coaxial lead-in cable to the receiver in the Omega Laboratory. The electrical environment of this receiving antenna is one of considerable interfering noise. The noise is primarily from two sources: (1) 60 Hz harmonics radiated by high-powered electrical equipment in the building; and (2) audio modulation of a nearby AM radio transmitter. Therefore, the ground-based data is of worst-case variety. The data without strong station North Dakota was collected as that station was going off-the-air for scheduled maintenance.

The airborne data was collected with the equipment set-up of Figure B-1 installed onboard the Avionics Engineering Center DC-3 flying laboratory. The data was collected outbound to Chicago O'Hare International Airport from Ohio University Airport at Albany, Ohio (and also inbound on the return flight). The

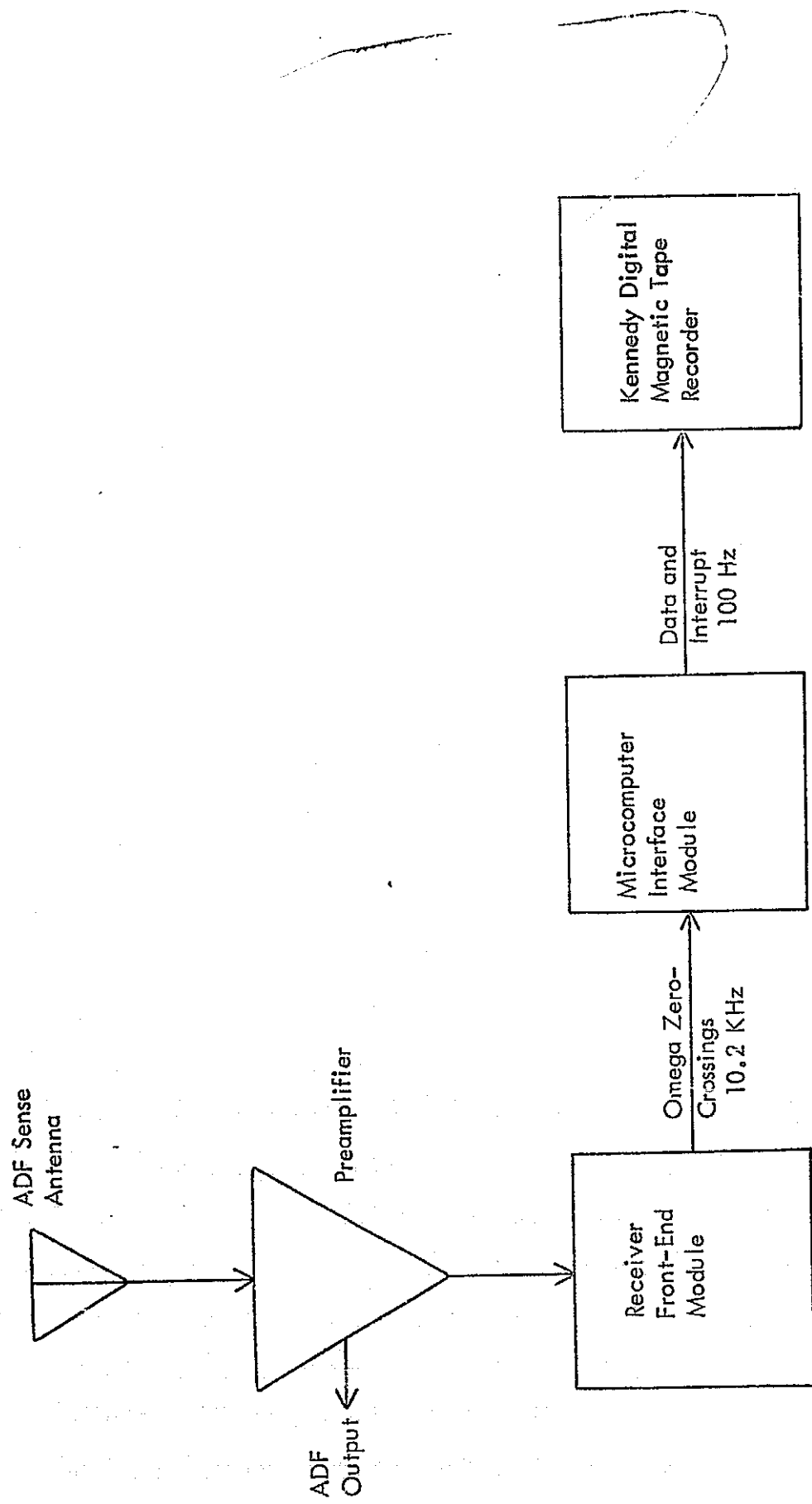


Figure B-1. Omega Data Collection Setup.

outbound flight was conducted between the hours of 7:00 and 8:30 AM on October 20, 1976. The cruise altitude was 2438 meters and VFR conditions persisted throughout the flight. The return flight was between the hours of 6:00 and 7:00 PM on the same day and the cruise altitude was 2743 meters in VFR conditions. The aircraft's ADF sense antenna mounted on top of the fuselage was used with the preamplifier mounted on the ceiling inside the aircraft. The preamplifier fed approximately 6.1 meters of coaxial lead-in cable to the receiver.

All data was recorded on magnetic tape in the binary format presented by the microcomputer interface module. The phase of the Omega signal is recorded every ten milliseconds, each data point being quantized into the interval from zero to 255. The OSP[®]'s temperature compensated crystal oscillator (TCXO) was used as the local reference clock; therefore, the slight frequency offset of the TCXO appears as a constant-velocity phase ramp in the data.

Figure B-2 summarizes the contents of the data base.

<u>File #</u>	<u>Type Data</u>	<u>Date Collected</u>	<u>Location</u>	<u>Stations Transmitting</u>
1	Ground (24 hours)	January, 1976	Athens, Ohio	B,C,D,G
2	Ground (D off air)	June, 1976	Athens, Ohio	B,C,G
3	Ground (D off air)	June, 1976	Athens, Ohio	B,C,G
4	Flight (VFR)	October, 1976	Athens-Chicago	B,C,D,G
5	Flight (VFR)	October, 1976	Chicago-Athens	B,C,D,G

Figure B-2. Omega Data Base Summary.

C. Omega Sensor Processor Circuitry. The Omega sensor processor is composed of three distinct hardware modules and a general-purpose microcomputer. The circuit details of the Omega preamplifier, receiver front-end, and microcomputer interface modules are given in Figures C-1, C-2 and C-3, respectively. The microcomputer system is described in Appendix D.

D. JOLT Microcomputer System.

1. Hardware. The JOLT Microcomputer System is available from Microcomputer Associates, Inc., Santa Clara, California. As implemented in the Omega Sensor Processor, the JOLT system consists of a CPU board and a memory board. The CPU board containing the 6502 CPU chip, 6530 chip (PIA, TTY Monitor ROM, and Interval Timer), 6520 PIA chip, TTY interface circuitry, and 512 bytes RAM is available in kit form for \$150. The 4K RAM memory board is available in kit form for \$200. Circuit diagrams for the CPU and memory boards appear in Figures D-1 and D-2. [22]

As can be seen from these diagrams, the JOLT incorporates a 16-line address bus and an 8-line data bus, along with an adjustable 700 KHz - 1 MHz oscillator. System architecture includes one accumulator, two index registers, one processor status register, one stack pointer register, and one program counter register. All are 8-bit registers except for the program counter which is 16-bits long.

The system accommodates two fully vectored interrupts. One is a non-maskable interrupt (NMI), and the other is an interrupt request (IRQ) which can be disabled and thereafter ignored by the software.

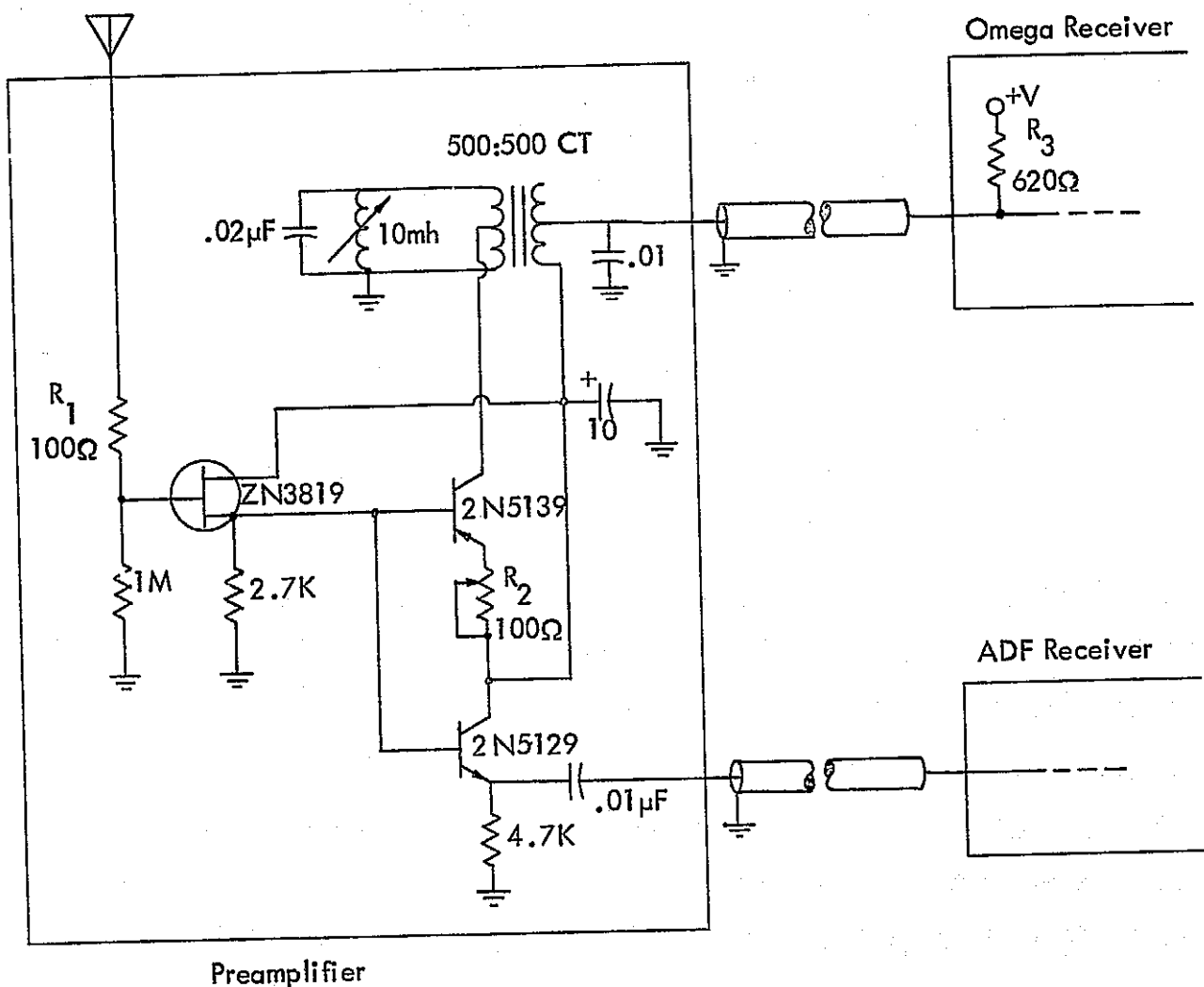


Figure C-1. Dual Purpose Preamplifier Module.

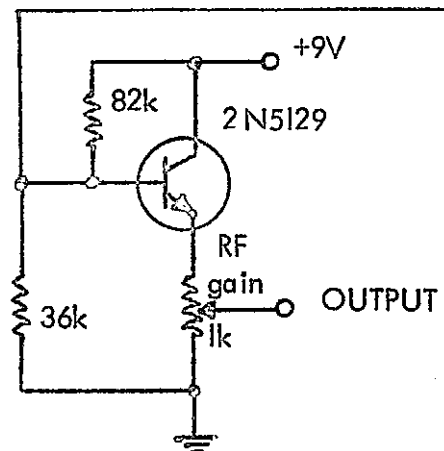
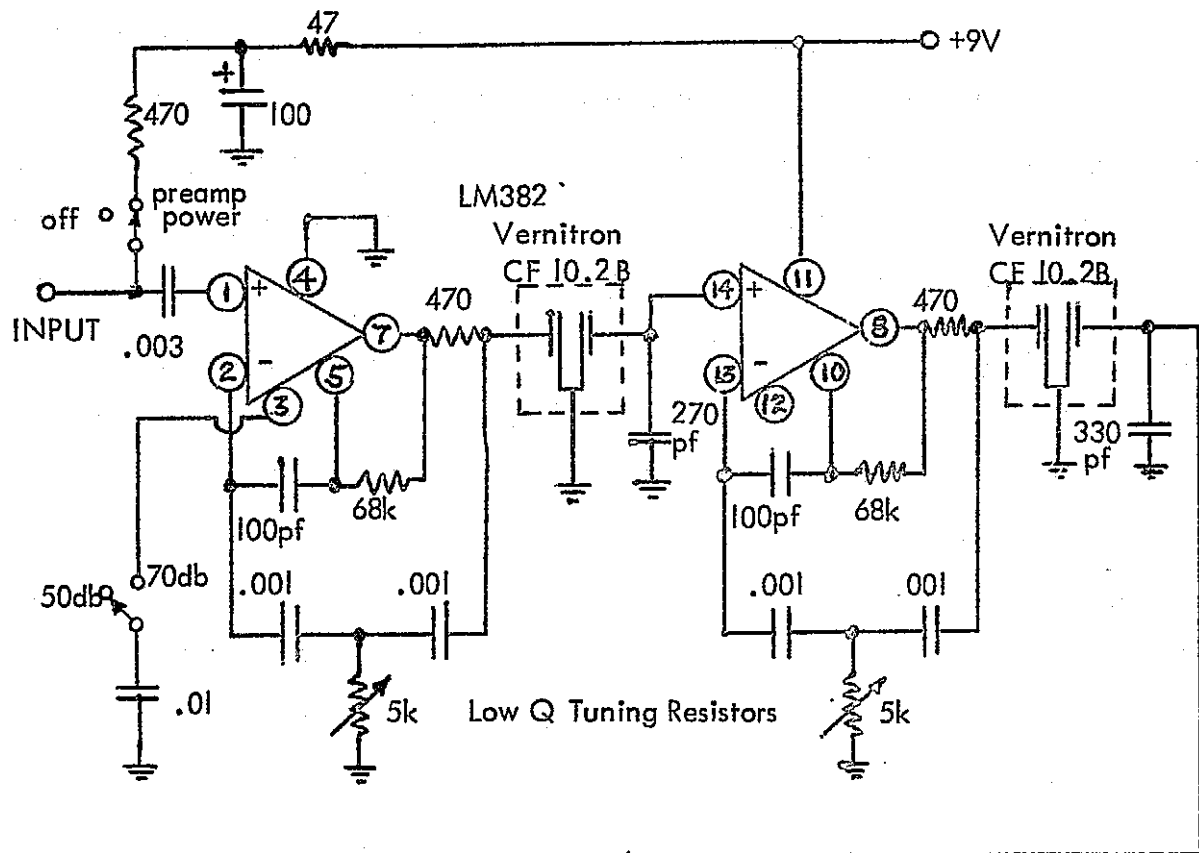


Figure C-2a. Receiver Front-End Module, Two-Stage VLF Bandpass Amplifier.

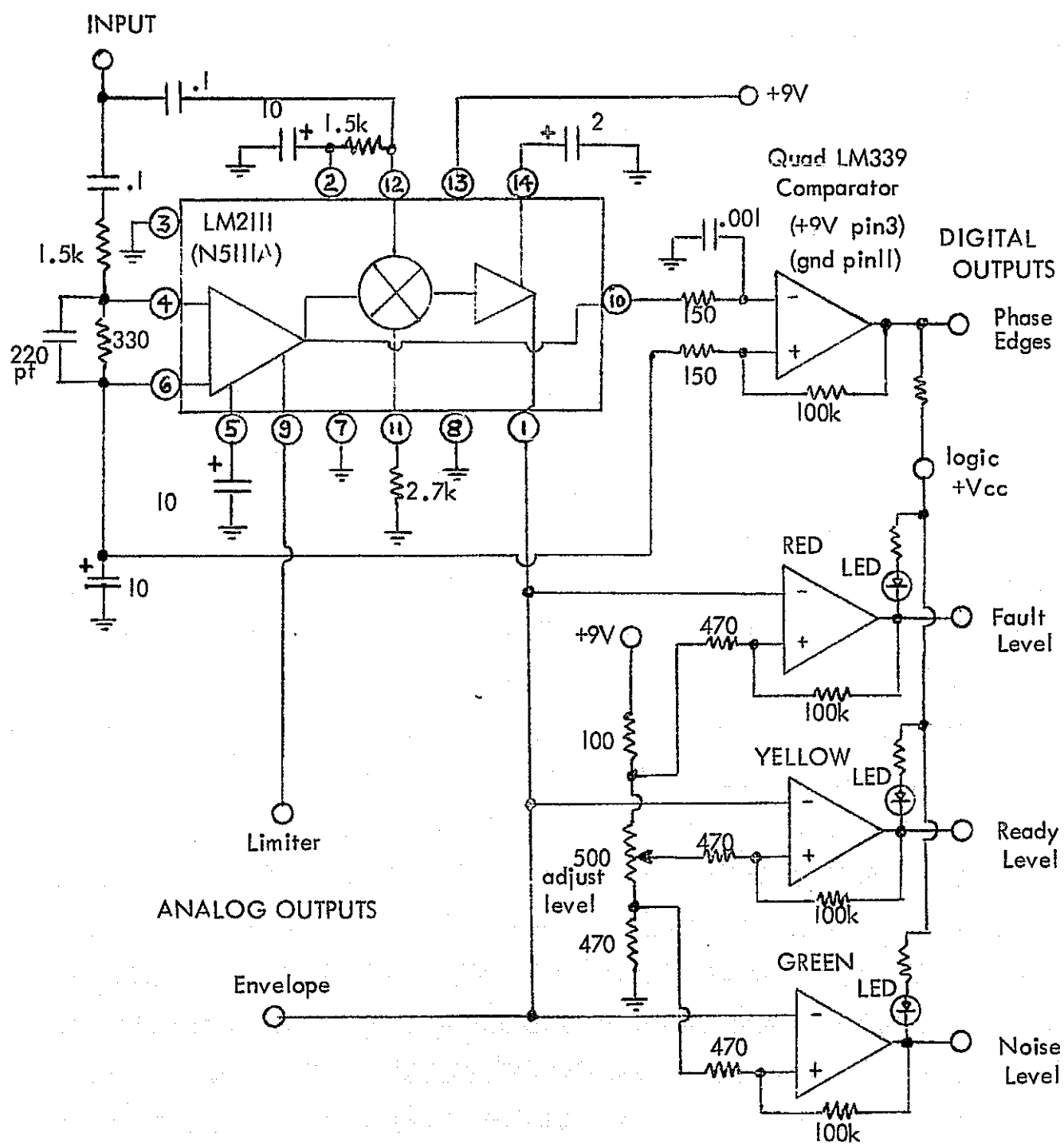


Figure C-2b. Receiver Front-End Module, Limiter - Comparator Circuit.

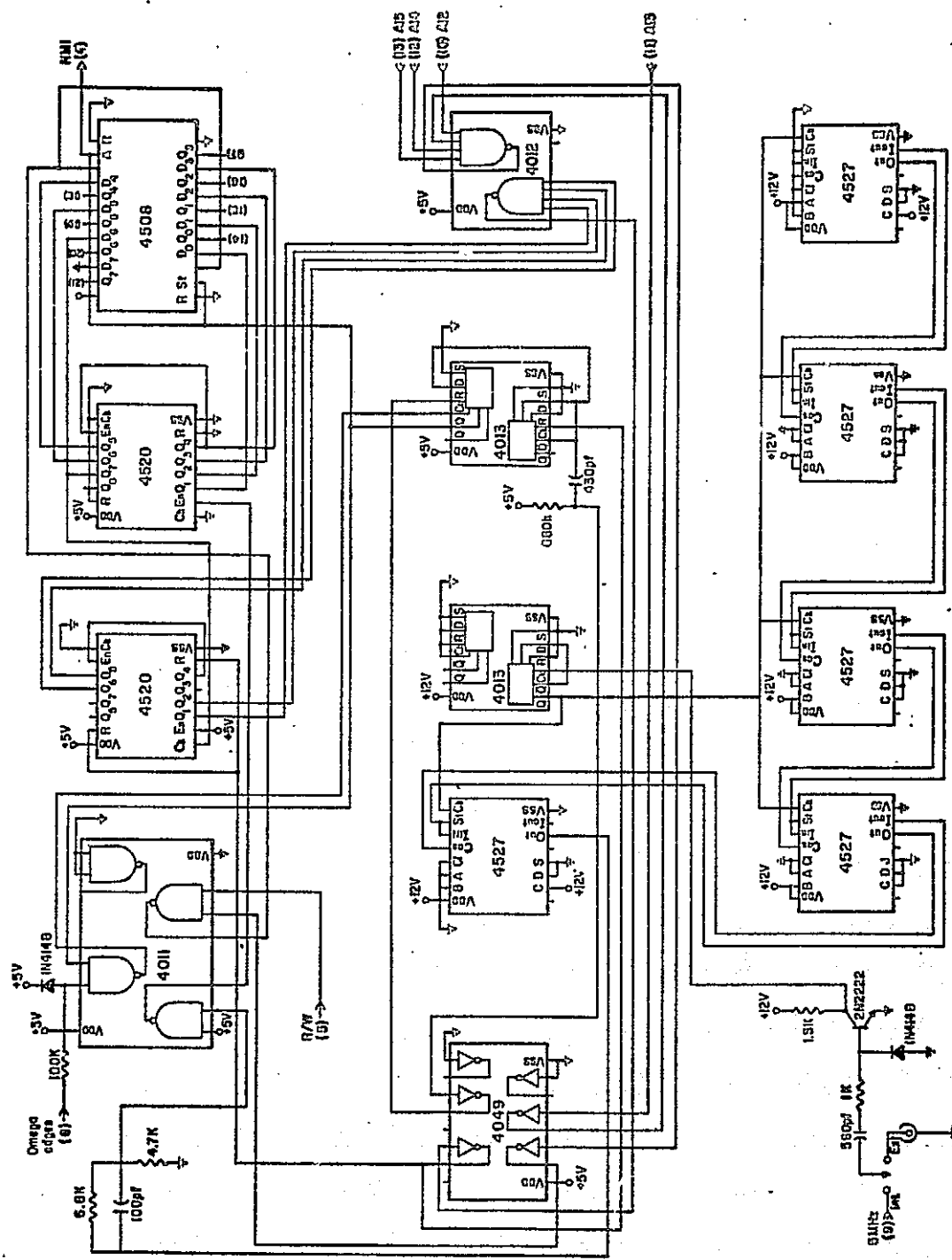


Figure C-3. Microcomputer Interface Module Circuit Diagram.

ORIGINAL PAGE IS
OF POOR QUALITY

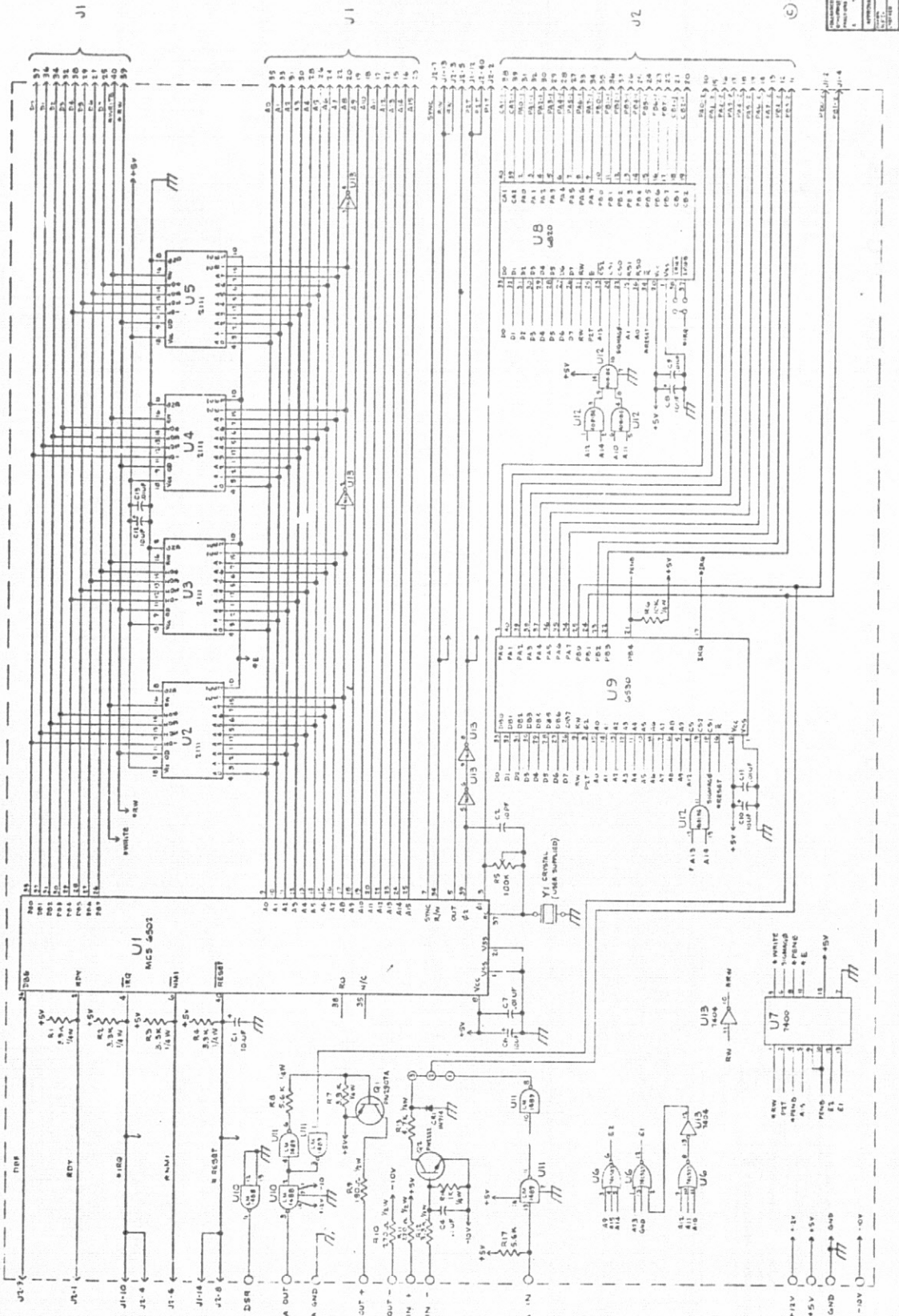


Figure D-1. JOLT CPU Board Schematic Diagram.

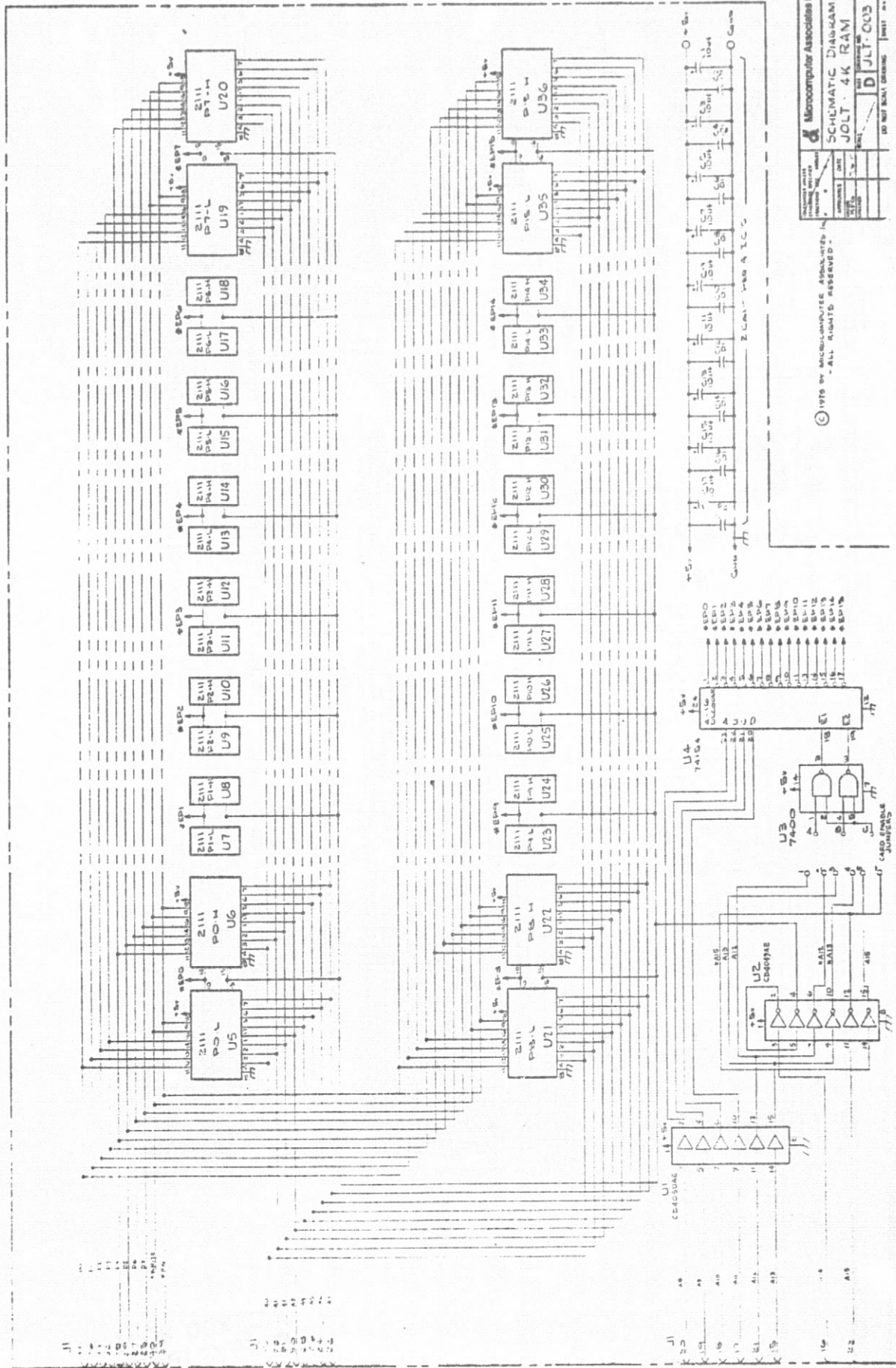


Figure D-2. JOLT 4K RAM Memory Board Schematic Diagram.

The JOLT system requires approximately 2 amps at +5 volts and 50 milliamps at -10 volts DC. After these supplies have been turned on, the user need only push the system reset button and the system is ready to accept user-commands from a TTY keyboard.

2. Software. Figure D-3 gives the instruction set for the JOLT system and details about each instruction. It can be seen that the average instruction fetch and execute time is about 3 microseconds. The 52 instructions combined with their various addressing modes provide one hundred and fifty unique operations. Figure D-4 gives more software details and Figure D-5 gives the [22] JOLT system memory map.

The TTY monitor routine which is resident on the 6530 1K ROM chip allows the user to operate the JOLT from a TTY keyboard. Commands include: (1) display contents of memory; (2) display contents of CPU registers; (3) alter contents of memory or CPU registers; (4) begin program execution; and (5) punch and read paper tape. In addition, several monitor subroutines can be called to type data on the TTY printer.

In addition, a 6502 Assembler which can be executed via a larger computer system employing FORTRAN IV, has been obtained. [23] This Assembler capability allows the programmer to write microcomputer programs in mnemonics rather than hexadecimal number codes, and allows for use of variable names and labels rather than numerical codes and locations.

E. FORTRAN Simulation Analysis. In order to test the feasibility of performing OSP functions of automatic synchronization and PLL phase tracking in

INSTRUCTIONS	IMMEDIATE	ABSOLUTE	ZERO PAGE	ACCUM	IMPLIED	(IND.X)	(IND.Y)	Z.PAGE,X	ABS,X	ABS,Y	RELATIVE	INDIRECT	Z.PAGE,Y	CONDITION CODES
BASICOPIC														
ADC A+M → A	161	69 2 2	6D 4	3 66 3 2				61 6 2 77 5 2 75 4 2	1D 4 2 3 79 4 3					/ - J - - I
ADD A+M+N → A	162	69 2 2	6D 4	3 26 3 2				31 6 2 31 5 2 35 4 2	20D 4 3 30 4 3					/ - J - - I
ASL C ← D, E → D	163	69 6 2	6D 6 2	3 66 5 2	DA 2 1			16 6 2 1E 7 3						
BCC BRANCH ON C=I	164													
BCS BRANCH ON C=I	165													
BEQ BRANCH ON Z=I	166													
BGT A>B	167													
BMI BRANCH ON N=I	168													
BNE BRANCH ON N≠I	169													
BPL BRANCH ON N=0	170													
BRK (See Fig. 1)								89 2 2						
CMC NEGATION ON V=0	171													
BVS BRANCH ON V=1	172													
CLC C=0	173							16 2 2						
CLD D=0	174							08 2 1						
CLI I=1	175							06 2 1						
CMV V=M	176							08 2 1						
CMP A-M	177	CB 2 2	CD 4 3	CB 3 2				C1 6 2 01 5 2 05 4 2 00 4 3 09 4 3						
CPA A=M	178	CB 2 2	CC 4 3	CB 3 2										
CPY V-M	179	CB 2 2	CC 4 3	CA 3 2										
DEC M+I-M	180	CE 0 2	CE 5 2											
LSR X→Z	181							CA 9 1						
DEY V-I-Y	182							08 2 1						
EOR M+I-M	183	ED 2 2	ID 4 3	05 3 2				47 6 2 51 5 2 55 4 2 00 4 3 09 4 3						
INC M+I-M	184	EE 6 2	EE 5 2					FA 6 2 FE 7 3						
INX X+I-X	185							EB 2 1						
INY Y+I-Y	186							CF 2 1						
JMP JUMP TO NEW LOC	187	AC 2 2												
JSR (See Fig. 1) (PAGE 105)	188	29 6 2												
LDA M→A	189	AD 2 2	AD 4 3	AS 3 2				A1 6 2 81 5 2 85 4 2 BD 4 3 89 4 3						

INSTRUCTIONS	IMMEDIATE	ABSOLUTE	ZERO PAGE	ACCUM	IMPLIED	(IND.X)	(IND.Y)	Z.PAGE,X	ABS,X	ABS,Y	RELATIVE	INDIRECT	Z.PAGE,Y	CONDITION CODES
LOX M→X	191	A2 2 2	AE 4 3	AS 3 2										
LSD M+N-Y	192	BE 2 2	AC 4 3 66 3 2						94 6 2 30 4 3					
LSR P→C	193	BE 0 3	40 5 2	BA 2 1					56 6 2 5E 7 3					
ROR R+I-R	194													
ORA AVM+A	195	BB 2 2	BD 4 3	BS 3 2				81 6 2 17 5 7 15 4 2 1D 4 3 19 4 3						
PHA A→M, S-I-S	196							4B 3 1						
PHB PH-M, S1-S2-S	197							4B 3 2						
PLA S1-S-S M→A	198							68 4 1						
PLB S1-S-S M-S-S	199							20 4 1						
ROL M-L (See 1)	200	2E 8 3	28 5 2	2A 2 1					38 6 2 3E 7 3					
ROR M-L (See 1)	201	BE 6 3	66 5 2	BA 2 1					76 6 2 7E 7 3					
RTS (See Fig. 2) RTN SUB	202							4B 6 1						
SEC A+P-Z→A	203	ED 2 2	ED 4 3	ES 3 2				EE 8 2 F1 9 2 F2 4 2 FD 4 3 FF 4 3						
SEC 1→C	204							38 2 1						
SED 1→D	205							FB 2 1						
SEI 1→I	206							7B 2 1						
STA A→M	207	80 6 3	85 3 2					81 6 2 81 6 2 05 4 2 20 5 3 99 5 3						
STH H→M	208	88 4 3	88 3 2											
STY Y→M	209	8C 4 3	84 3 2											
TAX A→X	210							AA 2 1						
TAY Y→X	211							AB 2 1						
TSX S→X	212							BA 2 1						
TXA X→R	213							CA 2 1						
TXS X+S	214							DA 2 1						
TYA Y→A	215							DB 2 1						

(1) ADD TO "N" IF PAGE BOUNDARY IS CROSSED
 (2) ADD TO "N" IF BRANCH OCCURS TO SAME PAGE.
 ADD 2 TO "N" IF BRANCH OCCURS TO DIFFERENT PAGE.
 (3) CARRY NOT = BORROW
 (4) IF IN DECIMAL MODE Z FLAG IS INVALID,
 ACCUMULATOR MUST BE CHECKED FOR ZERO RESULT.

X INDEX, X
 Y INDEX, Y
 A ACCUMULATOR
 M MEMORY PER EFFECTIVE ADDRESS
 M₁ MEMORY PER STACK POINTER
 V OR
 M₂ MEMORY BIT 7

* EXCLUSIVE OR
 / MODIFIED
 - NOT MODIFIED
 M MEMORY BIT 7
 M₂ MEMORY BIT 5

LSD	0	1	2	3	4	5	6	7	B	B	A	B	C	D	E	F	LSD
MID																	
0	BRK	ORA IND, X							ORA Z, Page	ASL P, PAGE							#
1	CMV	CMV IND, Y							ORA E, Page	ASL E, Page							
2	JSR	AND IND, X							BIT E, Page	AND E, Page	ROL E, Page	PLP	AND MM	ROL A			1
3	BRK	AND IND, Y							AND E, Page	AND E, Page	ROL E, Page	SEC	AND MM	ROL A			2
4	RTI	EDR IND, X							EDR E, Page	EDR E, Page	EDR E, Page	PHA	EDR MM	EDR A			3
5	PHB	PHB IND, Y							EDR E, Page	EDR E, Page	EDR E, Page	CLI	EDR MM	EDR A			4
6	RTS	ADC IND, X							ADC E, Page			FLA	ADC MM		JMP IND		5
7	DI	ADC IND, Y										SCI	ADC MM				6
8	STA	STA IND, X							STA E, Page	STA E, Page	STA E, Page	TAY	STA MM				7
9	STC	STC IND, Y							STA E, Page	STA E, Page	STA E, Page	TVA	STA MM				8
A	LDS	LDS IND, X							LDS E, Page	LDS E, Page	LDS E, Page	TAY	LDS MM				9
B	LDY	LDY IND, Y							LDY E, Page	LDY E, Page	LDY E, Page	TAY	LDY MM				10
C	CPY	CPY IND, X							CPY E, Page	CPY E, Page	CPY E, Page	INY	CPY MM				11
D	LDZ	LDZ IND, Y							LDZ E, Page	LDZ E, Page	LDZ E, Page	CLO	LDZ MM				12
E	CPX	CPX IND, X							CPX E, Page	CPX E, Page	CPX E, Page	INX	CPX MM				13
F	LDX	LDX IND, Y							LDX E, Page	LDX E, Page	LDX E, Page	EDO	LDX MM				14

IMM — IMMEDIATE ADDRESSING — THE OPERAND IS CONTAINED IN THE SECOND BYTE OF THE INSTRUCTION.

ABS — ABSOLUTE ADDRESSING — THE SECOND BYTE OF THE INSTRUCTION CONTAINS THE 8 LOW ORDER BITS OF THE EFFECTIVE ADDRESS. THE THIRD BYTE CONTAINS THE 8 HIGH ORDER BITS OF THE EFFECTIVE ADDRESS.

PAGE X, Z PAGE ADDRESSING — SECOND BYTE CONTAINS THE 8 LOW ORDER BITS OF THE EFFECTIVE ADDRESS. THE 8 HIGH ORDER BITS ARE ZERO.

ACCUMULATOR — ONE BYTE INSTRUCTION OPERATING ON THE ACCUMULATOR.

PAGE X, Z PAGE Y, ZERO PAGE INDEXED — THE SECOND BYTE OF THE INSTRUCTION IS ADDED TO THE INDEX. (CARRY IS DROPPED) TO FORM THE LOW ORDER BYTE OF THE EA. THE EA, THE HIGH ORDER BYTE OF THE EA IS ZEROS.

ABS, X ABS, Y ABSOLUTE INDEXED — THE EFFECTIVE ADDRESS IS FORMED BY ADDING THE INDEX TO THE SECOND AND THIRD BYTE OF THE INSTRUCTION.

IND, X, IND, Y INDEXED INDIRECT — THE SECOND BYTE OF THE INSTRUCTION IS ADDED TO THE X INDEX. DISCARDING THE CARRY. THE RESULTS POINTS TO A LOCATION ON PAGE ZERO WHICH CONTAINS THE 8 LOW ORDER BITS OF THE EA. THE NEXT BYTE CONTAINS THE 8 HIGH ORDER BITS.

INDIVL INDIRECT INDEXED — THE SECOND BYTE OF THE INSTRUCTION POINTS TO A LOCATION IN PAGE ZERO. THE CONTENTS OF THIS MEMORY LOCATION IS ADDED TO THE Y INDEX. THE RESULT BEING THE LOW ORDER EIGHT BITS OF THE EA. THE CARRY FROM THIS OPERATION IS ADDED TO THE CONTENTS OF THE NEXT PAGE ZERO LOCATION, THE RESULT BEING THE 8 HIGH ORDER BITS OF THE EA.

ORIGINAL PAGE IS
OF POOR QUALITY

Figure D-3. Instruction Set for MOS Technology 6502 CPU.

<u>COMMAND</u>	<u>OPERATION</u>
R	Print out the CPU registers.
M	Print out contents of memory.
:	Alter contents of CPU registers or memory.
G	Begin program execution.
WH	Write contents of memory in hexadecimal.
LH	Read punched paper tape.

Figure D-4. JOLT System TTY Monitor Commands Summary.

FFFF	INTERRUPT VECTORS
F3C0	RAM (1)
F3BF	RESERVED
C000	FOR
BFFF	JOLT EXPANSION
8000	USER ROM AND RAM AREA
7FFF	(RECOMMENDED LOCATION FOR ADDITIONAL RAM BOARDS)
7000	DEMON MONITOR
6FFF	(RCM) (1)
6E40	RESERVED FOR JOLT PERIPHERALS
6E3F	
6200	6530 I/O TIMER (1)
61FF	
6000	RESERVED FOR USER I/O
5FFF	CPU PIA (1)
4000	USER PIAs
3FFF	
1000	USER RAM AREA
0FFF	(RECOMMENDED LOCATIONS FOR FIRST THREE 4K RAM BOARDS)
0200	SPARE RAM SPACE (NORMALLY UNUSED)
01FF	
0100	USER AREA AND STACK (1)
00FF	
0000	USER AREA AND DEMON (1)

INTERRUPT VECTORS

A

6530

B

USER PIAs

C

PAGE ONE

D

PAGE ZERO

E

(1) Standard on JOLT CPU board.

Figure D-5. JOLT System Memory Map.

software, a FORTRAN simulation analysis was performed. This simulation also served to optimize parameters in both algorithms before they were assembled in microcomputer code. The input data for much of the simulation analysis was the real Omega data base described in Appendix B; however, since the specification of system performance requires complete and absolute knowledge of the input data, computer generated data was also used.

Each simulation is summarily described, and the actual listing for each FORTRAN simulation appears at the end of this Appendix.

1. Noise Modeling. Since the real Omega data base contained uncertainties such as signal-to-noise ratios (SNR), phase measurements designed to approximate the data at the output of the OSP front-end and microcomputer interface modules were generated with the computer. The Omega noise is both gaussian and impulsive. Gaussian noise is easily generated by the computer and was judged to sufficiently approximate real Omega noise following comparisons of statistics of the real and modeled noise.

The noise model must simulate the gaussian distributed input noise being bandpassed through the 30 Hz narrowband Omega receiver front-end module. The basis for such a model of a sinusoidal signal embedded in gaussian noise and received through a narrowband receiver is developed by Schwartz. [24]

The signal developed across the antenna can be expressed as: $s(t) = (x+A)\cos(\omega t+\phi)+(y)\sin(\omega t)$. This expression neglects possible interfering carrier terms from other Omega frequencies and other strong signals near the desired frequency. $A\cos(\omega t+\phi)$ is the desired signal term, and x and y are the white, gaussian noise terms (with x and y independent, of zero mean, and variance σ^2).

These noise terms can be generated by calls to system library random number generator routines, RANDNR and RANDNRB. The narrowband receiver front-end module is simulated by a low-pass filter (LPF) subroutine, GRANGE. Passing the random noise terms through the LPF results in correlated noise samples.

The phase angle detected at the output of the LPF front-end can be simulated by taking $\theta = \arctan(\frac{y}{x+A})$. The density function of phase obtained in this

manner is:

$$f(\theta) = \frac{e^{-s^2}}{2\pi} + \frac{1}{2} \sqrt{\frac{s^2}{\pi}} \cos \theta e^{-s^2 \sin^2 \theta} [1 + \operatorname{erf}(s \cos \theta)]$$

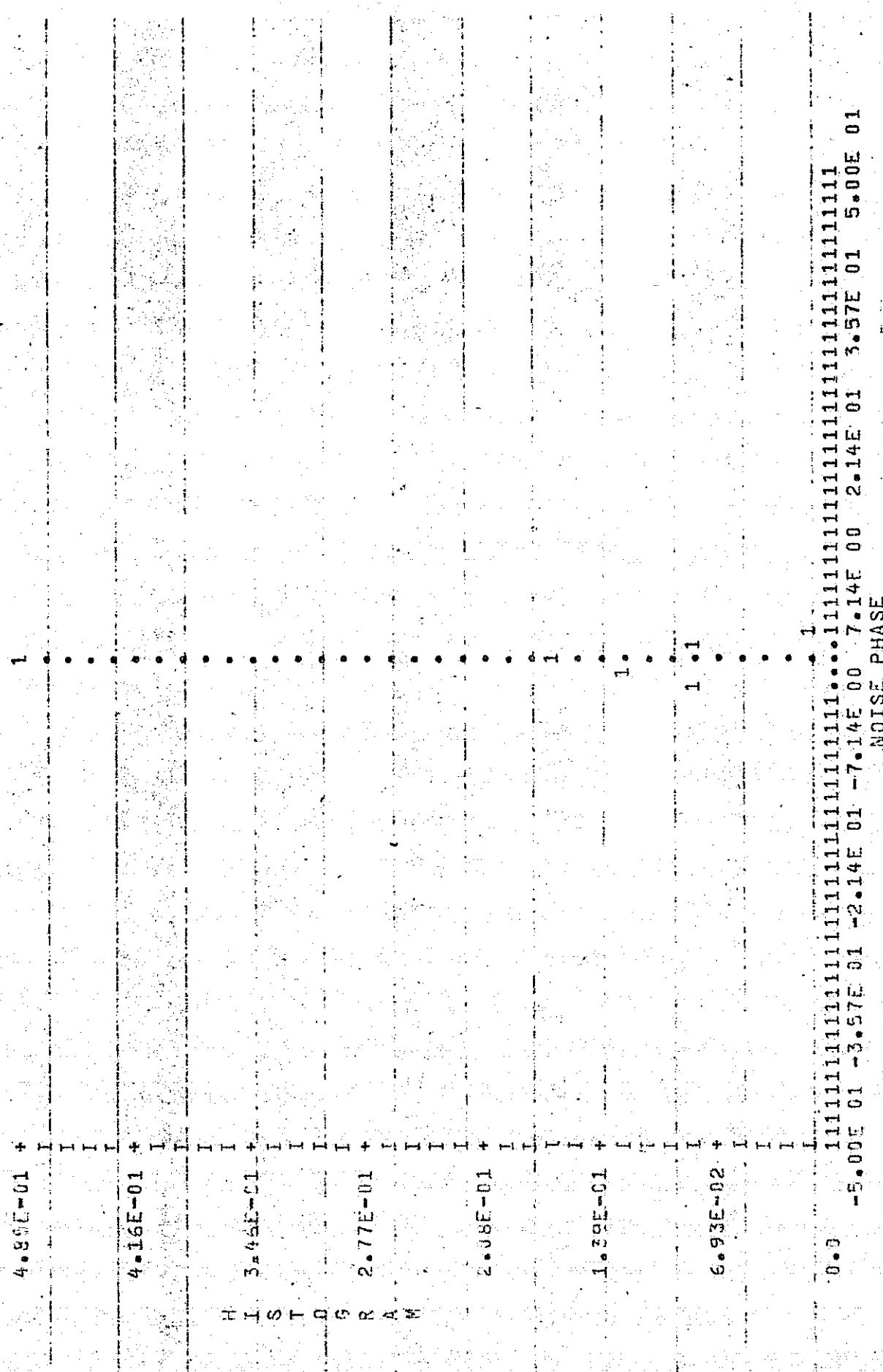
where s^2 is the power signal-to-noise ratio equal to $\frac{A^2}{2\sigma^2}$.

Comparison of the histograms and autocorrelation plots in Figures E-1, E-2 versus E-3, E-4 gives an example of how well the modeled noise approximates the real Omega noise. Lack of autocorrelation of the simulated narrowband noise is due to the fact that the LPF subroutine GRANGE simulates a single-pole RC low-pass rather than the multiple-pole low-pass filter provided by the real Omega front-end. However, the amplitude of the R(O) term (noise variance) closely approximates that of the real data, and the histograms are fairly well matched (remember that the signal-to-noise ratios for the real data are only approximations).

All plots were generated via calls to the system library routine MMPLOTT.

2. Automatic Synchronization Simulation. The automatic synchronization simulation is flow charted in Figure E-5.

The real Omega data base was used as the input data for this simulation, and the subroutine DATA is first called to insure a random starting point in the data base (simulating a random OSP turn-on time). After a completed 10-second frame of data is read, the data is "mirrored". Figure E-6 shows the 10-second



ORIGINAL PAGE IS
OF POOR QUALITY

Figure E-1. Normalized Histogram of Simulated Noise Phase Vs. Phase in cec for +20 dB SNR.

2.50E 00 1

1

1

1

1

1

1

1

1

1

1

1

1

1

1

1

1

1

1

1

1

1

1

1

1

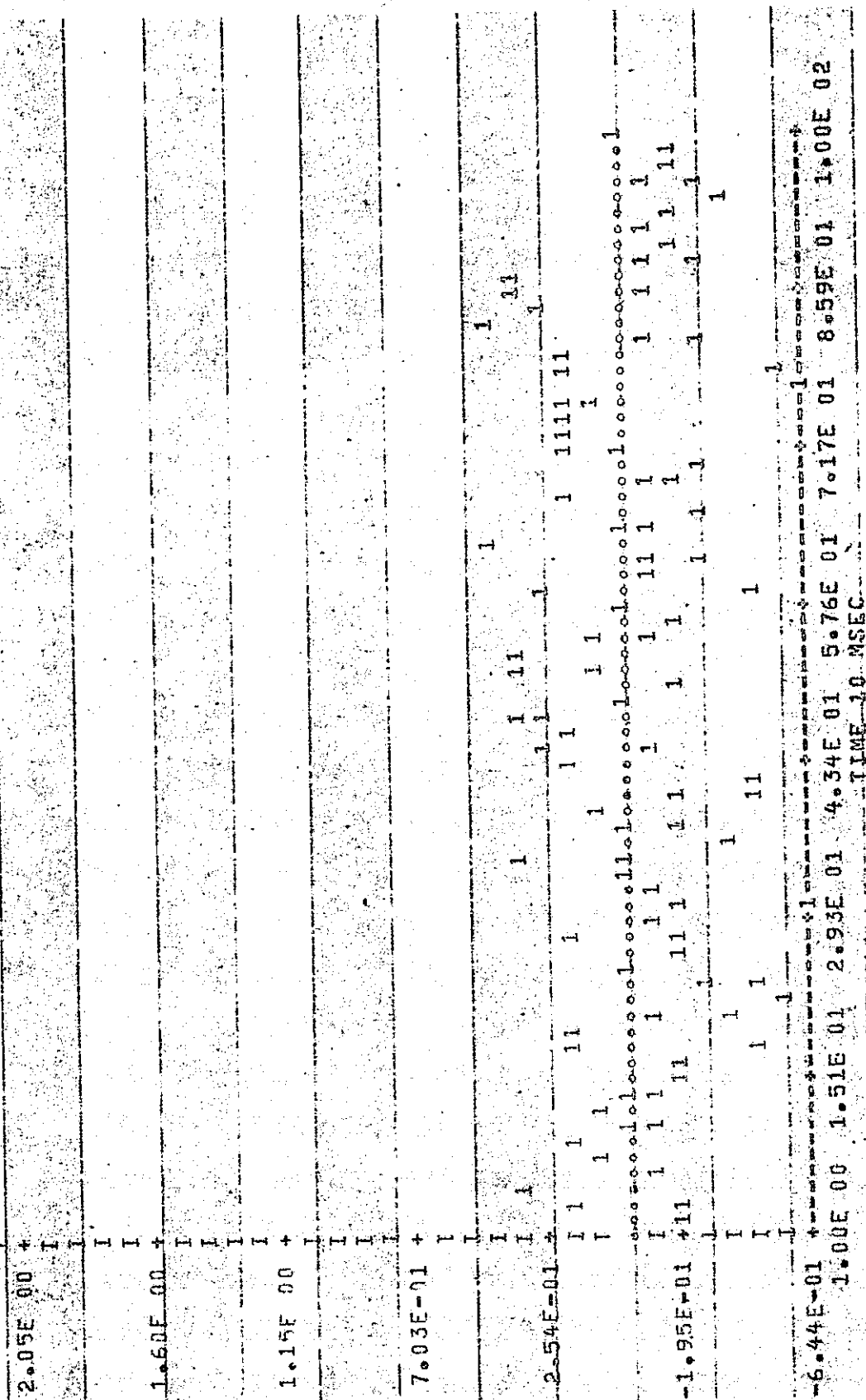
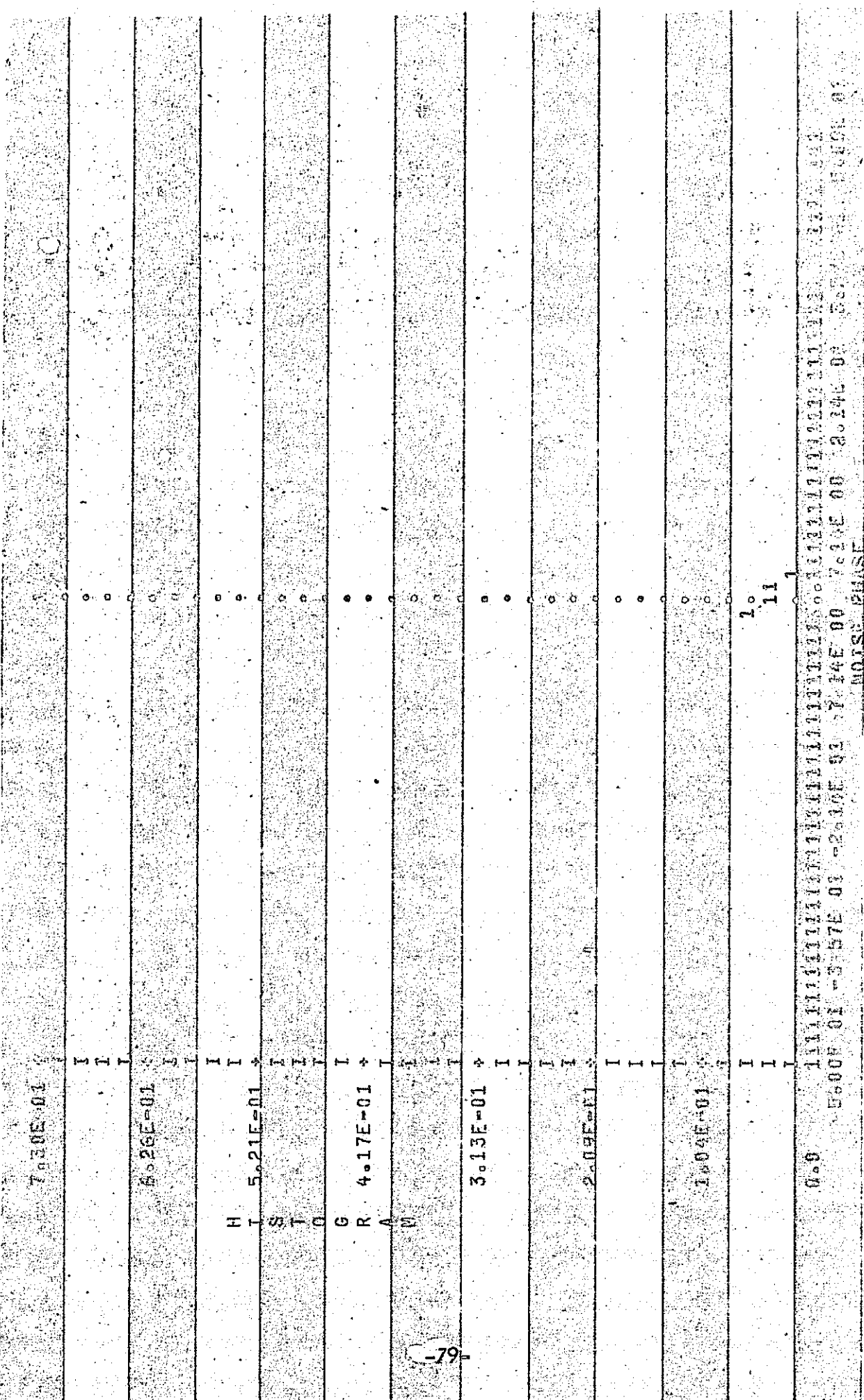
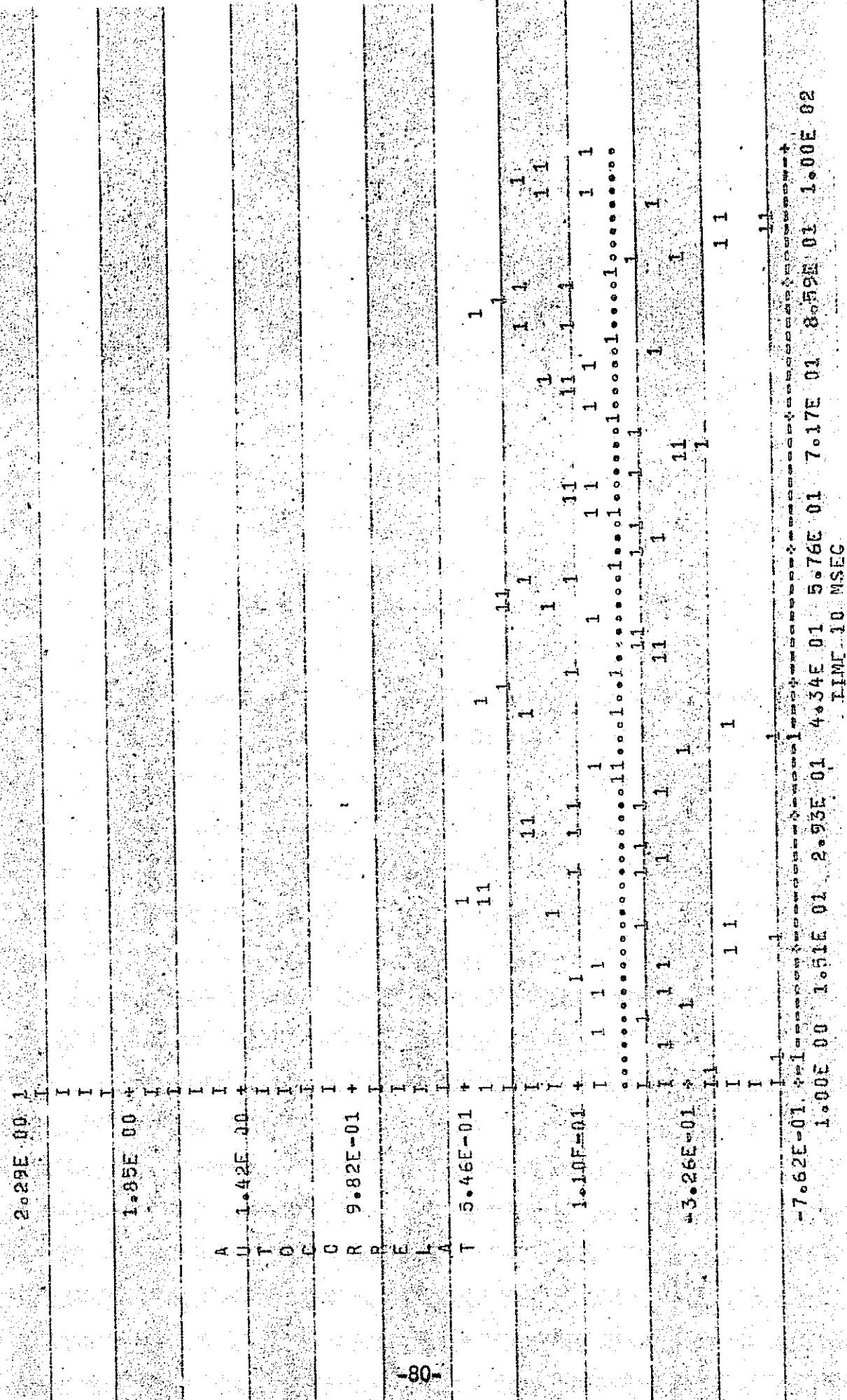


Figure E-2. Autocorrelation for Simulated Noise Phase for +20 dB SNR.

ORIGINAL PAGE
POOR QUALITY





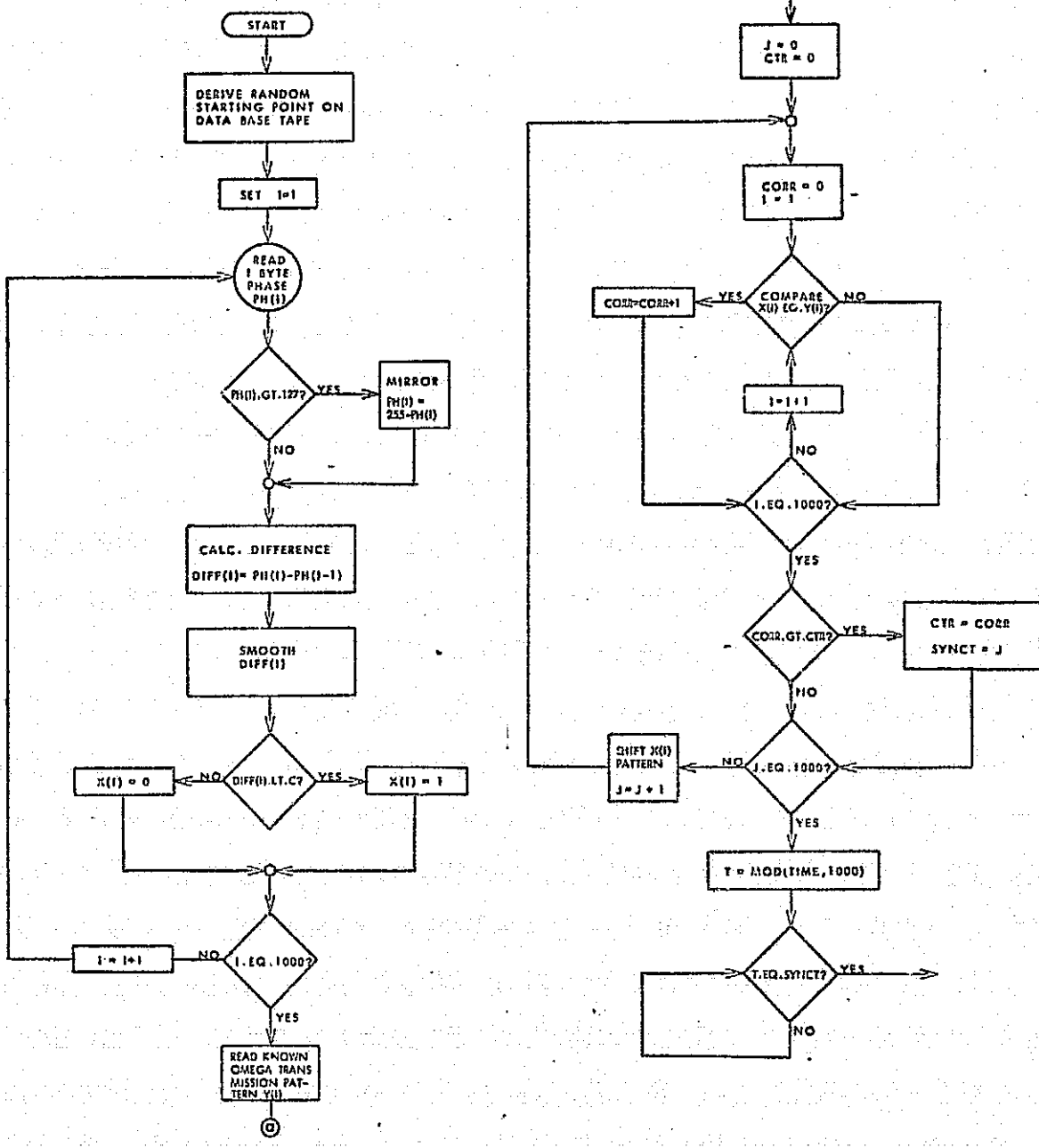


Figure E-5. Automatic Synchronization Flow Chart.

ORIGINAL PAGE IS
OF POOR QUALITY

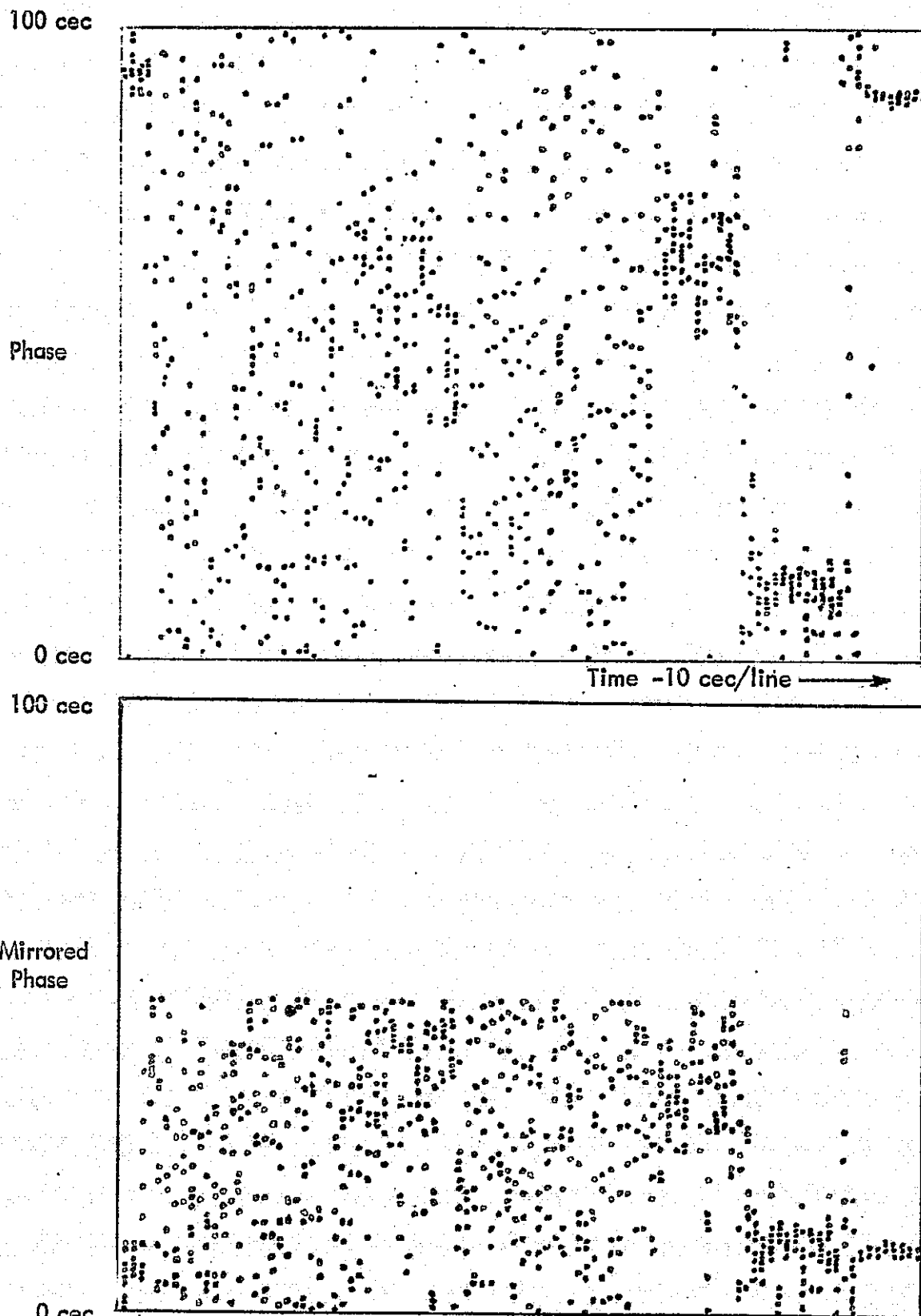


Figure E-6. 10 Second Frame of Data Plotted 10 Points Per Line.
Top = Real Data, Bottom = Mirrored Data.

frame of data and its corresponding mirrored values plotted 10 points per line.

Next, sample-to-sample differences are computed (see Figure E-7). Each difference value is compared to the predetermined threshold constant, and a vector of "1" and "0" is generated which represents the correlated and uncorrelated samples.

Before generating the vector of "1" and "0" by comparing phase differences to the threshold constant, it is helpful to smooth or average these differences.

Several types of smoothing filter were tried, including straight averager, one and two-sided exponential, and median three, with various amounts of points tried in each filter. The most successful was found to be the 9-point straight averager. Using this filter, the accumulated sum of nine differences is compared to nine times the threshold constant.

The threshold constant is most critical and has been determined (approximately) using the decision theory approach as well as by simulation. The constants determined by both techniques are in close agreement, thereby lending credence to the value chosen.

Having determined this constant, the vector of "1" and "0" is created by comparing each phase difference to it. Then the vector represents the received correlation pattern. This received correlation pattern can be compared (or cross-correlated) "bit-by-bit" in a bilevel correlation process with the stored unique Omega transmission pattern. A correlation counter is incremented for each coincidence of the stored and received patterns. Then the received pattern is shifted one bit and the entire cross-correlation process is repeated until all possible starting points have been tested. The number of shifts necessary to yield the highest

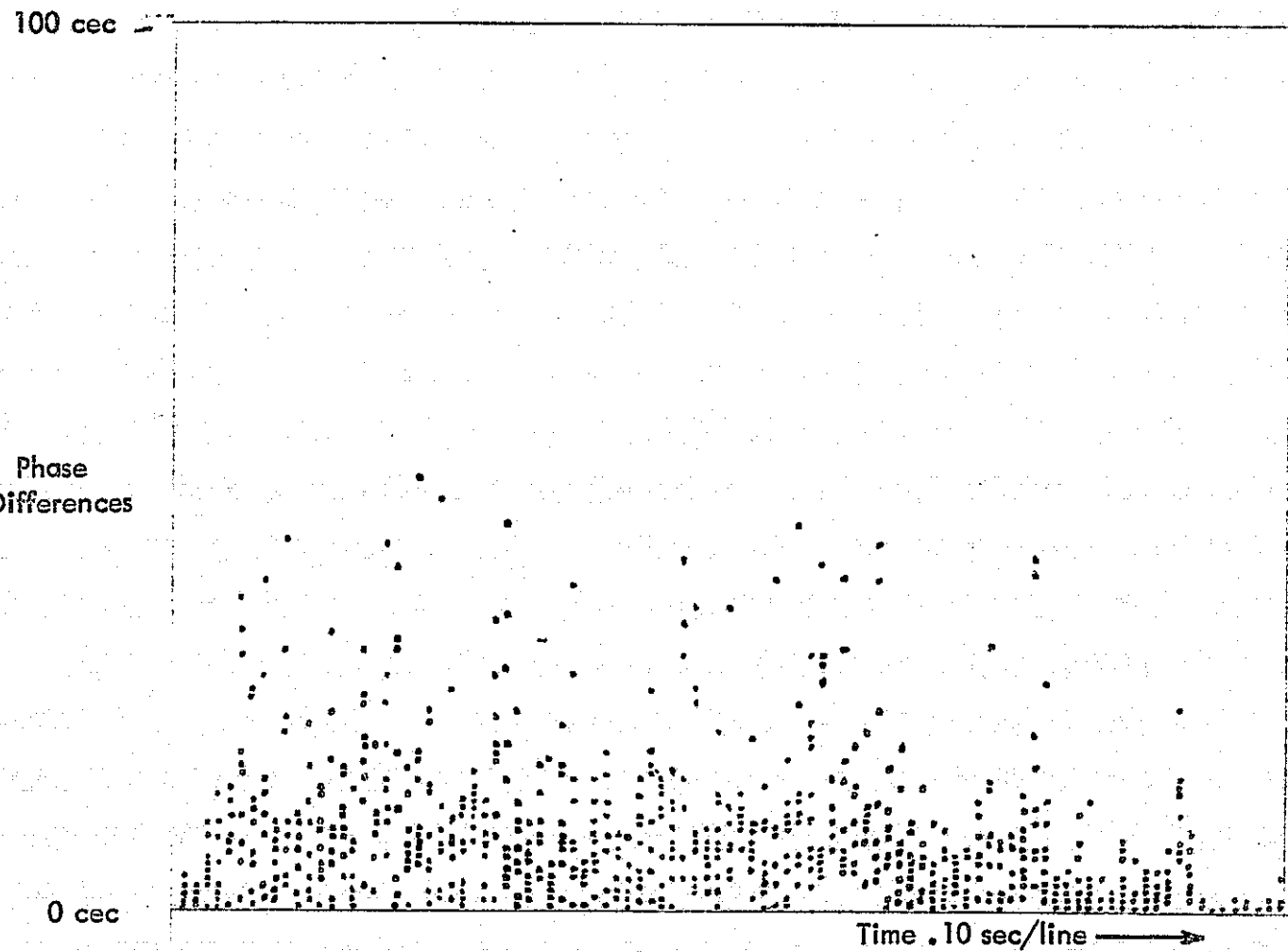


Figure E-7. Sample-to-Sample Phase Differences Plotted Ten Points Per Line.

correlation counter value is assumed to be the desired starting point for the "A" time-slot of the Omega data frame. After shifting the original data the determined number shifts, Figure 9 (in text) shows the Omega phase samples plotted ten points per line.

The routine's performance is improved if the operator inserts the stations which are expected to give coherent phase data samples (i.e. those stations received at or above 0 dB SNR). There was no noticeable difference in the routines ability to sync on ground or flight data, nor on data with the strong station North Dakota off-the-air. However, it is obvious that the technique depends on at least two stations being received above 0 dB SNR. Therefore, if only one station was sufficiently received the operator would have to identify which station it was. Note that if a two or three frequency system was available, only one station would be needed for sync (due to the unique lengths of adjacent time-slots).

3. Phase Locked Loop Simulation. Since the phase-tracking structure presented in the text (SMAPLL2) does not readily fit conventional models analyzed in the literature, computer simulation has been chosen rather than theoretical analysis to optimize loop parameters for the airborne Omega application. Computer-generated data has been used to optimize the parameters and specify SMAPLL2 performance. Finally, the real Omega data base was used to confirm expected tracking performance. Worst-case conditions of -20 dB SNR in the 30 Hz pre-detection bandwidth and 300 knots velocity of input signal phase in a direction radially to/from Omega stations have been simulated.

There are two SMAPLL2 response modes of interest: transient (including lock-up mode) and steady-state response. The transient response is evaluated by

beginning with the loop in lock with the input signal; then step and ramp input signals are applied. The response to these inputs is observed for the entire range of -20 dB to +20 dB input SNR. Steady-state response is evaluated by initializing the loop to a locked condition for various velocities of ramping input signals and calculating the loop's output error for each input signal after several hundred time-slots have been simulated. This response is also observed for the entire range of input SNR's.

A three-step approach has been utilized to "home-in" on the best choices for the parameters of first-order bandwidth and second-order gain via this simulation:

(1) With the loop in the first-order configuration (SMAPLL1),

the steady-state response for a range of first-order filter constants is examined. The value of loop filtering which results in an output standard deviation of or near zero over the desired operating range of input SNR is chosen.

(2) With the loop in the second-order configuration (SMAPLL2),

and using the chosen value of first-order filtering, the transient

response is examined for a wide range of second-order gains. It

is desirable to choose the value of second-order gain which results

in best transient response (fastest lock-up time). If this minimum

lock-up time is excessive, the data rate from the first-order filter

is too slow, and step #1 must be repeated to choose a lower value

of first-order filtering (i.e. to increase the loop's data rate).

(3) With the chosen values of first-order filtering and second-order

gain, the steady-state response of the SMAPLL2 to various velocity

ramp inputs is examined. If the output error standard deviation is not within acceptable limits over the SNR operating range, steps #1 and #2 are repeated. A greater amount of first-order filtering is chosen while sacrificing some lock-up time. This trade-off is the design optimization that must be made to achieve the best combination of transient and steady-state performance for each particular application.

Executing step #1 of this approach, the SMAPLL1 yields the graph in Figure E-8. This graph gives the SMAPLL1 steady-state response to zero-velocity input signals over the desired tracking range of SNR's. Since a first-order filter of 5 bits (32 counts) (or .02 Hz bandwidth) is seen to give an output standard deviation of near zero cec over the operating range of SNR, this value was initially chosen. However, it was found that this amount of first-order filtering reduced the data rate to below acceptable limits (i.e. in step #2 the lock-up time was found to be prohibitive). Therefore, the first-order filter constant of 4 bits (16 counts or .05 Hz bandwidth) was chosen.

The .05 Hz first-order loop bandwidth yields acceptable lock-up times for several values of second-order gain (again, determined by executing step #2). Therefore, the best value of second-order gain is chosen as that which provides best steady-state performance for ramp inputs over the desired range of input SNR's (step #3). Figure E-9 shows the steady-state response of SMAPLL2 to a zero-velocity input for several values of second-order gain. Figure E-10 gives the same data for a 300-knot input ramp. It can be seen that a value of .25 for the second-order gain gives the best response for both input velocities.

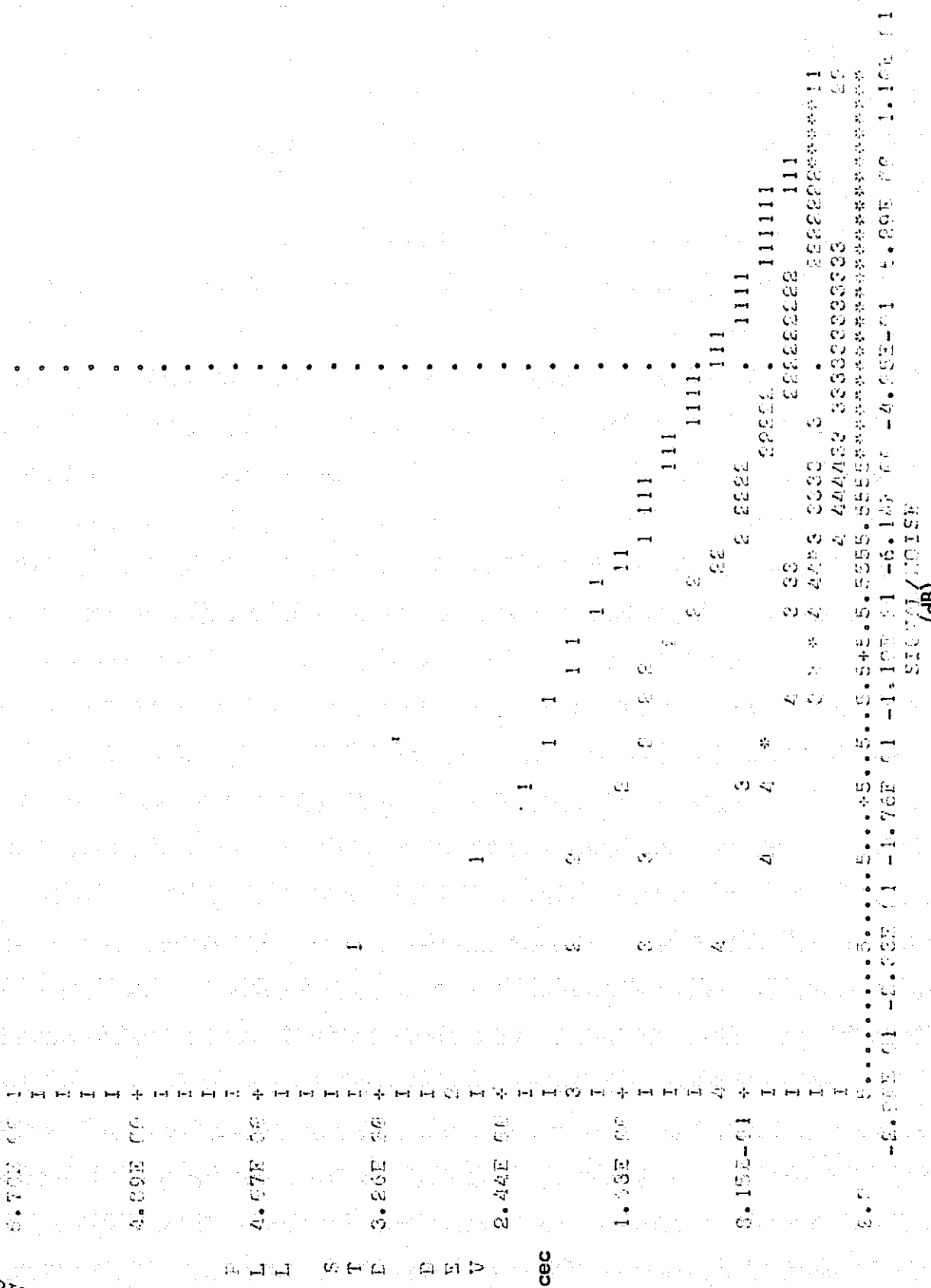


Figure E-8. SMAPLL Steady-State Response to O-Velocity Input for First-Order Filter Equal to 2 Counts (1), 4 counts (2), 8 counts (3), 16 counts (4) and 32 counts (5).

ORIGINAL PAGE IS
OF POOR QUALITY

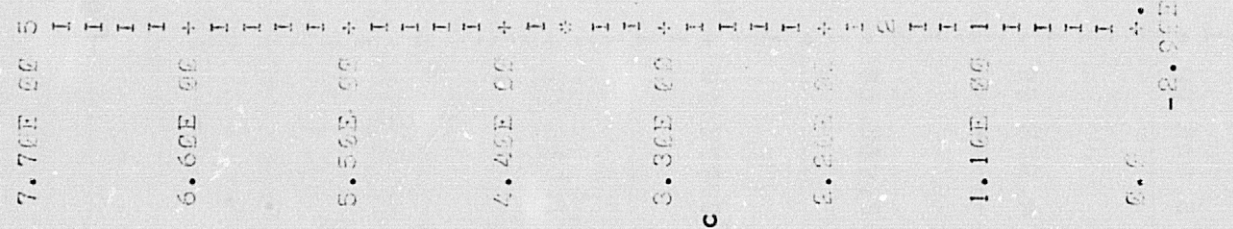
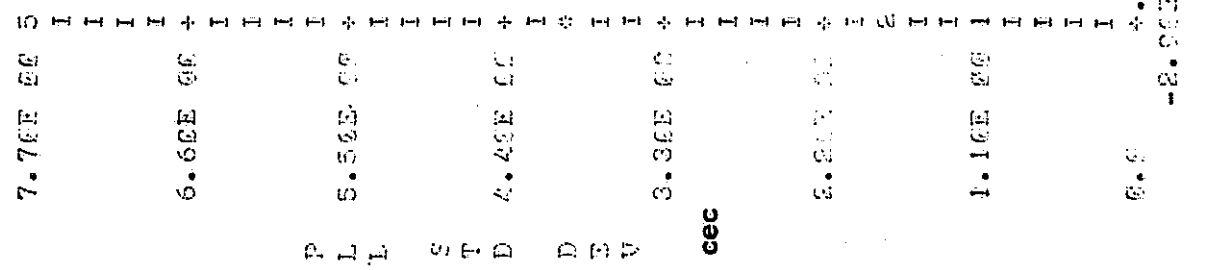


Figure E-9. SMAPLL2 Steady-State Response to Zero-Velocity Input for Second-Order Gain Equal to Zero (1), .125 (2), .250 (3), .375 (4), .500 (5).



ORIGINAL PAGE IS
OF POOR QUALITY

Figure E-9. SMAPLL2 Steady-State Response to Zero-Velocity Input for Second-Order Gain Equal to Zero (1), .125 (2), .250 (3), .375 (4), .500 (5).

6. .53E 63

+ 5. 94E 00

I I I I

P L 4. 95E 00

I I I I

S T 1. 5

D 3. 96E 00

I I *

D E I

V 2. 97E 00

I I *

1. 98E 00

I I *

9. 98E-01

I I *

6. 0

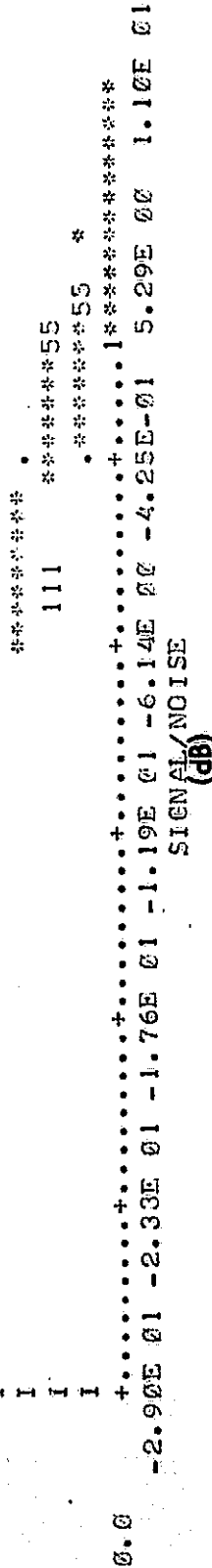


Figure E-10. SMAP112 Steady-State Response to 300-Knot Ramp Input for Second-Order Gain Equal to .125 (1), .250 (2), .375 (3), .500 (4), .625 (5).

The transient response of the optimized SMAPLL2 to 180 degree step and 300-knot ramp inputs is plotted in Figures E-11 and E-12. Since a general aviation aircraft is usually on the ground for at least ten minutes after aircraft power is turned on, a lock-up time of this length is considered acceptable.

The FORTRAN language listings for computer simulations of Omega noise, the automatic synchronization algorithm, and the performance simulation of the SMAPLL2 are given as Figures E-13, E-14 and E-15, respectively.

100 cec

Phase

0 cec

100 cec

Phase

0 cec

Time 1sec/line →

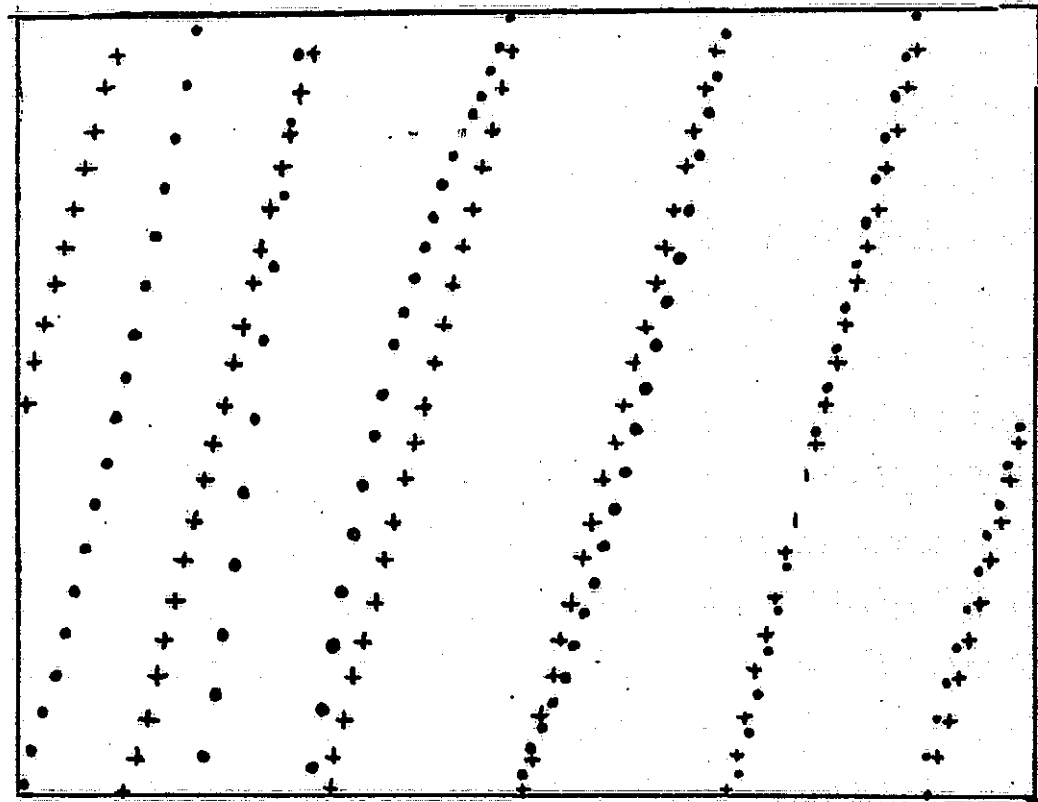
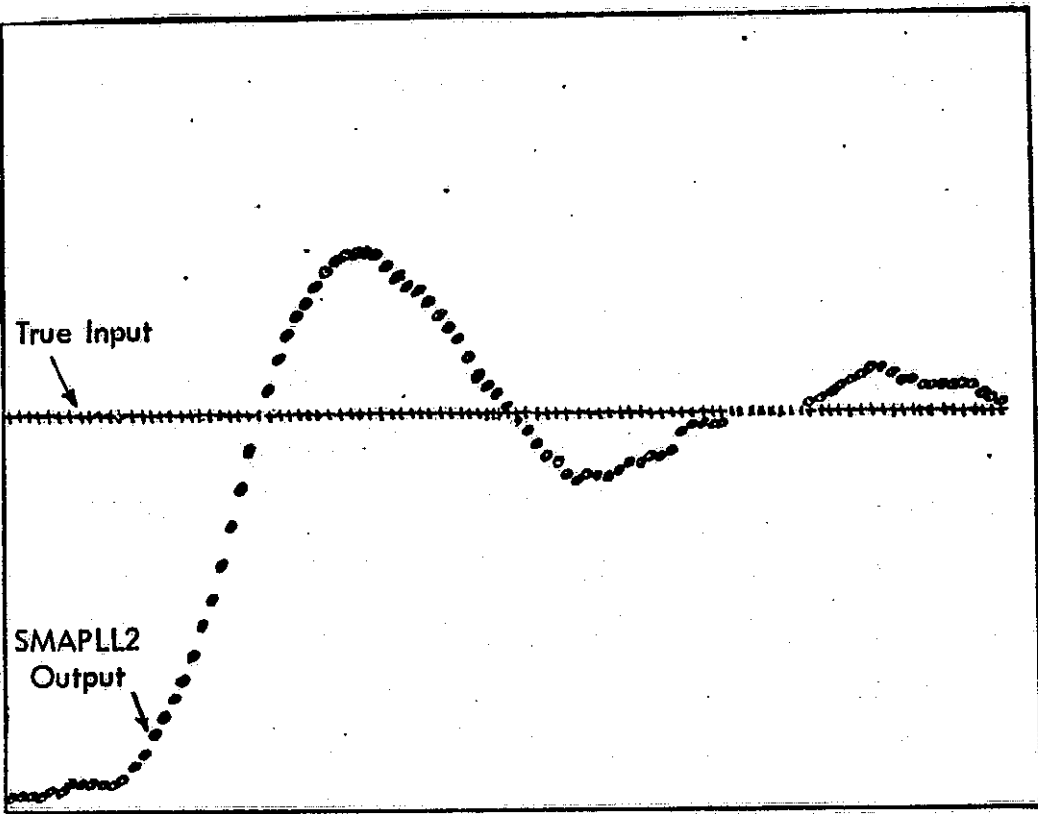


Figure E-11. SMAPLL2 Transient (Lock-Up Mode) Response to 180° Step (Top) and 300-Knot Ramp (Bottom) Input of -10 dB SNR.

100 cec

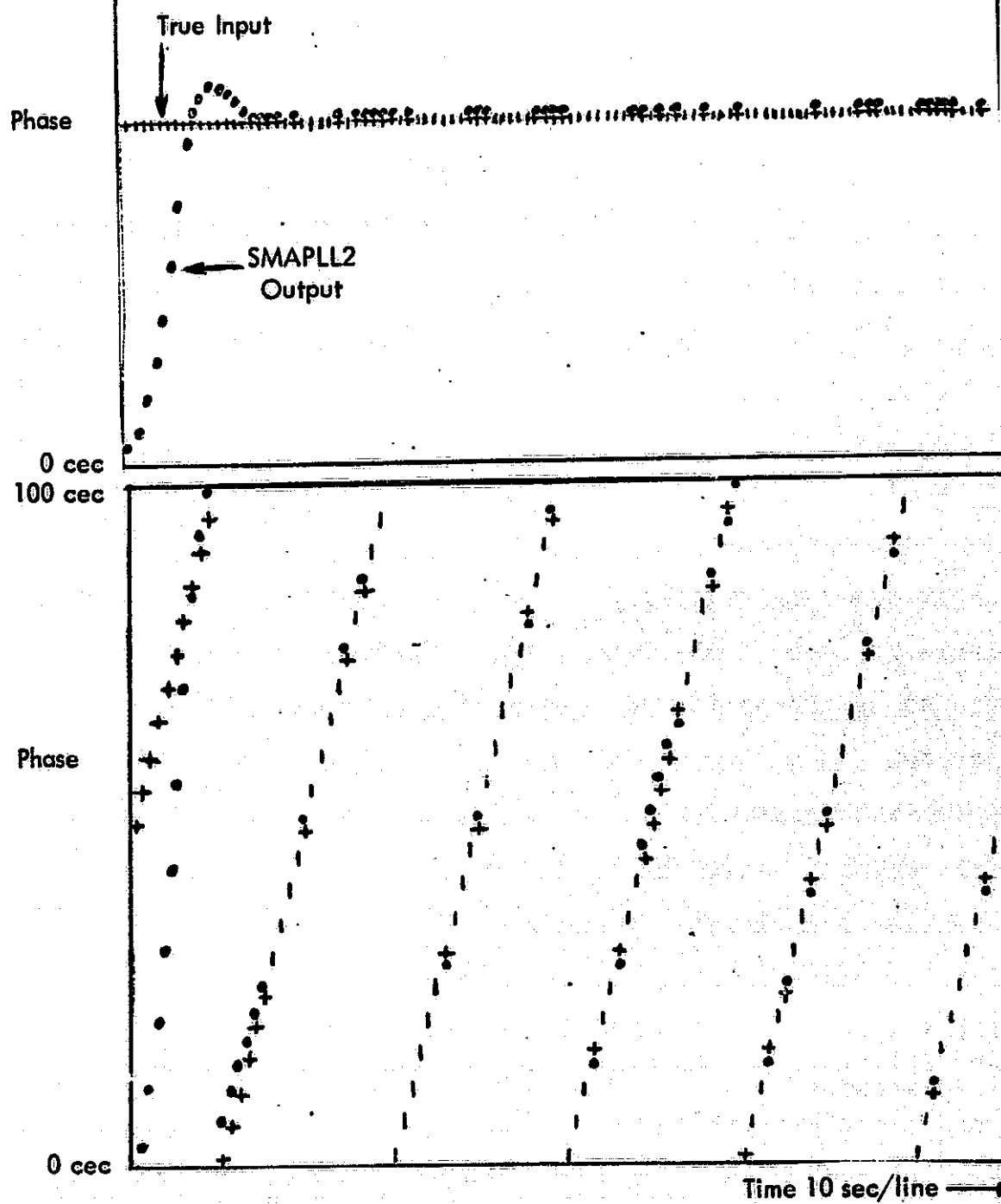


Figure E-12. SMAPLL2 Transient (Lock-Up Mode) Response to 180° Step (Top) and 300-Knot Ramp (Bottom) Inputs at +10 dB SNR.

```

C ROUTINE COMPUTES THE AUTOCORRELATION R(T) OF BOTH REAL OMEGA
C NOISE AND SIMULATED NOISE, AND PLOTS R(T) ON SEPARATE GRAPHS.
C
C ROUTINE COMPUTES AND PLOTS THE HISTOGRAMS OF BOTH REAL OMEGA
C NOISE AND SIMULATED NOISE PHASE ON SEPARATE GRAPHS.
C
C OPERATOR MUST SELECT SNR FOR SIMULATED NOISE BY SETTING A.
C OPERATOR MUST SELECT SNR FOR REAL OMEGA NOISE BY READING OVER
C DATA ON DATA BASE WHICH IS NOT WANTED.
C
C INTEGER TME
C REAL X(200),XX(100),R(100),XXA(100)
C REAL Y(200),YY(200),XXL(12),YYL(12),INTVL
C DATA XXL/'T','I','M','E',' ','1','0',' ','M','S','E','C'/
C DATA YYL/'A','U','T','O','C','O','R','R','E','L','A','T'/
C CALL RANDOM NUMBER GENERATOR AND LPF TO GET SIMULATED NOISE.
C SET PARAMETERS ON LPF TO SIMULATE 30HZ BW AND 100HZ SAMPLES.
C CALL INTGEN(5**11)
C BW=15.
C SMALLA=BW*12.57
C CAPA=2.*SQRT(4./SMALLA)
C INTVL=.01
C TME=200
C CALL GRANGE(YY,INTVL,CAPA,SMALLA,TME)
C CALL INTGEN(5**17)
C CALL GRANGE(Y,INTVL,CAPA,SMALLA,TME)
C TAKE ARCTAN OF RANDOM NUMBER RATIOS TO GET NOISE PHASE.
C A IS THE SIGNAL VOLTAGE AMPLITUDE: POWER SNR IS (A*A)/(2*N*N).
C
555 DO 5 I=1,200
A=0.001
X(I)=ATAN2(YY(I),(Y(I)+A))
C CHANGE UNITS FROM RADIANS TO CEC.
X(I)=X(I)/0.062831853
5 CONTINUE
C CALL AUTCOR SUBROUTINE TO COMPUTE AND PLOT R(T).
CALL AUTCOR(X)
PRINT 102
102 FORMAT(1X,'THIS IS THE AUTOCORRELATION FOR SIMULATED NOISE PHASE')
SNR=10.* ALOG10(A*A*.5)
BW2=2.*BW
PRINT 101,SNR,BW2,INTVL
101 FORMAT(1X,10X,'SNR = ',F6.2,' DB',10X,'BW = ',F3.0,' HZ',10X,
C'SAMPLING TIME = ',F5.3,' SEC')
C CALL TO HISTO SUBROUTINE PLOTS HISTOGRAM OF SIMULATED PHASE
C NOISE VS. PHASE IN CEC.
CALL HISTO(X)
PRINT 105
105 FORMAT(1X,'THIS IS THE HISTOGRAM OF SIMULATED NOISE PHASE VS.
C PHASE IN CEC.')
PRINT 101,SNR,BW2,INTVL
C
C CALL DATA SUBROUTINE TO RETURN REAL OMEGA PHASE PLUS NOISE.
C FIRST SELECT SNR OF REAL DATA BY READING OVER UNWANTED DATA.
500 CONTINUE
DO 1 I=1,130

```

Figure E-13. FORTRAN Program RSRAND Used to Analyze Real and Simulated Omega Noise.

```

CALL DATA(IOUT,6100)
ISKIP=I
1 CONTINUE
DO 2 I=1,100
CALL DATA(IOUT,6100)
X(I)=FLOAT(IOUT)
2 CONTINUE
LANE=255
HALFLN=128.
SUM=0
DO 6 I=1,100
SUM=SUM+X(I)
6 CONTINUE
AVE=SUM/100.
DO 7 I=1,100
X(I)=X(I)-AVE
IF(X(I).GT.HALFLN) X(I)=X(I)-LANE
IF(X(I).LT.-HALFLN) X(I)=X(I)+LANE
C CHANGE UNITS FROM 255THS TO CEC.
X(I)=X(I)*100./255.
7 CONTINUE
DO 3 I=1,900
CALL DATA(IOUT,6100)
3 CONTINUE
DO 4 I=101,200
CALL DATA(IOUT,6100)
X(I)=FLOAT(IOUT)
4 CONTINUE
SUM=0.
DO 8 I=1,100
SUM=SUM+X(100+I)
8 CONTINUE
AVE=SUM/100.
DO 9 I=101,200
X(I)=X(I)-AVE
IF(X(I).GT.HALFLN) X(I)=X(I)-LANE
IF(X(I).LT.-HALFLN) X(I)=X(I)+LANE
C CHANGE UNITS FROM 255THS TO CEC.
X(I)=X(I)*100./255.
9 CONTINUE
C CALL AUTCOR SUBROUTINE TO COMPUTE AND PLOT R(T).
CALL AUTCOR(X)
PRINT 103
103 FORMAT(1X,'THIS IS THE AUTOCORRELATION OF REAL OMEGA NOISE')
PRINT 104,ISKIP
104 FORMAT(1X,'THE DATA STARTED ',I5,'SAMPLES AFTER THE START OF
CTHE D TIME SLOT')
C CALL THE HISTOGRAM SUBROUTINE FOR REAL OMEGA NOISE PHASE .
CALL HISTO(X)
PRINT 106
106 FORMAT(1X,'THIS IS THE HISTOGRAM OF REAL OMEGA NOISE PHASE VS.
C PHASE IN CEC.')
PRINT 104,ISKIP
100 STOP
END

```

ORIGINAL PAGE IS
OF POOR QUALITY

Figure E-13. (Continued)

```

C      XXXXXXXXXXXXXXXXXXXXXXXXXXXXXXXXXXXXXXXXXXXXXXXXX
      SUBROUTINE AUTCOR(X)
      REAL X(200), XX(100), R(100), XXA(100), XXL(12), YYL(12)
      DATA XXL/'T','I','M','E',' ','1','0',' ','M','S','E','C'/
      DATA YYL/'A','U','T','O','C','O','R','R','E','L','A','T'/
C      COMPUTE AND PLOT AUTOCORRELATION OF THE NOISE.
      DO 10 I=1,100
      XX(I)=X(I)
 10 CONTINUE
C      COMPUTE AUTOCORRELATION FOR ONE VALUE OF TAU.
      DO 20 II=1,100
      SUM=0.
      DO 30 I=1,100
      IF(II.EQ.1)GO TO 16
      GO TO 15
 16 J=I
      GO TO 17
 15 J=I+II
 17 CONTINUE
      PROD=XX(I)*X(J)
      SUM=SUM+PROD
 30 CONTINUE
      R(II)=SUM/100.
 20 CONTINUE
      DO 50 I=1,100
      XXA(I)=FLOAT(I)
 50 CONTINUE
      CALL MMPLT(XXA,R,100,1,XXL,YYL)
      RETURN
      END
C      XXXXXXXXXXXXXXXXXXXXXXXXXXXXXXXXXXXXXXXXXXXXXXXXX
      SUBROUTINE GRANGE(Y,INTVL,A,SMALLA, TME)
      INTEGER TME
      REAL Y(5000), INTVL
      TAU=INTVL
      R=EXP(-SMALLA*TAU)
      PSI=(A*A*SMALLA)/4.
      CONS=SQRT(PSI*(1.-(R*R)))
      CALL ANORM(AN)
      Y(1)=AN*PSI
      DO 10 I=2,TME
      J=I-1
      CALL ANORM(AN)
 9 FORMAT(1X,10E10.2)
      Y(I)=AN*CONS+R*Y(J)
 10 CONTINUE
      RETURN
      END
C      XXXXXXXXXXXXXXXXXXXXXXXXXXXXXXXXXXXXXXXXXXXXXXXXX
      SUBROUTINE DATA(IOUT,*)
C... DEBLOCKS OMEGA TAPE DATA AND RETURNS ONE DATA SAMPLE TO MAIN PROGRAM
C...
C... ON TAPE EOF, RETURNS TO *
C...
C... R. W. LILLEY, AVIONICS, JANUARY, 1976

```

Figure E-13. (Continued)

```

INTEGER I/O/
LOGICAL*1 IN(1000),INB(4)
EQUIVALENCE(IL,INE(1))
II=0
IF(I.EQ.0)GO TO 10
30 INB(4)=IN(I)
IOUT=II
I=I+1
IF(I.GT.1000)I=0
RETURN

C...
10 I=1
17 READ(11,5,END=20) IN
 5 FORMAT(5(200A1))
 GO TO 30

C...
20 RETURN 1
C...
 ENTRY START
C...STARTS DATA OUTPUT AT A RANDOM POINT ON TAPE. READS UP TO
C... 25 RECORDS, AND STARTS BETWEEN BYTE 1-1000.
C...
C...SEED WITH UNDEFINED VARIABLE
 IF(IQ.EQ.0)IQ=5**13
 IQ=IABS(IQ/2)*2+1
 CALL INTGEN(IQ)
 RETURN
 ENTRY RAND(NBYTE)
 CALL IRAND(NREC,24)
 CALL IRAND(NBYTE,999)

C...
 DO 51 IR=1,NREC
51 READ(11,5)IN
 I=NBYTE+1
 PRINT 52,NREC,NBYTE
52 FORMAT(' THIS RUN STARTS AFTER ',/1X,I2,' SKIPPED RECORDS AND',
 *1X,I4,' SKIPPED BYTES ')
 GO TO 17
END

C XXXXXXXXXXXXXXXXXXXXXXXXXXXXXXXXXXXXXXXXXXXXXXX
C SUBROUTINE ILPF(Y,TAU,A,BW,NUM)
C PRINT 14,TAU,BW
14 FORMAT(1X,2F10.3)
C ROUTINE RETURNS 'NUM' IDEAL LOW-PASS-FILTERED, GAUSSIANLY
C DISTRIBUTED RANDOM VARTABLES.

C
C Y IS THE VECTOR OF SIN(X)/X CORRELATED NUMBERS; TAU IS THE INDEP-
C ENDENT TIME SHIFT VARIABLE; A IS A WASTE; BW IS THE BANDWIDTH
C OF THE FILTER (ONE-SIDED); NUM IS THE NUMBER OF NUMBERS RETURNED.
REAL Y(5000)
R=(SIN(6.283185*BW*TAU))/(6.283185*BW*TAU)
CONS=SQRT(ABS(1.-(R*R)))
PRINT 12,R,CONS
12 FORMAT(1X,2F10.3)
CALL ANORM(AN)

```

Figure E-13. (Continued)

```

Y(1)=AN
DO 10 I=2,NUM
J=I-1
CALL ANORM(AN)
Y(I)=AN*CONS+R*Y(J)
11 FORMAT(1X,2F8.2)
10 CONTINUE
RETURN
END
C XXXXXXXXXXXXXXXXXXXXXXXXXXXXXXXXXXXXXXXXXXXXXXXXX
C SUBROUTINE HISTO(X)
C ROUTINE PLOTS HISTOGRAM OF NUMBERS IN VECTOR (X(200)).
INTEGER IX(200)
REAL X(200), YA(101), XL(12), YL(12)
DATA XL/'N','O','I','S','E',' ',' ','P','H','A','S','E',' ',' '
DATA YL/'H','I','S','T','O','G','R','A','M',' ',' ',' ',' '
DO 10 I=1,200
IX(I)=INT(X(I))
10 CONTINUE
C CREATE X-AXIS VECTOR OF -50. TO 50. CEC.
DEV=-50.
DO 60 I=1,101
YA(I)=0.
XA(I)=DEV
DEV=DEV+1.
60 CONTINUE
C CREATE Y-AXIS VECTOR OF FREQ. OF OCCURENCE OF EACH CEC VALUE.
DO 70 I=1,200
DO 80 J=1,101
IF(IX(I).EQ.INT(XA(J))) YA(J)=YA(J)+1.
80 CONTINUE
70 CONTINUE
C NORMALIZE RELATIVE FREQ. OF OCCURENCE.
DO 90 I=1,101
YA(I)=YA(I)/200.
90 CONTINUE
CALL MMPLT(XA,YA,101,1,XL,YL)
RETURN
END

```

Figure E-13. (Continued)

```

C OMEGA SENSOR PROCESSOR SIMULATION.
C MAIN PROGRAM
C
C R. SALTER, AVIONICS ENGINEERING CENTER, MARCH 1976
C ****
C OMEGA AUTO-SYNC ROUTINE
C INTEGER LOP(1000)
C INTEGER X(1000), DIFF(1000), C, LIVSLT(1000), CORR, CTR, SYNCPT
C INTEGER SLOT(1000)
C INTEGER SMDIFF(1000)
C INTEGER STA(8)
C INTEGER WITHIN, V(1000)
C INTEGER IMMIR(1000)
C INTEGER PHASE(8)
C INTEGER XX(2048), YY(2048), XL(12), YL(12)
C INTEGER*2 TSLOT(8) /90,100,110,120,90,110,120,100/
C INTEGER LCW(8), PHI
C INTEGER CPHI(8,1000), CCPHI(1000)
C INTEGER II(8), SOGAIN(8), VEL(8), RATE
C INTEGER CONST, SUMDIF(8), VAR(8,1000), VVAR(1000)
C DERIVE RANDOM STARTING POINT ON DATA-BASE TAPE
C SKIP 'NSKIP' FILES ON DATA BASE TAPE.
C NSKIP=4
C CALL START
C CALL RAND(NBYTE)
C TAKE ONE RECORD (1000 BYTES) OF DATA AND MIRROR IT
C DO 1 I=1,1000
C CALL DATA(X(I),650)
C CALL MIRR(X(I),INMIR(I))
1 CONTINUE
CALL PLOT10(X,1)
CALL PLOT10(INMIR,1)
C OBTAIN A 1000 BYTE VECTOR OF DIFFERENCES TO BE USED AS A MEASURE
C OF PHASE COHERENCE IN EACH 10 MSFC SAMPLE SLOT
CALL DIFFER(INMIR,DIFF)
CALL PLOT10(DIFF,1)
4 FORMAT(1X,25I4)
C SMOOTH DIFFERENCES (OPTIONAL).
CALL SMOOTH(DIFF,SMDIFF)
PRINT 151
151 FORMAT(1X,'9 PT. STRAIGHT AVERAGING SMOOTHER INSTALLED')
C GENERATE A 1000 BYTE VECTOR OF 1'S AND 0'S REPRESENTING SIGNAL
C AND NOISE SLOTS
C MUST SET THRESHOLD "C" TO COMPARE DIFFERENCES TO.
C =120
12 CONTINUE
CALL COMPAR(C,SMDIFF,LIVSLT)
C PERFORM BILEVEL CORRELATION OF KNOWN OMEGA PATTERN TO LIVE DATA
CORR=0
J=0
CALL PATERN(SLOT)
10 CALL BICOR(LIVSLT,CTR,SLOT)
I=J+1
IF(CTR.GE.CORR) CORR=CTR

```

ORIGINAL PAGE IS
OF POOR QUALITY

Figure E-14. FORTRAN Program RSOSP Used to Simulate Automatic Synchronization Routine.

```

IF (CTR.EQ.COHR) SYNCPT=J
J=J+1
IF (J.GT.1000) GO TO 100
NSHIFT=1
CALL SHIFT(LIVSLT,NSHIFT)
GO TO 10
C PRINT CORRELATION VALUE AND SYNCPOINT VALUE OBTAINED.
100 PRINT 110,C,COPR,SYNCPT
110 FORMAT(1X,'C = ',I3,3X,' CORR = ',I4,3X,'SYNCPT = ',I4)
WITHIN=10*(380+NBYTE-SYNCPT)
PRINT 13,WITHIN
13 FORMAT(1X,'SYNC WITHIN',I5,1X,'MSEC')
NSHIFT=SYNCPT
C SHIFT VECTOR OF PHASE VALUES TO SYNCPOINT AND PLOT THEM OUT.
CALL SHIFT(X,NSHIFT)
CALL PLOT10(X,1)
GO TO 50
PRINT 111
111 FORMAT(1X,'ALL STATIONS ON ALE')
C RESET DATA BASE TAPE TO SYNCPOINT.
NSHIFT=1000-NSHIFT
DO 14 I=1,NSHIFT
CALL DATA (IOUT,850)
14 CONTINUE
***** ****
C OMEGA BURST FILTER ROUTINE.
C PERFORM BURST PLL FILTERING TO INCOMING OMEGA PHASE MEASUREMENTS.
DO 18 I=1,8
LCW(I)=0
SOGAIN(I)=0
VEL(I)=0
18 II(I)=1
C READ 1000 OMEGA FRAMES.
DO 26 X=1,1000
C READ 8 TIME SLOTS IN EACH OMEGA FRAME.
19 DO 25 I=1,8
JJ=TSLOT(I)
C READ TSLOT(I) PHASE MEASUREMENTS IN EACH TIME SLOT.
LPCTR=0
RATE=0
SUMDIF(I)=0
DO 20 J=1,JJ
CALL DATA(PHI,850)
CONST=2
CALL SMAPLL(PHI,LPCTR,LCW(I),CONST,RATE,SUMDIF(I))
IDIF=SUMDIF(I)
LLCW=LCW(I)
21 FORMAT(1X,5I10)
20 CONTINUE
22 FORMAT(1X)
CPHI(I,II(I))=LCW(I)
C COMPUTE SIGNAL VARIANCE IN TIMESLOT.
SUMDIF(I)=SUMDIF(I)/TSLOT(I)
VAR(I,II(I))=SUMDIF(I)
IF (RATE.LT.0) VEL(I)=VEL(I)-RATE*SOGAIN(I)

```

Figure E-14. (Continued)

```

IF(RATE.GT.0) VEL(I)=VEL(I)+RATE*SOGAIN(I)
LCW(I)=LCW(I)+VEL(I)
IF(LCW(I).LT.0) LCW(I)=256+LCW(I)
IF(LCW(I).GT.255) LCW(I)=LCW(I)-256
II(I)=II(I)+1
C SKIP SAMPLES FROM .2 SEC. NOISE GAP.
DO 23 K=1,20
23 CALL DATA(PHI,550)
25 CONTINUE
26 CONTINUE
C DUMP EACH STATION'S TIMESLOT PHASE ESTIMATE INTO VECTOR TO BE FLO-
C TTED BY PLOT1 SUBROUTINE.
30 DO 40 I=1,8
DO 35 J=1,1000
CCPHI(J)=CPHI(I,J)
C DUMP EACH STATION'S VARIANCE INTO A VECTOR TO BE PRINTED OUT.
VVAR(J)=VAP(I,J)
35 CONTINUE
***** ****
C OMEGA LOP ROUTINE
PRINT 36,I
36 FORMAT(' PHASE OF STATION ',I2,' MINUS CLOCK')
PRINT 60,CCPHI
60 FORMAT(1X,10I10)
PRINT 61,I
61 FORMAT(' SIGNAL VARIANCE OF STATION ',I2)
PRINT 60,VVAR
CALL PLOT1(CCPHI,1)
40 CONTINUE
ISIA1=3
ISIA2=4
CALL LOPO(CPHI,ISIA1,ISIA2,LOP)
C PLOT LOP SPECIFIED BY ISIA1-ISIA2.
CALL PLOT1(LOP,1)
STOP
50 STOP 50
END
SUBROUTINE DIFFER(X,DIFF)
OMEGA AUTO-SYNC SIMULATION
C
C ROUTINE TAKES 1000 BYTE VECTOR OF INPUT PHASE DATA AND RETURNS A
C DIFFERENCE VALUE WHICH IS INVERSELY PROPORTIONAL TO THE PHASE
C COHERENCE (SIGNAL STRENGTH) IN EACH 10 MSEC SAMPLE SLOT.
C
C R. SALTER, AVIONICS ENGINEERING CENTER, MARCH 1976
C
INTEGER DIFF(1000),X(1000)
DO 20 I=1,999
J=I+1
DIFF(I)=IABS(X(I)-X(J))
20 CONTINUE
DIFF(1000)=IABS(X(1)-X(1000))
RETURN
END
SUBROUTINE COMPAR(C,DIFF,LIVSLT)

```

ORIGINAL PAGE IS
OF POOR QUALITY

Figure E-14. (Continued)

C OMEGA AUTO-SYNC SIMULATION

C ROUTINE COMPARES 1000 BYTE VECTOR OF DIFFERENCES TO THRESHOLD
C CONSTANT AND RETURNS A BILEVEL VECTOR CONTAINING 1'S FOR SIGNAL
C AND 0'S FOR NOISE

C E. SALTER, AVIONICS ENGINEERING CENTER, MARCH 1976

```
INTEGER C,DIFF(1000),LIVSLT(1000)
DO 10 I=1,1000
IF(DIFF(I).GE.C)LIVSLT(I)=0
IF(DIFF(I).LT.C)LIVSLT(I)=1
```

10 CONTINUE

RETURN

END

SUBROUTINE BICOR(LIVSLT,CTR,SLOT)

OMEGA AUTO-SYNC SIMULATION

C ROUTINE PERFORMS BILEVEL CROSS-CORRELATION OF OMEGA TRANSMISSION
C PATTERN OFF AIR WITH THE KNOWN PATTERN GENERATED BY "PATTERN" ,
C AND RETURNS VALUE PROPORTIONAL TO CORRELATION

C R. SALTER, AVIONICS ENGINEERING CENTER, MARCH 1976

```
INTEGER LIVSLT(1000),CTR
INTEGER SLOT(1000)
CTR=0
DO 10 I=1,1000
IF(LIVSLT(I).EQ.SLOT(I))CTR=CTR+1
```

10 CONTINUE

RETURN

END

SUBROUTINE SHIFT(LIVSLT,NSHIFT)

OMEGA AUTO-SYNC SIMULATION

C ROUTINE SHIFTS LIVSLT VECTOR "NSHIFT" SLOTS TO THE RIGHT.

C R. SALTER, AVIONICS ENGINEERING CENTER, MARCH 1976

C MODIFIED BY R. SALTER, APRIL, 1976

```
INTEGER LIVSLT(1000),AUXSLT(1000)
DO 30 K=1,NSHIFT
DO 10 I=2,1000
J=I-1
AUXSLT(I)=LIVSLT(J)
```

10 CONTINUE

AUXSLT(1)=LIVSLT(1000)

DO 20 I=1,1000

LIVSLT(I)=AUXSLT(I)

20 CONTINUE

30 CONTINUE

RETURN

END

SUBROUTINE PATERN(SLOT)

OMEGA AUTO-SYNC SIMULATION

Figure E-14. (Continued)

```

C ROUTINE CREATES KNOWN OMEGA TRANSMISSION PATTERN
C
C R. SALTER, AVIONICS ENGINEERING CENTER, MARCH 1976
C
1 INTEGER SLOT(1000),STA(8)
1 INTEGER JJ(8)/1,111,231,361,501,631,741,881/
1 INTEGER KK(8)/90,210,340,480,610,720,860,980/
1 READ(1,1)STA
1 FORMAT(8I1)
1 DO 10 I=1,8
1 J=JJ(I)
1 K=KK(I)
100 DO 110 L=J,K
1 SLOT(L)=STA(I)
110 CONTINUE
1 M=K+1
1 N=K+20
1 DO 120 L=M,N
1 SLOT(L)=0
120 CONTINUE
10 CONTINUE
130 RETURN
END
SUBROUTINE DATA(IOUT,*)
C...DEBLOCKS OMEGA TAPE DATA AND RETURNS ONE DATA SAMPLE TO MAIN PROGRAM
C...
C...ON TAPE EOF, RETURNS TO *
C...
C... R. W. LILLEY, AVIONICS, JANUARY, 1976
1 INTEGER I/O/
1 LOGICAL*1 IN(1000),INB(4)
1 EQUIVALENCE(II,INB(1))
1 II=0
1 IF(I.EQ.0)GO TO 10
30 INB(4)=IN(I)
1 IOUT=II
1 I=I+1
1 IF(I.GT.1000)I=0
1 RETURN
C...
10 I=1
17 READ(11,5,END=20)IN
5 FORMAT(5(20A1))
1 GO TO 30
C...
20 RETURN 1
C...
ENTRY START
C...STARTS DATA OUTPUT AT A RANDOM POINT ON TAPE. READS UP TO
C... 25 RECORDS, AND STARTS BETWEEN BYTE 1-1000.
C...
C...SEED WITH UNDEFINED VARIABLE
IF(IQ.EQ.0)IQ=5**13
IQ=IABS(IQ/2)*2+1

```

Figure E-14. (Continued)

```

CALI INTGEN(IQ)
RETURN
ENTRY RAND(NBYTE)
CALL IPAND(NREC,24)
CALL IRAND(NBYTE,999)

C...
DO 51 IR=1,NREC
51 READ(11,5) IN
I=NBYTE+1
PRINT 52,NREC,NBYTE
52 FORMAT(' THIS RUN STARTS AFTER ',/1X,I2,' SKIPPED RECORDS AND',
*1X,I4,' SKIPPED BYTES ')
GO TO 17
END
SUBROUTINE MIRR(IN,INMIR)
C...OMEGA DATA SIMULATION
C...ROUTINE REFLECTS COUNTS 128-255 MIRRORRED TO 127-0
C...
C... R. W. LILLEY, AVIONICS, JANUARY, 1976
C MODIFIED BY P. SALTER, APRIL, 1976
IF(IN.LE.127)GO TO 10
INMIR=255-IN
RETURN
10 INMIP=IN
RETURN
END
SUBROUTINE SMOOTH(DIFF,SMDIFF)
OMEGA AUTO-SYNC SIMULATION
C
C ROUTINE SMOOTH SMOOTH VECTOR OF 1000 DIFFERENCES BY PASSING EACH SAMPLE
C POINT THRU A 9 POINT EXPONENTIAL FILTER
C
C P. SALTER, AVIONICS ENGINEERING CENTER, MARCH 1976
C
INTEGER SMDIFF(1000)
INTEGER DIFF(1000)
DO 10 I=1,1000
IF(I.LT.5)GO TO 20
IF(I.GT.995)GO TO 30
J=I-1
K=I-2
L=I-3
M=I-4
25 JJ=I+1
KK=I+1
LL=I+3
MM=I+4
C TEMPORARY SMOOTHER --- NINE PT. STRAIGHT AVERAGER.
C USES 4 PTS. BEHIND , 4 PTS. AHEAD, AND CURRENT PT. EQUALLY WEIGHT
35 SMDIFF(I)=DIFF(I)+DIFF(J)+DIFF(K)+DIFF(L)+DIFF(M)+DIFF(JJ)+DIFF
*(KK)+DIFF(LL)+DIFF(MM)
10 CONTINUE
GO TO 40
20 J=1000-MOD(1000-I+1,1000)
K=1000-MOD(1000-I+2,1000)

```

Figure E-14. (Continued)

Figure E-14. (Continued)

```

RETURN
END
SUBROUTINE SMAPL(PHI,LPCTR,PHIREF,CONST,RATE,SUMDIF)
ROUTINE PERFORMS DIGITAL FILTERING ON INCOMING OMEGA PHASE
MEASUREMENTS( PLL, BURST FILTER). OPERATION AND TIME CONSTANTS
CLOSELY RESEMBLE HARDWARE MAPLL.
''CONST'' IS A VALUE TO BE SPECIFIED FOR MAX. LOOP CTR. VALUE
BEFORE ADJUSTING PHIREF. (LOOP TIME CONSTANT OF AMOUNT OF INTEGRA.

R. SALTER, AVIONICS ENGINEERING CENTER, JULY 1976.

INTEGER PHI,PHIREF,CONST,RATE,LPCTR
INTEGER DIFF,SUMDIF
COMPARE INCOMING PHASE TO LOOP CONTROL WORD(LCW) (PHASE REFERENCE
DIFF=PHI-PHIREF
KEEP A RUNNING SUM OF ABSOLUTE VALUES OF DIFFERENCES TO INDICATE
SIGNAL VARIANCE.
IF(DIFF) 10,50,20
CHECK FOR EDGE OF LANE AMBIGUITY.
10 IF(DIFF.LT.-128) GO TO 25
SUMDIF=SUMDIF+IABS(DIFF)
GO TO 40
20 IF(DIFF.GT.128) GO TO 35
SUMDIF=SUMDIF+IABS(DIFF)
GO TO 30
INCREMENT LOOP COUNTER.
30 LPCTR=LPCTR+1
EXAMINE LPCTR FOR INCR. MORE THAN 'CONST' TIMES CORRELATED.
IF(LPCTR.LE.CONST) RETURN
LPCTR=0
PHIREF=PHIREF+1
RATE=RATE+1
CHECK FOR MODULO 255 LANE COUNTS.
IF(PHIREF.GT.255) PHIREF=0
RETURN
DECREMENT LOOP COUNTER.
40 LPCTR=LPCTR-1
EXAMINE LPCTR FOR DECR. MORE THAN 'CONST' TIMES CORRELATED.
IF(LPCTR.GE.-CONST) RETURN
LPCTR=0
PHIREF=PHIREF-1
RATE=RATE-1
CHECK FOR MODULO 255 LANE COUNTS.
IF(PHIREF.LT.0) PHIREF=255
50 RETURN
25 PHI=PHI+256
DIFF=PHI-PHIREF
SUMDIF=SUMDIF+IABS(DIFF)
GO TO 30
35 PHI=PHI-256
DIFF=PHI-PHIREF
SUMDIF=SUMDIF+IABS(DIFF)
GO TO 40
END
SUBROUTINE PLOT1(X,LL)
```

ORIGINAL PAGE IS
OF POOR QUALITY

Figure E-14. (Continued)

C ROUTINE PLOTS DATA VECTOR "X" WITH STARS, ONE POINT PER LINE ON A
C 1-128 SCALE.

C IF VALUES OF "X" CAN FALL BETWEEN 128-255, SET LL=1 AND ROUTINE
C WILL HALVE EACH VALUE BEFORE PLOTTING. OTHERWISE, IF VALUES OF
C "X" ARE ALL LESS THAN 128, ROUTINE WILL PLOT STRAIGHT VALUES IF
C LL=0

C MUST DIMENSION X = VECTOR OF VALUES TO BE PLOTTED.

C R.W. LILLEY, AVIONICS, JANUARY, 1976

C MODIFIED BY R. SALTER, AVIONICS, APRIL, 1976.

INTEGER BK/' /,ST/'**/,LIN(128)

INTEGER X(1000)

DO 10 I=1,128

10 LIN(I)=BK

DO 20 I=1,200

IF(LL.EQ.0)GO TO 12

MM=X(I)/2+1

GO TO 13

12 CONTINUE

MM=X(I)

13 CONTINUE

LIN(MM)=ST

PRINT 11,LIN

11 FORMAT(1X,128A1)

LIN(MM)=BK

20 CONTINUE

RETURN

END

Figure E-14. (Continued)

Figure E-15. FORTRAN Program RSSIM Used to Simulate SMAPLL2 and Evaluate Performance.

```

C      PERFORM CALCULATION OF LOOP VARIANCE FOR SEVERAL SNRS
C      SEVERAL TIMES. EACH TIME INCREASING THE LOOP TIME CONSTANT
C      (M) (MORE INTEGRATION OR SKIPPED BITS IN THE COUNTER).
DO 45 MM=1,8
PRINT 46,SOGAIN
46 FORMAT(1X,'SECOND ORDER GAIN = ',F5.2)
DO 40 M=1,1
CONST=16
PRINT 11,CONST
11 FORMAT(3X,'LOOP CONSTANT = ',I5)
C      PERFORM CALLS TO SMAPL AND CALCULATE OUTPUT VARIANCE FOR
C      100 GIVEN SNRS . INCREASE SNR EACH AROUND THIS LOOP.
DO 30 L=1,1
C      CALCULATE NEW NOISE PHASE INPUTS FOR EACH SNR.
3 DO 10 I=1,5000
G(I)=ATAN2(GR(I),(GA(I)+A))
G(I)=G(I)*57.2957795
114 FORMAT(1X,E9.1)
112 FORMAT(1X,E12.3)
NOISE(I)=INT(G(I))
10 CONTINUE
IF(COMTRL.LT.10.)GO TO 14
C      CALL HIST1 SUBROUTINE TO PLOT HISTOGRAM OF INPUT NOISE PHASE.
CALL HIST1(NOISE,5000,SNR,VAR)
14 CONTINUE
K=TSLOT
ERPSUM=0
SUMDIF=0
CTR2=0
C      CALCULATE RATE FOR 2ND ORDER LOOP STEADY STATE TRACKING FOR GIVEN
C      VELOCITY SIGNAL INPUT. (I.E. START LOOP OUT BEING LOCKED IN SS).
IF(SOGAIN.EQ.0.)GO TO 17
RATE=INT(VEL*FLOAT(LEVELS)/(5760.*SOGAIN))
17 CONTINUE
PHIOUT=0
BATF=0
LPCTR=0
JJ=1
J=0
VEL=VEL1
DELTA=INT(VEL/16.)
PHASE=0
C      CALCULATE PHASE INPUT TO LOOP BY ADDING TRUE PHASE PLUS NOISE PHAS
15 DO 20 I=1,K
PHI(I+J)=PHASE
PHIIN=PHI(I+J)+NOISE(I+J)
PHIIN=MOD(PHIIN,360)
IF(PHIIN.LT.0) PHIIN=PHIIN+360
X=FLOAT(PHIIN)
CALL QUANT(X,LEVELS)
PHIIN=INT(X)
PHIIN=MOD(PHIIN,LEVELS)
IF(PHIIN.LT.0) PHIIN=PHIIN+LANE+1
CALL SMAPL(PHIIN,LPCTR,PHIOUT,CONST,CTR2,SUMDIF)
111 FORMAT(1X,6I4)

```

Figure E-15. (Continued)

20 CONTINUE

XX

C
C CALCULATE LOOP ERROR BY TAKING PHI(TRUE PHASE IN) - PHIOUT
(LOOP ESTIMATE OF PHI).

X=FLOAT(PHI(I+J))
CALL QUANT(X,LEVELS)
PHI(I+J)=INT(X)
PHI(I+J)=MOD(PHI(I+J),LEVELS)
IF(PHI(I+J).LT.0)PHI(I+J)=PHI(I+J)+LANE+1
IQUANT=PHI(I+J)
LQUANT=PHIOUT
CONTRL=11.
IF(CONTRL.LT.10.)GO TO 16
CALL PLTPHS(LQUANT,IQUANT)

16 CONTINUE

CONTREL=0.

ERROR(JJ)=PHIOUT-PHI(I+J)
IF(ERROR(JJ).GT.HALFLN)ERROR(JJ)=ERROR(JJ)-LEVELS
IF(ERROR(JJ).LT.-HALFLN)ERROR(JJ)=ERROR(JJ)+LEVELS
ERROR(JJ)=INT(FLOAT(ERROR(JJ))*5.625)

XX

C
C PERFORM RATE-AIDING FOR 2ND ORDER SNAPLL.

RATE=RATE+CTR2
XA=FLOAT(PHIOUT)+FLOAT(RATE)*SOGAIN
PHIOUT=INT(XA)
PHIOUT=MOD(PHIOUT,LEVELS)
IF(PHIOUT.LT.0)PHIOUT=PHIOUT+LEVELS
CALCULATE PHASE AT TIME OF NEXT TIME SLOT (10 SEC LATER).
DELTA=INT(VEL/16.)
PHASE=PHASE+DELTA
PHASE=MOD(PHASE,360)
IF(PHASE.LT.0)PHASE=PHASE+360
J=J+TSLOT
SUMDIF=0
CTR2=0
LPCTE=0
JJ=JJ+1
IF(J.GT.2500)VEL=-VEL1
IF(J.LT.5000)GO TO 15

XX

C
C PLOT HISTOGRAM OF LOOP OUTPUT ERRORS VS PHASE IN CEC.

CONTRL=11.
IF(CONTRL.LT.10.)GOTO 31
CALL HIST1(ERROR,NUM,SNR,VAR)

31 CONTINUE

CONTREL=0.

SNR=10.* ALOG10(A**2/(VARI*2.))
XX(L)=SNR
YY(L)=VAR

Figure E-15. (Continued)

```

YY(L)=SQRT(VAR)
S(LL)=SNR
STD(LL)=YY(L)
LL=LL+1
A=A+0.1
29 FORMAT(1X,'INPUT SNR = ',F7.3,10X,'OUTPUT VARIANCE = ',F8.3)
30 CONTINUE
999 NPTSPP=100
NPLOTS=1
GO TO 40
CALL MMPLT(XX,YY,NPTSPP,NPLOTS,XXL,YYL)
A=0.1
40 CONTINUE
GO TO 44
44 CONTINUE
SOGAIN=SOGAIN+.125
45 CONTINUE
CALL MMPLT(S,STD,100,6,XXL,YYL)
STOP
200 STOP
END
C XXXXXXXXXXXXXXXXXXXXXXXXXXXXXXXXXXXXXXXXXXXXXXX
C SUBROUTINE QUANT(X,LEVELS)
C ROUTINE QUANTIZES REAL X TO NUMBER OF LEVELS = LEVELS.
C RETURNS REAL X QUANTIZED.
XX=FLOAT(LEVELS)
X=(XX/360.)*X
I=INT(X)
X=FLOAT(I)
RETURN
END
C XXXXXXXXXXXXXXXXXXXXXXXXXXXXXXXXXXXXXXXXXXXXXXX
C SUBROUTINE GRANGE(Y,INTVL,A,SMALLA, TME)
INTEGER TME
REAL Y(5000), INTVL
TAU=INTVL
R=EXP(-SMALLA*TAU)
PSI=(A*A*SMALLA)/4.
CONS=SQRT(PSI*(1.-(R*R)))
CALL ANORM(AN)
Y(1)=AN*PSI
DO 10 I=2,TME
J=I-1
CALL ANORM(AN)
9 FORMAT(1X,10E10.2)
Y(I)=AN*CONS+R*Y(J)
10 CONTINUE
RETURN
END
C XXXXXXXXXXXXXXXXXXXXXXXXXXXXXXXXXXXXXXXXXXXXXXX
C SUBROUTINE SMAPLL(PHI,LPCTR,PHIREF,CONST,CTR2,SUMDIF)
C ROUTINE PERFORMS DIGITAL FILTERING ON INCOMING OMEGA PHASE
C MEASUREMENTS( PLL, BURST FILTER). OPERATION AND TIME CONSTANTS
C CLOSELY RESEMBLE HARDWARE MAPLL.
C ''CONST'' IS A VALUE TO BE SPECIFIED FOR MAX. LOOP CTR. VALUE

```

Figure E-15. (Continued)

C BEFORE ADJUSTING PHIREF. (LOOP TIME CONSTANT OF AMOUNT OF INTEGRA.
C

C R. SALTER, AVIONICS ENGINEERING CENTER, JULY 1976.
C

INTEGER PHI,PHIREF,CONST,CTR2,LPCTR

INTEGER DIFF,SUMDIF,HALFLN,LANE

HALFLN=64

LANE=127

COMPARE INCOMING PHASE TO LOOP CONTROL WORD(LCW) (PHASE REFERENCE

DIFF=PHI-PHIREF

KEEP A RUNNING SUM OF ABSOLUTE VALUES OF DIFFERENCES TO INDICATE
SIGNAL VARIANCE.

IF(DIFF).10,.50,.20

CHECK FOR EDGE OF LANE AMBIGUITY.

10 IF(DIFF.LT.-HALFLN) GO TO 25

SUMDIF=SUMDIF+IABS(DIFF)

GO TO 40

20 IF(DIFF.GT.HALFLN) GO TO 35

SUMDIF=SUMDIF+IABS(DIFF)

GO TO 30

C INCREMENT LOOP COUNTER.

30 LPCTR=LPCTR+1

C EXAMINE LPCTR FOR INCR. MORE THAN 'CONST' TIMES CORRELATED.

IF(LPCTR.LE.CONST) RETURN

LPCTR=0

PHIREF=PHIREF+1

CTR2=CTR2+1

C CHECK FOR MODULO 256 LANE COUNTS.

IF(PHIREF.GT.LANE) PHIREF=0

RETURN

C DECREMENT LOOP COUNTER.

40 LPCTR=LPCTR-1

C EXAMINE LPCTR FOR DECR. MORE THAN 'CONST' TIMES CORRELATED.

IF(LPCTR.GE.-CONST) RETURN

LPCTR=0

PHIREF=PHIREF-1

CTR2=CTR2-1

C CHECK FOR MODULO 256 LANE COUNTS.

IF(PHIREF.LT.0) PHIREF=LANE

50 RETURN

25 PHI=PHI+LANE

DIFF=PHI-PHIREF

SUMDIF=SUMDIF+IABS(DIFF)

GO TO 30

35 PHI=PHI-LANE

DIFF=PHI-PHIREF

SUMDIF=SUMDIF+IABS(DIFF)

GO TO 40

END

C XXX

ROUTINE PLOT1(X,LL)

C ROUTINE PLOTS DATA VECTOR "X" WITH STARS, ONE POINT PER LINE ON A
1-128 SCALE.

C IF VALUES OF "X" CAN FALL BETWEEN 128-256, SET LL=1 AND ROUTINE

Figure E-15. (Continued)

```

C      WILL HALVE EACH VALUE BEFORE PLOTTING. OTHERWISE, IF VALUES OF
C      "X" ARE ALL LESS THAN 128, ROUTINE WILL PLOT STRAIGHT VALUES IF
C      LL=0
C
C      MUST DIMENSION X = VECTOR OF VALUES TO BE PLOTTED.
C      R.W. LILLEY, AVIONICS, JANUARY, 1976
C      MODIFIED BY R. SALTER, AVIONICS, APRIL, 1976.
C
C      INTEGER BK//*,ST/**/,LIN(128)
C      INTEGER X(1000)
C      DO 10 I=1,128
10 LIN(I)=BK
C      DO 20 I=1,200
C      IF(LL.EQ.0)GO TO 12
C      MM=X(I)/2+1
C      GO TO 13
12 CONTINUE
C      MM=X(I)
13 CONTINUE
C      LIN(MM)=ST
C      PRINT 11,LIN
11 FORMAT(1X,128A1)
C      LIN(MM)=BK
20 CONTINUE
C      RETURN
C      END
C      XXXXXXXXXXXXXXXXXXXXXXXXXXXXXXXXXXXXXXXXXXXXXXXXX
C      SUBROUTINE GRANGB(Y,INTVL,A,SMALLA, TME)
C      INTEGER TME
C      REAL Y(5000), INTVL
C      TAU=INTVL
C      R=EXP(-SMALLA*TAU)
C      PSI=(A*A*SMALLA)/4.
C      CONS=SQRT(PSI*(1.-(R*R)))
C      CALL BNORM(AN)
C      Y(1)=AN*PSI
C      DO 10 I=2,TME
C      J=I-1
C      CALL BNORM(AN)
C      Y(I)=AN*CONS+R*Y(J)
10 CONTINUE
C      RETURN
C      END
C      XXXXXXXXXXXXXXXXXXXXXXXXXXXXXXXXXXXXXXXXXXXXXXXXX
C      SUBROUTINE PLTPHS(LQUANT,IQUANT)
C      PLTPHS PLOTS THE QUANTIZED PHASE VALUE OF THE INPUT PHASE (+) AND THE
C      OUTPUT PHASE (*)
C      INTEGER BLANK,STAR,PT,CROSS
C      DATA BLANK//,STAR/**/,PT//-,CROSS//+
C      DIMENSION LINE(128)
C      DO 10 K=1,128
10 LINE(K)=BLANK
C      LINE(LQUANT+1)=STAR
C      IF IT IS DESIRED THAT ONLY THE OUTPUT PHASE BE PLOTTED, SET
C      LINE(IQUANT)= BLANK

```

Figure E-15. (Continued)

ORIGINAL PAGE IS
OF POOR QUALITY

```

LINE(IQUANT+1)=CROSS
IF(LQUANT.EQ.IQUANT) LINE(LQUANT+1)=PT
PRINT 1,LINE
1 FORMAT(1X,128A1)
RETURN
END
C XXXXXXXXXXXXXXXXXXXXXXXXXXXXXXXXXXXXXXXXXXXXXXXXX
SUBROUTINE MNVAR(GA,AVE,VAR)
REAL GA(5000)
C COMPUTE MEAN AND VARIANCE OF R.V.'S RETURNED FROM RANDOM NUMBER
C GENERATOR AND LOW PASS FILTER.
SUM=0.
DO 5 I=1,5000
SUM=SUM+GA(I)
5 CONTINUE
AVE=SUM/5000.
SUM2=0.
DO 6 I=1,5000
SUM2=SUM2+(GA(I)-AVE)**2
6 CONTINUE
VAR=SUM2/5000
PRINT 7,AVE,VAR
7 FORMAT(1X,2E20.9)
RETURN
END
C XXXXXXXXXXXXXXXXXXXXXXXXXXXXXXXXXXXXXXXXXXXXXXXXX
SUBROUTINE HIST1(NOISE,NUM,SNR,VAR2)
INTEGER NOISE(5000),NN(5000)
REAL YYY(101),XXX(101),XXXL(12),YYYL(12),XXL(12),YYL(12)

DATA XXL/'S','I','G','N','A','L','/','N','O','I','S','E'/
DATA YYL/'P','L','L',' ','S','T','D',' ','D','E','V',' '
DATA XXXL/'N','O','I','S','E',' ','P','H','A','S','E',' '
DATA YYYL/'H','I','S','T','O','G','R','A','M',' ',' ',' '
C COMPUTE AND PLOT PROBABILITY DENSITY OF THE INPUT NOISE BEFORE
C IT IS ADDED TO THE SIGNAL PHASE, QUANTIZED, AND SENT TO SMAPLL.
ICEC=-50
DO 18 J=1,101
YYY(J)=0
DO 8 J=1,NUM
NN(J)=INT(FLOAT(NOISE(J))/3.6)
IF(NN(J).EQ.ICEC) YYY(J)=YYY(J)+1.
307 FORMAT(1X,I5,F6.1)
8 CONTINUE
XXX(I)=FLOAT(ICEC)
ICEC=ICEC+1
18 CONTINUE
DO 19 IK=1,101
YYY(IK)=YYY(IK)/FLOAT(NUM)
19 CONTINUE
GO TO 20
CALL MMPLT(XXX,YYY,101,1,XXXL,YYYL)
20 CONTINUE
ISUM=0
DO 115 I=1,NUM

```

Figure E-15. (Continued)

```
ISUM=ISUM+NN(I)
115 CONTINUE
AVE=FLOAT(ISUM)/FLOAT(NUM)
SUM=0
DO 116 I=1,NUM
ERR=FLOAT(NN(I))-AVE
SUM=SUM+ERR**2
116 CONTINUE
VAR2=SUM/FLOAT(NUM)
RETURN
PRINT 117,AVE,VAR2,SNR
117 FORMAT(1X,'MEAN=',F10.5,10X,'VARIANCE=',F10.5,10X,'SNR=',F10.5)
RETURN
END
```

Figure E-15. (Continued)

F. OSP Microcomputer Routines.

1. Main Routine. The "main" routine in this version of the OSP is simply an initialization and idling routine. This program initializes all the memory words needed by the OSP data processing subroutines and then simply waits to be interrupted by the microcomputer interface module with new Omega data, as flow charted in Figure F-1 and listed in Figure F-2. This main routine would be replaced by a more meaningful area navigation routine in a full-blown ONS. The navigation routine could perform navigation processing functions in the time between Omega data interrupts.

2. Interrupt Service Routine. When the main program is interrupted by the microcomputer interface module with new Omega data, the interrupt service routine is implemented as flow charted in Figure F-3 and listed in Figure F-4. The service routine first loads the new Omega data and updates a time-keeping register. It then checks a system status word to see if auto-sync is complete. If not, the data is passed to the auto-sync subroutine. If auto-sync is complete the time-keeping register is consulted to determine whether the current data sample is to be treated as Omega signal information or a transmission gap sample. If the sample falls in a time-slot the SMAPLL2 subroutine is called and the data used to update the estimate of phase for that time-slot. If the data is noise-gap information the time-keeping register is again consulted to determine if this is the first measurement taken during the current gap. If so, the data output subroutine is called and the rate-aiding for the second order SMAPLL2 is performed. Otherwise, the new data is simply forgotten and control is returned to the main routine to wait for the next interrupt.

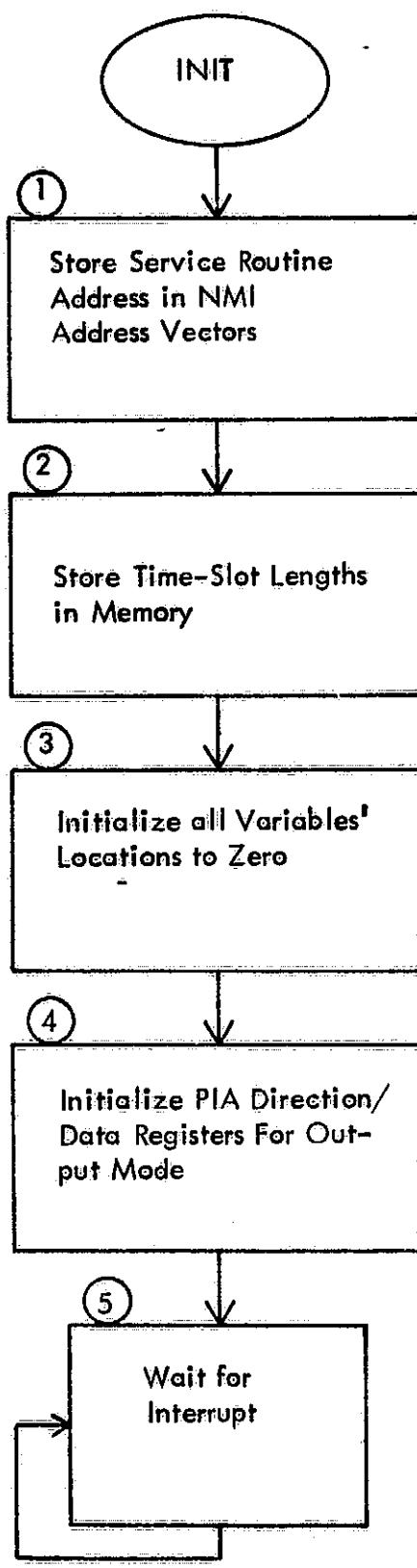


Figure F-1. Main (Initialization) Routine Flow Chart.

END PASS 1: 0 ERRORS

1	0000	ORG	00
2	0000	NMIL	EQU \$FFFA
3	0000	NMIH	EQU \$FFFFB
4	0000	OPTION	EQU 00
5	0000	LOP1	EQU 01
6	0000	LOP2	EQU 02
7	0000	STAST	EQU 03
8	0000	STAST2	EQU 74
9	0000	LENGTH	EQU 04
10	0000	GAP	EQU 12
11	0000	TIMCTR	EQU 13
12	0000	SYNCST	EQU 15
13	0000	TEMP	EQU 16
14	0000	PHI	EQU 17
15	0000	PREVPH	EQU 18
16	0000	FIRST	EQU 19
17	0000	FTP1	EQU 20
18	0000	SKFCTR	EQU 21
19	0000	NSHIFT	EQU 23
20	0000	CORCTR	EQU 25
21	0000	MAXCOR	EQU 27
22	0000	SYNCPT	EQU 29
23	0000	CTR1	EQU 31
24	0000	CTR2	EQU 32
25	0000	WASTE	EQU 33
26	0000	LCW	EQU 34
27	0000	RATE	EQU 42
28	0000	SN	EQU 50
29	0000	TSLOT	EQU 66
30	0000	PTR3	EQU 67
31	0000	PTR4	EQU 68
32	0000	PTR2	EQU 69
33	0000	TEMP2	EQU 70
34	0000	MUXCTR	EQU 71
35	0000	BITTRN	EQU 90
36	0000	INPORT	EQU \$D000
37	0000	OUTPRT	EQU \$BC00
38	0000	HALFLN	EQU 63
39	0000	LANE	EQU 127
40	0000	THRESH	EQU 4
41	0000	NBYTE	EQU 125
42	0000	CCNST	EQU 03
43	0000	LAF	EQU 90
44	0000	LBH	EQU 100
45	0000	LCE	EQU 110
46	0000	LDG	EQU 120
47	0000	LGAP	EQU 20
48	0000	SERVL	EQU \$60
49	0000	SLRVH	EQU \$10
50	1000		ORG \$1000
51	1000 78		SEI
52	1001 A9 60	ONE	LDA =SERVL

Figure F-2. Microcomputer Program INIT Listing.

53	1003	8D	FA	FF		STA	NMIL
54	1006	A9	10			LDA	=SERVH
55	1008	8D	FB	FF		STA	NMIH
56	100E	A9	5A		TWO	LDA	=LAF
57	100D	85	04			STA	LENGTH
58	100F	85	09			STA	LENGTH+5
59	1011	A9	64			LDA	=LBH
60	1013	85	05			STA	LENGTH+1
61	1015	85	0E			STA	LENGTH+7
62	1017	A9	6E			LDA	=LCE
63	1019	85	06			STA	LENGTH+2
64	101B	85	08			STA	LENGTH+4
65	101D	A9	78			LDA	=LDG
66	101F	85	0A			STA	LENGTH+6
67	1021	85	07			STA	LENGTH+3
68	1023	A9	14			LDA	=LGAP
69	1025	85	0C			STA	GAP
70	1027	A2	0D		THREE	LDX	=TIMCTR
71	1029	A9	00			LDA	=00
72	102B	95	00		FOUR	STA	OPTION,X
73	102D	E8				INX	
74	102E	E0	4A			CPX	=STAST2
75	1030	D0	F9			BNE	FOUR
76	1032	A9	00		SIX	LDA	=00
77	1034	85	0F			SIA	SYNCST
78	1036	A5	03			LDA	STAST
79	1038	85	-4A			STA	STAST2
80	103A	A9	00			LDA	=00
81	103C	8D	01	5C		STA	\$5C01
82	103F	A9	FF			LDA	=\$FF
83	1041	8D	00	5C		STA	\$5C00
84	1044	A9	04			LDA	=04
85	1046	8D	01	5C		STA	\$5C01
86	1049	A9	01			LDA	=\$01
87	104B	85	42			SIA	TSLOT
88	104D	58				CLI	
89	104E	4C	4E	10	FIVE	JMP	FIVE
90						END	

END PASS 2: 0 ERRORS

Figure F-2. (Continued)

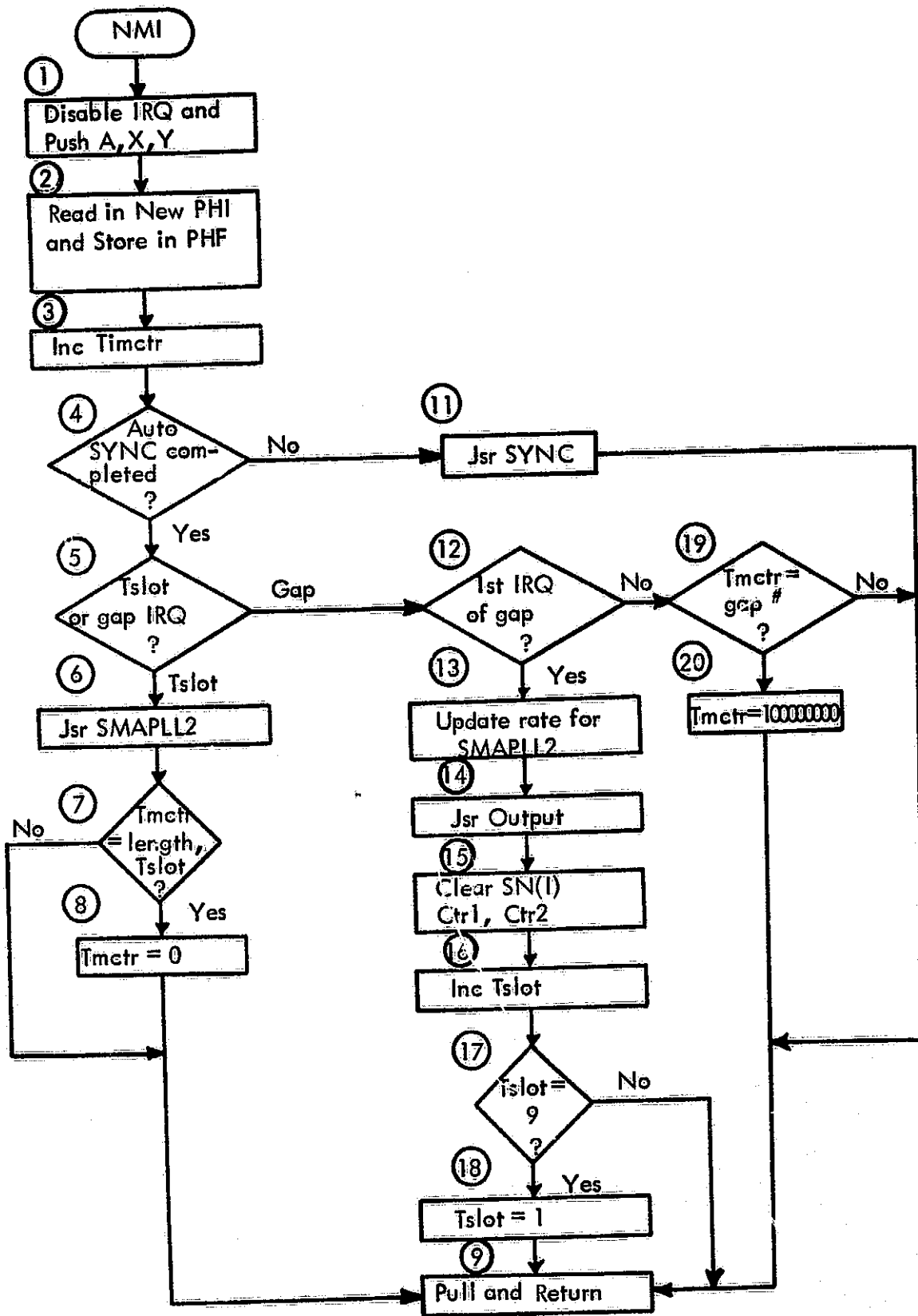


Figure F-3. Interrupt Service Routine Flow Chart.

END PASS 1: 0 ERRORS

1	0000		ORG	00
2	0000	IMPORT	EQU	\$D000
3	0000	PHI	EQU	17
4	0000	TIMCTR	EQU	13
5	0000	SYNCST	EQU	15
6	0000	TSLOT	EQU	66
7	0000	LENGTH	EQU	04
8	0000	PREVPH	EQU	18
9	0000	CTR2	EQU	32
10	0000	RATE	EQU	42
11	0000	CTR1	EQU	31
12	0000	SN	EQU	50
13	0000	GAP	EQU	20
14	0000	SYNC	EQU	\$1100
15	0000	SMAPLL	EQU	\$1300
16	0000	OUTPUT	EQU	\$1400
17	1060		ORG	\$1060
18	1060 78	ONE	SEI	
19	1061 48		PHA	
20	1062 8A		TXA	
21	1063 48		PHA	
22	1064 98		TYA	
23	1065 48		PHA	
24	1066 AD 00 D0	TWO	LDA	IMPORT
25	1069 85 11		STA	PHI
26	106B E6 0E	THREE	INC	TIMCTR+1
27	106D D0 02		BNE	FOUR
28	106F E6 0D		INC	TIMCTR
29	1071 A5 0F	FOUR	LDA	SYNCST
30	1073 C9 Q3		CMP	=03
31	1075 D0 1D		BNE	ELEVEN
32	1077 A5 0E	FIVE	LDA	TIMCTR+1
33	1079 10 31		BPL	TWELVE
34	107B 46 11	SIX	LSR	PHI
35	107D 20 00 13		JSR	SMAPLL
36	1080 A9 7F	SEVEN	LDA	=%01111111
37	1082 25 0E		AND	TIMCTR+1
38	1084 A6 42		LDX	TSLOT
39	1086 D5 03		CMP	LENGTH-1,X
40	1088 D0 04		BNE	NINE
41	108A A9 00	EIGHT	LDA	=00
42	108C 85 0E		STA	TIMCTR+1
43	108E 68	NINE	PLA	
44	108F A8		TAY	
45	1090 68		PLA	
46	1091 AA		TAX	
47	1092 68		PLA	
48	1093 40		RTI	
49	1094 20 00 11	ELEVEN	JSR	SYNC
50	1097 A5 0E		LDA	TIMCTR+1
51	1099 C9 E8		CMP	=\$E8
52	109B D0 0C		BNE	B11

Figure F-4. Microcomputer Program OSERV Listing.

53	109D	A5	0D		LDA	TIMCTR
54	109F	C9	03		CMP	=\$03
55	10A1	D0	06		BNE	B11
56	10A3	A9	00		LDA	=00
57	10A5	85	0E		STA	TIMCTR+1
58	10A7	85	0D		STA	TIMCTR
59	10A9	4C	8E	10	B11	JMP NINE
60	10AC	C9	01		TWELEV	CMP =01
61	10AE	D0	3D			BNE NINETN
62	10B0	A6	42		THIRTN	LDX TSLOT
63	10B2	A5	20			LDA CTR2
64	10B4	30	08			BMI LABEL1
65	10B6	18				CLC
66	10B7	75	29			ADC RATE-1,X
67	10B9	95	29			STA RATE-1,X
68	10BE	4C	CC	10		JMP FOURTN
69	10BE	49	FF		LABEL1	EOR =\$FF
70	10C0	18				CLC
71	10C1	69	01			ADC =01
72	10C3	85	20			STA CTR2
73	10C5	B5	29			LDA RATE-1,X
74	10C7	38				SEC
75	10C8	55	20			SBC CTR2
76	10CA	95	29			STA RATE-1,X
77	10CC	20	00	14	FOURTN	JSE OUTPUT
78	10CF	8A			FIFTN	TXA
79	10D0	18				CLC
80	10D1	65	42			ADC TSLOT
81	10D3	AA				TAX
82	10D4	A9	00			LDA =00
83	10D6	95	30			STA SN-2,X
84	10D8	95	31			STA SN-1,X
85	10DA	85	1F			STA CTR1
86	10DC	85	20			STA CTR2
87	10DF	E6	42		SISTN	INC TSLOT
88	10E0	A9	09		SEVTN	LDA =09
89	10E2	C5	42			CMP TSLCT
90	10E4	D0	A8			BNE NINE
91	10E6	A9	01		EIGHTN	LDA =01
92	10E8	85	42			STA TSLOT
93	10EA	4C	8E	10		JMP NINE
94	10ED	C9	14		NINETN	CMP =GAP
95	10EF	D0	9D			BNE NINE
96	10F1	A9	80		TWENTY	LDA =\$80
97	10F3	85	0E			STA TIMCTR+1
98	10F5	4C	8E	10		JMP NINE
99						END

END PASS 2: 0 ERRORS

Figure F-4. (Continued)

3. Automatic Synchronization Subroutine. The auto-sync procedure is explained in the main text, and the microcomputer program is flow charted in Figure F-5. The microcomputer language listing appears in Figure F-6.

4. SMAPLL2 Tracking Subroutine. The memory-aided second order phase locked loop (SMAPLL2) operation is also functionally outlined in the text. More details on the performance which can be expected from this tracking configuration is given in Appendix E. The SMAPLL2 procedure as implemented in the OSP microcomputer is charted in Figure F-7, and the program listing appears in Figure F-8.

5. Data Output Subroutine. The data output operation is described in the text and is flow charted in Figure F-9. The microcomputer output subroutine is listed in Figure F-10.

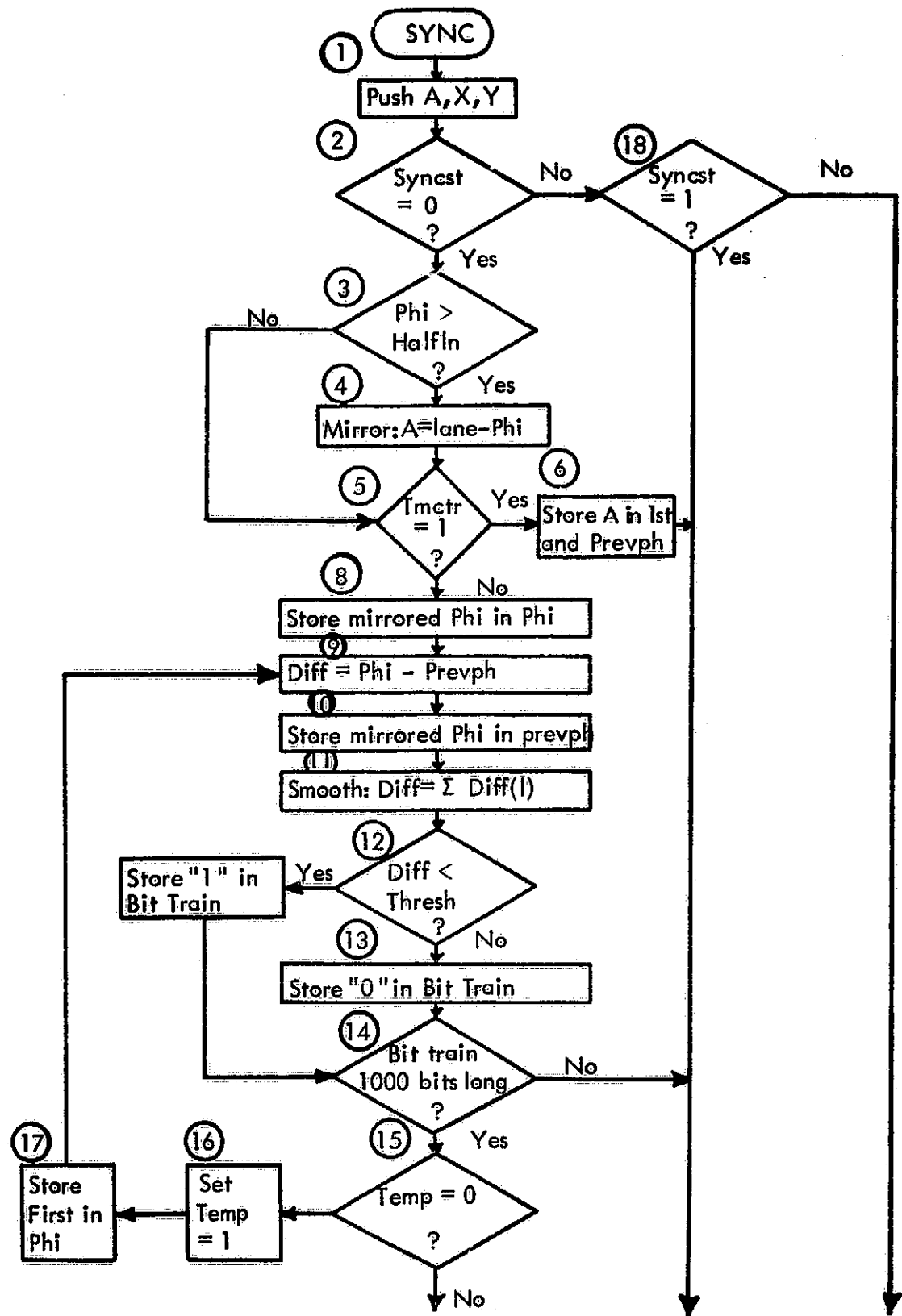


Figure F-5. Automatic Synchronization Subroutine Flow Chart.

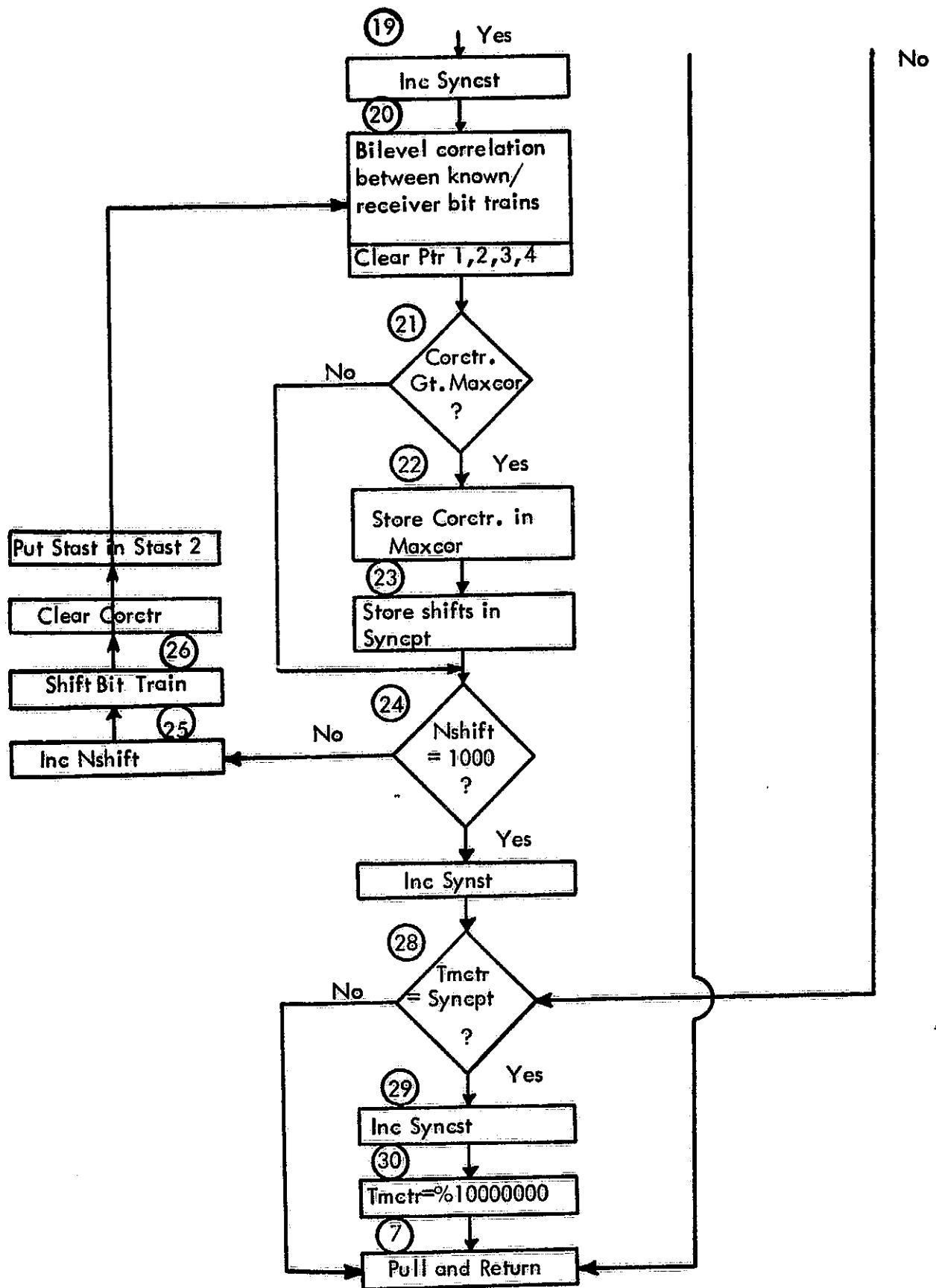


Figure F-5. (Continued)

END PASS 1: 0 ERRORS

1	0000		ORG	00
2	0000		SYNCST	EQU 15
3	0000		TEMP	EQU 16
4	0000		PHI	EQU 17
5	0000		SPhi	EQU 72
6	0000		HALFLN	EQU 63
7	0000		LANE	EQU 127
8	0000		FIRST	EQU 19
9	0000		PREVPH	EQU 18
10	0000		THRESH	EQU 05
11	0000		NBYTE	EQU 125
12	0000		BITTRN	EQU 90
13	0000		TIMCTR	EQU 13
14	0000		PTR2	EQU 20
15	0000		PTR1	EQU 69
16	0000		PTR3	EQU 67
17	0000		PTR4	EQU 68
18	0000		LFNGTH	EQU 04
19	0000		STAST	EQU 03
20	0000		STAST2	EQU 74
21	0000		SHFCTR	EQU 21
22	0000		NSHIFT	EQU 23
23	0000		CORCTR	EQU 25
24	0000		MAXCOR	EQU 27
25	0000		SYNCPT	EQU 29
26	1100		ORG	\$1100
27	1100	48	SYNC	PHA
28	1101	98		TYA
29	1102	48		PHA
30	1103	8A		TXA
31	1104	48		PHA
32	1105	A5 0F	TWO	LDA SYNCST
33	1107	D0 5B		BNE EIGHTN
34	1109	A5 11	THREE	LDA PHI
35	110B	85 48		STA SPhi
36	110D	C9 3F		CMP =HALFLN
37	110F	90 05		BCC FIVE
38	1111	A9 7F	FOUR	LDA =LANE
39	1113	38		SEC
40	1114	E5 48		SBC SPhi
41	1116	A4 0E	FIVE	LDY TIMCTR+1
42	1118	C0 01		CPY =01
43	111A	D0 0A		BNE EIGHT
44	111C	85 13	SIX	STA FIRST
45	111E	85 12		STA PREVPH
46	1120	68	SEVEN	PLA
47	1121	A8		TAY
48	1122	68		PLA
49	1123	AA		TAX
50	1124	68		PLA
51	1125	60		RTS
52	1126	85 48	EIGHT	STA SPhi

Figure F-6. Microcomputer Program SYNC Listing.

53	1128	38	NINE	SEC
54	1129	E5 12		SBC PREVPH
55	112B	B0 05		BCS TEN
56	112D	49 FF		BOR =\$FF
57	112F	18		CLC
58	1130	69 01		ADC =01
59	1132	A4 48	TEN	LDY SPHI
60	1134	84 12		STY PREVPH
61	1136	EA	ELEVEN	NOP
62	1137	EA		NOP
63	1138	EA		NOP
64	1139	C9 05	TWELEV	CMP =THRESH
65	113B	90 04		BCC SIGNAL
66	113D	18	THIRTN	CLC
67	113E	4C 42 11		JMP STORE
68	1141	38		SIGNAL SEC
69	1142	A2 7D		STORE LDX =NBYTE
70	1144	36 59		ROTATE ROL BITTRN-1,X
71	1146	CA		DEX
72	1147	D0 FE		BNE ROTATE
73	1149	A5 0D	FOURTN	LDA TIMCTE
74	114B	C9 03		CMP =\$03
75	114D	D0 D1		BNE SEVEN
76	114F	A5 0E		LDA TIMCTF+1
77	1151	C9 E8		CMP =\$E8
78	1153	D0 CB		BNE SEVEN
79	1155	A5 10	FIFTN	LDA TEMP
80	1157	D0 15		BNE NINETN
81	1159	A9 01	SIXTN	LDA =01
82	115B	85 10		STA TEMP
83	115D	A5 13	SEVTN	LDA FIRST
84	115F	85 48		STA SPHI
85	1161	4C 28 11		JMP NINE
86	1164	C9 01	EIGHTN	CMP =01
87	1166	D0 03		BNE A19
88	1168	4C 20 11		JMP SEVEN
89	116B	4C 06 12	A19	JMP TWENT8
90	116E	E6 0F	NINETN	INC SYNCST
91	1170	A9 00		LDA =00
92	1172	85 0E		STA TIMCTF+1
93	1174	85 0D		STA TIMCTR
94	1176	A6 14	TWENTA	LDX PTR2
95	1178	B5 04		LDA LENGTH,X
96	117A	85 15	TWENTB	STA SHFCTR
97	117C	26 4A	TWENTE	ROL STAST2
98	117E	90 06		BCC PLUS
99	1180	A9 01		LDA =01
100	1182	85 10		STA TEMP
101	1184	10 04		BPL TWENTF
102	1186	A9 00	PLUS	LDA =00
103	1188	85 10		STA TEMP
104	118A	A6 43	TWENTF	LDX PTR3
105	118C	B5 5A		LDA BITTRN,X
106	118E	A4 44	TWENTG	LDY PTR4
107	1190	F0 04	B20G	BEQ TWENTH

Figure F-6. (Continued)

108	1192	2A	ROL A
109	1193	88	DEY
110	1194	10 FA	BPL B20G
111	1196	2A	TWENTH ROL A
112	1197	A9 00	TWENTI LDA =00
113	1199	65 10	ADC TEMP
114	119B	C9 01	TWENTJ CMP =01
115	119D	F0 06	BEQ TWENTK
116	119F	E6 1A	INC CORCTR+1
117	11A1	D0 02	BNE TWENTK
118	11A3	E6 19	INC CORCTR
119	11A5	A4 44	TWENTK LDY PTR4
120	11A7	C8	INY
121	11A8	C0 08	TWENTL CPY =08
122	11AA	D0 04	BNE TWENTM
123	11AC	A0 00	LDY =00
124	11AE	E6 43	INC PTR3
125	11B0	84 44	TWENTM STY PTR4
126	11B2	C6 15	DEC SHFCTF
127	11B4	D0 D4	TWENTN BNE TWENTF
128	11B6	A5 45	TWENTO LDA PTR1
129	11B8	D0 08	BNE TWENTQ
130	11BA	A9 14	TWENTP LDA =20
131	11BC	85 15	STA SHFCTR
132	11BE	E6 45	INC PTR1
133	11C0	10 C4	BPL PLUS
134	11C2	A5 14	TWENTQ LDA PTR2
135	11C4	C9 07	CMP =07
136	11C6	F0 08	BEQ TWENT1
137	11C8	E6 14	TWENTT INC PTR2
138	11CA	A9 00	LDA =00
139	11CC	85 45	STA PTR1
140	11CF	F0 A6	BEQ TWENTA
141	11D0	A9 00	TWENT1 LDA =00
142	11D2	85 45	STA PTR1
143	11D4	85 14	STA PTR2
144	11D6	85 43	STA PTR3
145	11D8	85 44	STA PTR4
146	11DA	A5 19	LDA CORCTR
147	11DC	C5 1B	CMP MAXCOR
148	11DE	90 18	BCC TWENT4
149	11E0	D0 06	BNE TWENT2
150	11E2	A5 1A	LDA CORCTR+1
151	11E4	C5 1C	CMP MAXCOR+1
152	11E6	90 10	BCC TWENT4
153	11E8	A5 19	TWENT2 LDA CORCTR
154	11EA	85 1B	STA MAXCOR
155	11EC	A5 1A	LDA CORCTR+1
156	11EE	85 1C	STA MAXCOR+1
157	11F0	A5 17	TWENT3 LDA NSHIFT
158	11F2	85 1D	STA SYNCPT
159	11F4	A5 18	LDA NSHIFT+1
160	11F6	85 1F	STA SYNCPT+1
161	11F8	A5 18	TWENT4 LDA NSHIFT+1
162	11FA	C9 E8	CMP =\$E8

Figure F-6. (Continued)

163	11FC	D0	1D		BNE	TWENT5
164	11FL	A5	17		LDA	NSHIFT
165	120C	C9	03		CMP	=\$03
166	1202	D0	17		BNE	TWENT5
167	1204	E6	0F	TWENT7	INC	SYNCST
168	1206	A5	0D	TWENT8	LDA	TIMCTR
169	1208	C5	1D		CMP	SYNCPT
170	120A	D0	0C		BNE	A25
171	120C	A5	0E		LDA	TIMCTR+1
172	120E	C5	1E		CMP	SYNCPT+1
173	1210	D0	06		BNE	A25
174	1212	E6	0F	TWENT9	INC	SYNCST
175	1214	A9	80	THIRTY	LDA	=\$80
176	1216	85	0E		STA	TIMCTR+1
177	1218	4C	20	11	A25	JMP SEVEN
178	121E	E6	18	TWENT5	INC	NSHIFT+1
179	121D	D0	02		BNE	TWENT6
180	121F	E6	17		INC	NSHIFT
181	1221	A2	7D	TWENT6	LDX	=NBYTE
182	1223	A5	5A		LDA	BITTRN
183	1225	30	03		BMI	MINUS
184	1227	18			CLC	
185	1228	90	01		BCC	DOIT
186	122A	38		MINUS	SEC	
187	122B	36	59	DOIT	ROL	BITTRN-1,X
188	122D	CA			DEX	
189	122E	D0	FB		BNE	DOIT
190	1230	A9	00		LDA	=00
191	1232	85	19		STA	CORCTR
192	1234	85	1A		STA	CORCTR+1
193	1236	A5	03		LDA	STAST
194	1238	85	4A		STA	STAST2
195	123A	4C	76	11	JMP	TWENTA
196					END	

END PASS 2: 0 ERRORS

Figure F-6. (Continued)

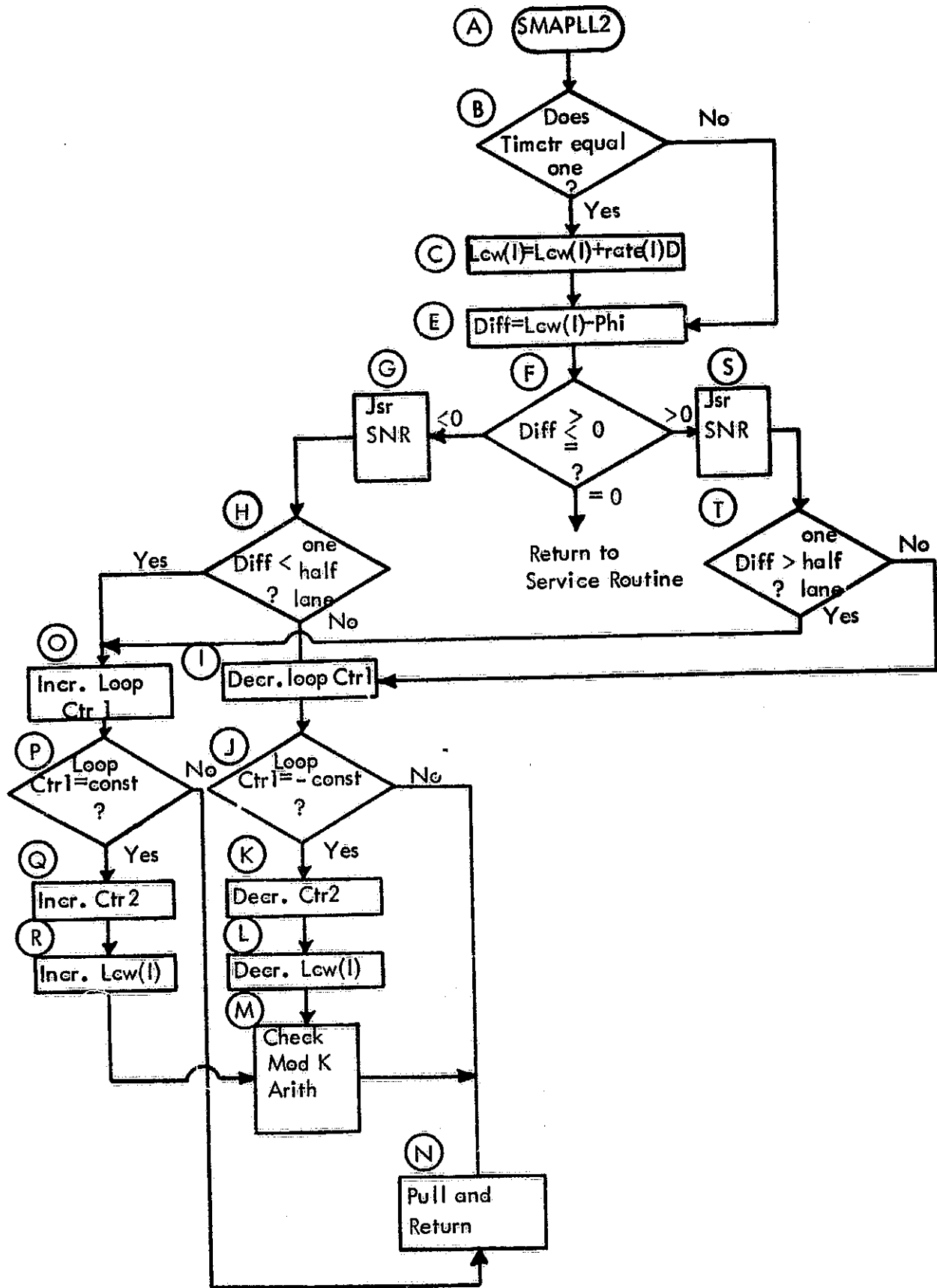


Figure F-7. SMAPLL2 Subroutine Flow Chart.

END PASS 1: 0 ERRORS

1	0000		ORG 00
2	0000		TIMCTR EQU 13
3	0000		CTR1 EQU 31
4	0000		CTR2 EQU 32
5	0000		RATE EQU 42
6	0000		LCW EQU 34
7	0000		SN EQU 50
8	0000		PHI EQU 17
9	0000		TSLOT EQU 66
10	0000		PREVPH EQU 18
11	0000		TEMP EQU 16
12	0000		TEMP2 EQU 70
13	0000		HALFLN EQU 32
14	0000		CONST EQU 08
15	0000		MOD64 EQU \$1390
16	0000		SNR EQU \$13C0
17	1300		ORG \$1300
18	1300 48		SMAPLL PHA
19	1301 8A		TXA
20	1302 48		PHA
21	1303 98		TYA
22	1304 48		PHA
23	1305 A5 0E	B1	LDA TIMCTR+1
24	1307 C9 81		CMP =\$81
25	1309 D0 25		BNE E1
26	130B A6 42	C1	LDX TSLOT
27	130D B5 29		LDA RATE-1,X
28	130F 30 0C		BMI LABEL1
29	1311 4A		LSR A
30	1312 4A		LSR A
31	1313 85 46		STA TEMP2
32	1315 B5 21		LDA LCW-1,X
33	1317 18		CLC
34	1318 65 46		ADC TEMP2
35	131A 4C 2E 13		JMP D1
36	131D 49 FF	LABEL1	EOR =\$FF
37	131F 18		CLC
38	1320 69 01		ADC =01
39	1322 4A		LSR A
40	1323 4A		LSR A
41	1324 85 46		STA TEMP2
42	1326 B5 21		LDA LCW-1,X
43	1328 38		SEC
44	1329 B5 46		SBC TEMP2
45	132B 20 90 13	D1	JSR MOD64
46	132E 95 21		STA LCW-1,X
47	1330 A6 42	E1	LDX TSLOT
48	1332 B5 21		LDA LCW-1,X
49	1334 38		SEC
50	1335 E5 11		SBC PHI
51	1337 F0 2A	F1	BEQ N1
52	1339 B0 41		BCS S1

Figure F-8. Microcomputer Program SMAPLL2 Listing.

53	133B	A5	11	H1	LDA	PHI	
54	133D	38			SFC		
55	133E	F5	21		SBC	LCW-1,X	
56	1340	20	C0	13	JSR	SNR	
57	1343	C9	20	G1	CMP	=HALFLN	
58	1345	90	22		BCC	O1	
59	1347	C6	1F	I1	DEC	CTR1	
60	1349	A9	FF		LDA	=255	
61	134B	45	1F	J1	EOR	CTR1	
62	134D	18			CLC		
63	134E	69	01		ADC	=01	
64	1350	C9	08		CMP	=CONST	
65	1352	D0	0F		BNE	N1	
66	1354	A9	00		LDA	=00	
67	1356	85	1F		STA	CTR1	
68	1358	C6	20	K1	DEC	CTR2	
69	135A	D6	21	L1	DEC	LCW-1,X	
70	135C	B5	21	CKMOD	LDA	LCW-1,X	
71	135E	20	90	13	M1	JSR	MOD64
72	1361	95	21		STA	LCW-1,X	
73	1363	68		N1	PLA		
74	1364	A8			TAY		
75	1365	68			PLA		
76	1366	AA			TAX		
77	1367	68			PLA		
78	1368	60			RTS		
79	1369	E6	1F	O1	INC	CTR1	
80	136B	A9	08	P1	LDA	=CONST	
81	136D	C5	1F		CMP	CTR1	
82	136F	D0	F2		BNE	N1	
83	1371	A9	00		LDA	=00	
84	1373	85	1F		STA	CTR1	
85	1375	E6	20	Q1	INC	CTR2	
86	1377	F6	21	R1	INC	LCW-1,X	
87	1379	4C	5C	13	JMP	CKMOD	
88	137C	20	C0	13	S1	JSR	SNR
89	137F	C9	20		T1	CMP	=HALFLN
90	1381	B0	E6		BCS	O1	
91	1383	4C	47	13	JMP	I1	
92					END		

END PASS 2: 0 ERRORS

Figure F-8. (Continued)

END PASS 1: 0 ERRORS

1	0000		ORG 00
2	0000	TEMP2	EQU 70
3	1390		ORG \$1390
4	1390 85 46	MOD64	STA TEMP2
5	1392 8A		TXA
6	1393 48		PHA
7	1394 98		TYA
8	1395 48		PHA
9	1396 A5 46	TWO	LDA TEMP2
10	1398 30 11		BMI SEVEN
11	139A 29 40	THREE	AND =%01000000
12	139C F0 06		BEQ SIX
13	139E A5 46	FOUR	LDA TEMP2
14	13A0 29 3F		AND =%00111111
15	13A2 85 46	FIVE	STA TEMP2
16	13A4 68	SIX	PLA
17	13A5 A8		TAY
18	13A6 68		PLA
19	13A7 AA		TAX
20	13A8 A5 46		LDA TEMP2
21	13AA 60		RTS
22	13AB 49 FF	SEVEN	EOR =\$FF
23	13AD 85 46		STA TEMP2
24	13AF E6 46		INC TEMP2
25	13B1 A9 3F		LDA =63
26	13B3 38		SEC
27	13B4 E5 46		SBC TEMP2
28	13B6 4C A2 13		JMP FIVE
29			END

END PASS 2: 0 ERRORS

Figure F-8. (Continued)

END PASS 1: 0 ERRORS

1	0000		ORG 0
2	0000	TEMP2	EQU 70
3	0000	TSLOT	EQU 66
4	0000	SN	EQU 50
5	13C0		ORG \$13C0
6	13C0 85 46	SNR	STA TEMP2
7	13C2 8A		TXA
8	13C3 48		PHA
9	13C4 98		TYA
10	13C5 48		PHA
11	13C6 A5 42	TWO	LDA TSLOT
12	13C8 18		CLC
13	13C9 65 42		ADC TSLOT
14	13CB AA		TAX
15	13CC A5 46		LDA TEMP2
16	13CE 18		CLC
17	13CF 75 31		ADC SN-1,X
18	13D1 95 31		STA SN-1,X
19	13D3 90 03		BCC THREE
20	13D5 CA		DEX
21	13D6 F6 31		INC SN-1,X
22	13D8 68	THREE	PLA
23	13D9 A8		TAY
24	13DA 68		PLA
25	13DB AA		TAX
26	13DC A5 46		LDA TEMP2
27	13DE 60		RTS
28			END

END PASS 2: 0 ERRORS

Figure F-8. (Continued)

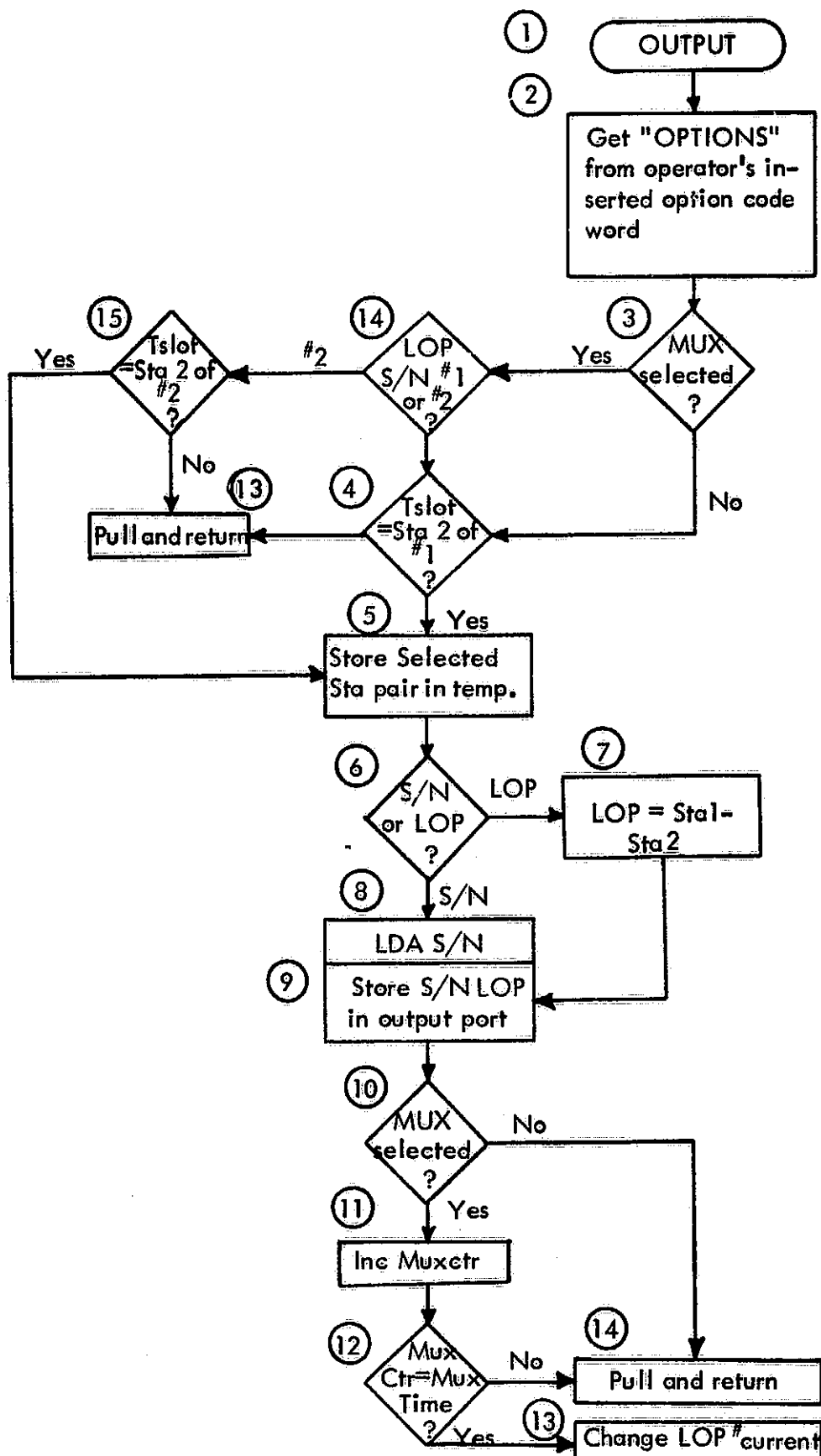


Figure F-9. Data OUTPUT Subroutine Flow Chart.

END PASS 1: 0 ERRORS

1	0000		ORG	00
2	0000		OPTION	EQU 00
3	0000		LOP1	EQU 01
4	0000		LOP2	EQU 02
5	0000		MUXCTR	EQU 71
6	0000		WASTE	EQU 33
7	0000		LCW	EQU 34
8	0000		SN	EQU 50
9	0000		TSLOT	EQU 66
10	0000		TEMP	EQU 16
11	0000		LANE	EQU 64
12	0000		OUTPRT	EQU \$5C00
13	1400			ORG \$1400
14	1400 48		OUTPUT	PHA
15	1401 8A			TXA
16	1402 48			PHA
17	1403 98			TYA
18	1404 48			PHA
19	1405 A5 00		TWO	LDA OPTION
20	1407 30 6E		THREE	BMI MUX
21	1409 A5 01		FOUR	LDA LOP1
22	140B 85 10		FIVE	STA TEMP
23	140D 29 0F			AND =%00000111
24	140F C5 42			CMP TSLOT
25	1411 D0 5E			BNE FOURTN
26	1413 A5 00		SIX	LDA OPTION
27	1415 29 40			AND =%01000000
28	1417 F0 21			BEQ EIGHT
29	1419 A5 10		SEVEN	LDA TEMP
30	141B 29 F0			AND =\$F0
31	141D 4A			LSR A
32	141E 4A			LSR A
33	141F 4A			LSR A
34	1420 4A			LSR A
35	1421 AA			TAX
36	1422 A5 10			LDA TEMP
37	1424 29 0F			AND =\$0F
38	1426 85 10			STA TEMP
39	1428 B5 21			LDA LCW-1,X
40	142A A6 10			LDX TEMP
41	142C 38			SEC
42	142D F5 21			SBC LCW-1,X
43	142F 30 03			BMI COMPL
44	1431 4C 51 14			JMP NINE
45	1434 18		COMPL	CLC
46	1435 69 40			ADC =LANE
47	1437 4C 51 14			JMP NINE
48	143A A5 42		EIGHT	LDA TSLOT
49	143C 18			CLC
50	143D 65 42			ADC TSLOT
51	143F AA			TAX
52	1440 B5 30			LDA SN-2,X

Figure F-10. Microcomputer Program OUTPUT Listing.

53	1442	0A		ASL A
54	1443	0A		ASL A
55	1444	0A		ASL A
56	1445	0A		ASL A
57	1446	0A		ASL A
58	1447	85 10		STA TEMP
59	1449	B5 31		LDA SN-1,X
60	144B	4A		LSR A
61	144C	4A		LSR A
62	144D	4A		LSR A
63	144E	18		CLC
64	144F	65 10		ADC TEMP
65	1451	8D 00	5C	NINE STA OUTFRT
66	1454	A5 00		TEN LDA OPTION
67	1456	10 19		BPL FOURTN
68	1458	E6 47		ELEVEN INC MUXCTR
69	145A	A5 47		TWELEV LDA MUXCTR
70	145C	29 3F		AND =%00111111
71	145E	85 10		STA TEMP
72	1460	A5 00		LDA OPTION
73	1462	29 3F		AND =%00111111
74	1464	C5 10		CMP TEMP
75	1466	D0 09		BNE FOURTN
76	1468	A5 47		THIRTN LDA MUXCTR
77	146A	29 C0		AND =%11000000
78	146C	18		CLC
79	146D	69 40		ADC =%01000000
80	146F	85 47		STA MUXCTR
81	1471	68		FOURTN PLA
82	1472	A8		TAY
83	1473	68		PLA
84	1474	AA		TAX
85	1475	68		PLA
86	1476	60		RTS
87	1477	A5 47	MUX	LDA MUXCTR
88	1479	29 40		AND =%01000000
89	147B	F0 8C		BEQ FOUR
90	147D	A5 02		FIFTEEN LDA LOP2
91	147F	4C 0B 14		JMP FIVE
92				END

END PASS 2: 0 ERRORS

Figure F-10. (Continued)